

An Architecture-Based Weight Estimation Method for Aircraft Fuel Systems

Carlos Daniel Rodriguez

A Thesis
in
The Department
of
Mechanical, Industrial, and Aerospace Engineering

Presented in Partial Fulfillment of the Requirements
for the Degree of Master of Applied Sciences in Mechanical Engineering at
Concordia University
Montreal, Québec, Canada

September 2022

©Carlos Daniel Rodriguez, 2022

CONCORDIA UNIVERSITY

School of Graduate Studies

This is to certify that the thesis prepared

By: Carlos D. Rodriguez

Entitled: An Architecture-Based Weight Estimation Method for Aircraft Fuel Systems

And submitted in partial fulfillment of the requirements for a degree of

Master of Applied Science Mechanical Engineering

Complies with the regulations of the University and meets the accepted standards with respect to originality and quality.

Signed by the final Examining Committee

Examiner and Chair

Dr. Charles Kiyanda

Examiner

Dr. Catharine Marsden

Supervisor

Dr. Susan Liscouët-Hanke

Approved by

Dr. Martin Pugh, Chair,

Department of Mechanical, Industrial, and Aerospace Engineering

2022

Mourad Debbabi, Dean

Gina Cody School of Engineering and Computer Science

Abstract

An Architecture-Based Weight Estimation Method for Aircraft Fuel Systems

Carlos Daniel Rodriguez

The development of hybrid-electric propulsion technologies for aircraft is believed to be a stepping stone for the aerospace industry to reduce greenhouse gas emissions and achieve 50% of the levels of 2005 by the year 2050. However, the introduction of batteries and power electronics significantly impacts the weight and size of new aircraft concepts that integrate these propulsion units. The traditional design techniques need to be adapted to account for this added weight and allow a more rapid evaluation and comparison between concepts and trade-off studies. New models and methods need to be developed to perform these concept studies in a multidisciplinary design, analysis, and optimization (MDAO) environment, to estimate the size, weight, and performance of non-conventional aircraft. This thesis proposes one such tool, focusing on the aircraft fuel system. The methodology to develop the tool is based on analyzing typical fuel system architectures across a wide range of conventional aircraft and how this approach can be adapted for hybrid-electric propulsion applications. This thesis breaks the system into four major groups (engine fuel feed, fuel transfer, fuel quantity & indicating, and tank venting) and how the weight of each can be estimated from existing component data. For conventional modern turboprop regional aircraft such as the ATR42, the methodology predicts the system weight within 10% of published data. The increased detail built into the tool implementation allows analysis of the variation in system weight arising from major changes to the fuel system architecture encountered in hybrid-electric aircraft. Two case studies of hybrid-electric variants of existing aircraft (the Dornier 228 and ATR42) are investigated to demonstrate the application of the tool. These studies also compare the estimated weight of the fuel system in the hybrid-electric aircraft architecture to that of the conventional propulsion variant, highlighting a reduction in system mass by approximately 10 to 15% relative to the conventional fuel system mass. Limitations and possible improvements of the proposed tool are also discussed. In summary, this thesis contributes to developing the design tool required for sizing the fuel system in conventional and hybrid-electric aircraft.

Acknowledgments

I want to thank Dr. Susan Liscouët-Hanke for her guidance and help throughout the entire time I have been carrying out my research into aircraft fuel systems; the accommodation and time she provided made a great difference in the completion of this project. I would also like to thank all my fellow Air Systems Lab student colleagues for their contributions and discussions, notably Dr. Florian Sanchez, Andrew Jayaraj, and Vijesh Mohan. I also want to thank my family, who encouraged and supported me throughout the last few years of these studies.

I thank God for the strength to see this project through to completion.

Table of Contents

LIST OF FIGURES.....	VII
LIST OF TABLES.....	IX
LIST OF ACRONYMS	XI
LIST OF SYMBOLS	XIII
1 INTRODUCTION.....	1
1.1 Background and Motivation	2
1.1.1 Aircraft Fuel Systems.....	3
1.1.2 Aircraft Propulsion and the Fuel System	4
1.2 Scope and Objectives of this Thesis.....	5
1.3 Organization of this Thesis	6
2 STATE OF THE ART FUEL SYSTEM WEIGHT ESTIMATION METHODS.....	7
2.1 Empirical Fuel System Weight Estimation Methods.....	8
2.2 Architecture-based Estimation Techniques.....	11
2.3 Summary / Gap Analysis.....	12
3 IMPROVED EMPIRICAL MODEL FOR COMMUTER AND REGIONAL AIRCRAFT FUEL SYSTEM WEIGHT PREDICTIONS	13
4 ARCHITECTURE-BASED WEIGHT ESTIMATION MODEL	19
4.1 Methodology Overview	19
4.2 Fuel Feed Subsystem	22
4.2.1 Fuel Feed Pumps Weight Estimation	24
4.2.2 Fuel Line Weight Estimation	26
4.2.3 Fuel Shut-off Valve Weight Estimation	30
4.3 Fuel Transfer Subsystem	31
4.3.1 Transfer fuel pumps	32
4.3.2 Transfer lines and valves	34
4.4 Fuel Quantity & Indicating Subsystem	36
4.5 Fuel Tank Venting Subsystem.....	39
4.5.1 Surge Tank and Vent Scoop Location.....	40
4.5.2 Vent Ducts.....	41
4.6 Validation of the Proposed Method and Ancillary Components Weight Factor Definition	43
4.7 ASSET Tool Implementation in MS Excel	44
5 VALIDATION AND APPLICATION TO HYBRID-ELECTRIC CASE STUDIES	51
5.1 ASSET Validation for Conventional Aircraft Fuel Systems	51

5.2	Case Study 1: Dornier 228	52
5.2.1	Conventional DO228 Fuel System.....	52
5.2.2	Hybrid-Electric Configurations 1 & 2.....	55
5.3	Case Study 2: ATR 42	59
5.3.1	Conventional ATR 42 Fuel System.....	59
5.3.2	Hybrid-Electric Configurations 1 & 2.....	62
6	CONCLUSIONS AND FUTURE WORK.....	67
6.1	Summary and contributions of this thesis.....	67
6.2	Limitations of the Implemented Methodology	68
6.3	Future Work	69
7	REFERENCES.....	71
	APPENDIX A ASSET FUEL SYSTEM WEIGHT ESTIMATION CONVENTIONS, ALGORITHM LOGIC, AND EQUATIONS.....	77
A.1	FUEL TANK GEOMETRY	77
A.2	ASSET EQUATIONS AND LOGIC	81
A.3	FUEL LINE & VENT DUCT WALL THICKNESS AND WEIGHT PER UNIT LENGTH.....	82
	APPENDIX B LIST OF TYPE CERTIFICATE DATASHEETS	84
	APPENDIX C AIRCRAFT FUEL SYSTEM SCHEMATICS.....	87
C.1	FEED AND TRANSFER SUBSYSTEM SCHEMATICS.....	87
C.2	FUEL QUANTITY & INDICATING SCHEMATICS	96
C.3	FUEL TANK VENTING SCHEMATICS.....	98
	APPENDIX D EMPIRICAL EQUATIONS FOR FUEL SYSTEM WEIGHT ESTIMATION.....	101

List of Figures

Figure 1: Hybrid-electric concept aircraft	1
Figure 2: Fuel system comparison between Cessna 100-series and Boeing 747-100	4
Figure 3: Comparison of conventional and hybrid-electric propulsion architectures	5
Figure 4: Fuel system logic tree from Liscouët-Hanke [32]	11
Figure 5: Fuel system weight as a function of maximum fuel capacity	13
Figure 6: Comparison of ASSET-L01, Roskam, and NASA FLOPS models	17
Figure 7: Architecture-based weight estimation process for fuel systems	21
Figure 8: CL605 fuel system with auxiliary fuel tanks	22
Figure 9: Common circuit arrangements for engine feed subsystems	25
Figure 10: Fuel line length estimation	27
Figure 11: Fuel line OD relationship to engine thrust or power	28
Figure 12: Fuel line OD and rated pump fuel flow	29
Figure 13: Engine feed line OD envelope as a function of engine fuel flow at take-off	30
Figure 14: Ejector pump weight as a function of induced flow	33
Figure 15: OD size for different fuel transfer subsystem lines	34
Figure 16: Capacitance-type fuel probe weight as a function of probe length	36
Figure 17: Survey of number of wing tank probes and aircraft wing span	37
Figure 18: Relationship showing number of wing tank FQI probes against tank span	38
Figure 19: Assumptions for vent line geometry definitions	40
Figure 20: Trend of vent duct OD as a function of max fuel capacity	42
Figure 21: Fokker F27 and ATR42 estimated fuel system weight breakdown	44
Figure 22: ASSET inputs page	46
Figure 23: ASSET Aircraft Geometry view	47
Figure 24: ASSET Engine Feed subsystem view	48

Figure 25: ASSET Fuel Transfer subsystem view	48
Figure 26: ASSET FQIS view	49
Figure 27: ASSET Vent subsystem view	49
Figure 28: ASSET Dashboard and weight estimation outputs	50
Figure 29: Conventional propulsion DO228-100 fuel system	52
Figure 30: DO228-100 aircraft geometry	53
Figure 31: DO228-100 hybrid-electric configuration HE01	56
Figure 32: DO228-100 hybrid-electric configuration HE02	57
Figure 33: ATR 42/72 fuel system schematic	59
Figure 34: ATR42 aircraft geometry	60
Figure 35: ATR42 hybrid-electric configuration HE01	63
Figure 36: ATR42 hybrid-electric configuration HE02	64
Figure 37: Estimating fuel tank boundaries (right-side) from aircraft geometry	78

List of Tables

Table 1: Preliminary design parameters at the aircraft level	7
Table 2: Estimated fuel system weights for light aircraft from Roskam.....	9
Table 3: Estimated fuel system weights for commuter, regional, and commercial aircraft	10
Table 4: Sample of light, commuter, regional, and narrow-body aircraft	14
Table 5: Summary of variables used in ASSET linear regression modeling.....	16
Table 6: Overview of the validation of the improved empirical fuel system weight estimation model	16
Table 7: Linear regression model ASSET-L01 constants.....	17
Table 8: Electrical fuel pump data for various aircraft applications	24
Table 9: Lookup table for fuel valve weight estimation	31
Table 10: Rated flows and weights for commercial boost and transfer pumps.....	33
Table 11: ASSET tool individual scavenge pump weights	34
Table 12: Range of weights for various FQIS components	39
Table 13: Assumed weight & quantities of vent subsystem components.....	41
Table 14: Fuel subsystem weight estimation for commuter/regional aircraft.....	43
Table 15: Torenbeek, NASA FLOPS, and ASSET FS Weight Estimations for commercial aircraft.....	51
Table 16: DO228-100 conventional aircraft fuel system and geometry parameters	52
Table 17: ASSET estimation weight breakdown for the DO228-100 fuel system.....	54
Table 18: Comparison of FS weight estimation methods for conventional DO228-100	54
Table 19: ASSET fuel system analysis for the DO228 configurations.....	58
Table 20: Comparing conventional and hybrid-electric DO228 fuel system weight predictions	58
Table 21: ATR 42-400 conventional aircraft fuel system and geometry parameters	60
Table 22: ASSET estimation weight breakdown for the ATR 42 fuel system.....	61
Table 23: Comparison of FS weight estimation methods for conventional ATR42-400.....	61
Table 24: Fuel system weight breakdown for conventional and HE ATR42 configurations	65

Table 25: Comparing conventional and hybrid-electric ATR42 fuel system weights	65
Table 26: ASSET aircraft and fuel tank geometry parameters.....	78
Table 27: ASSET fuel system calculated parameters	81
Table 28: Aircraft Tubing Wall Thickness from AS18802	82
Table 29: Aircraft Tubing W/L parameter for fuel lines and vent ducts.....	83

List of Acronyms

APU	Auxiliary Power Unit
ASSET	Aircraft Systems Sizing Estimation Tool
ATR	Avion de Transport Régional (Aerei da Transporto Regionale)
BAe	British Aerospace
CAWM	Canadian Airworthiness Manual
CRJ	Canadair Regional Jet
CTA	Commercial Transport Aircraft
DHC	De Havilland Canada
EDP	Engine-driven pump
FAR	Federal Aviation Regulations
FLOPS	Flight Optimization System
FQI	Fuel Quantity & Indicating
FQIS	Fuel Quantity & Indicating Subsystem
FS-Lxx	ASSET Fuel System Linear model, xx representing the model/iteration number
GA	General Aviation
GD	General Dynamics
MDAO	Multi-disciplinary Design Analysis and Optimization
MLW	Maximum Landing Weight (W_{MLW} , lb)
MOWE	Maximum Operating Weight Empty (W_{OWE} , lb)
MPLW	Maximum Payload Weight (W_{PL} , lb)
MTOW	Maximum Take-Off Weight (W_{TO} , lb)
MWE	Maximum Weight Empty (W_E , lb)
NACA	National Advisory Committee for Aeronautics
NASA	National Aeronautics and Space Administration
NM	Nautical mile
OD	Outer diameter (in)
PAX	Passengers
PPA	Piston-propeller aircraft

RTX	Raytheon Technologies Corporation
SAF	Sustainable aviation fuels
SOV	Shut-off Valve
SUGAR	Subsonic Ultra Green Aircraft Research
TO	Take-Off
USAF	United States Air Force
USG	U.S Gallons
UTAP	United Technologies Advanced Projects
UTC	United Technologies (now Raytheon Technologies Corporation)
XFR	Transfer

List of symbols

A	Aspect ratio
APU	ASSET boolean; 1 = aircraft has an APU
$B_{x\ aft}$	ASSET parameter defining the chordwise location of the aft spar as a percent of the wing chord
$B_{x\ fwd}$	ASSET parameter defining the chordwise location of the front spar as a percent of the wing chord
$B_{y\ wt}$	ASSET parameter defining the spanwise end of the fuel tanks as a percent of the total wing span
C_L	Max lift coefficient
CWT	ASSET boolean; 1 = aircraft has a center wing tank or center tank
$FMXTOT$	FLOPS Mission fuel weight (same as W_F , lb)
$FNENG$	FLOPS Number of engines
$FS01, FS02 \dots$	ASSET fuselage geometry definition points
int	Fraction of fuel tanks that are integral (ex. Wet wing)
K_{fsp}	Fuel density
M_{jp}	ASSET boolean variable; 1 = aircraft engines have motive flow output
N_e	Number of engines
N_t	Number of fuel tanks
OD	Outer diameter (in)
S	Wing area (ft ²)
T_{TO}	Take-off thrust (lbf)
W_{aux}	Olives weight estimation for auxiliary fuel components (lb)
W_E	Maximum weight empty (lb)

\dot{m}_{Feng}	Engine fuel flow at take-off (lb/h)
W_j	ASSET ejector pump weight estimate (lb)
W_{lines}	Olives weight estimation for fuel lines and vent ducts (lb)
W_{MTOW}	Maximum take-off weight (lb)
W_{OWE}	Maximum operating weight empty (lb)
W_{PL}	Maximum payload weight (lb)
W_F	Mission fuel weight (lb)
W_{FS}	Fuel system weight (lb)
$W_{fuel\ management}$	Olives weight estimation for fuel management electronics (lb)
$W_{fuel\ sys}$	Olives fuel system weight (lb)
W_{FSYS}	FLOPS Fuel system weight (lb)
W_{pumps}	Olives weight estimation for (engine-driven and airframe) fuel pumps (lb)
$WS01, WS02 \dots$	ASSET wing geometry definition points; LE indicates 'leading edge', TE indicates 'trailing edge'
$W_{sealant}$	Olives weight estimation for fuel tank sealer material (lb)
W_{valves}	Olives weight estimation for fuel system valves (lb)
V_{MAX}	FLOPS maximum operating speed (Mach)

1 Introduction

The turn into the 21st century has seen an increasing emphasis on becoming more conscious of climate change across all industries. After the road transportation industry, aviation is the second largest producer of global greenhouse gas emissions, consuming about 13% of fossil fuels used for transportation [1]. Thus, at the 66th IATA AGM, member airlines agreed to set ambitious goals to improve fuel efficiency, cap net aviation CO₂ emissions from 2020, and reduce these emissions to 50% of the 2005 levels before the year 2050 [2].



(a) Boeing SUGAR Volt [3], a 150 PAX commercial transport concept with a truce-braced high-wing design.



(b) Airbus E-Fan X [4] is a 70 PAX regional transport based on the Bae-146 airframe.



(c) The NASA PEGASUS [5] concept is a 40-50 PAX aircraft based on the ATR42 regional transport.



(d) UTC Project 804 [6], [7] is a demonstrator platform using a DHC8-300 regional aircraft for hybrid-electric technologies.



(e) The VoltAero Cassio [8] is a 4-10 PAX prototype hybrid-electric aircraft in the commuter category. It is based on the Cessna 337 airframe and currently undergoing flight testing.

Figure 1: Hybrid-electric concept aircraft

Accomplishing this is not easy since commercial aviation is heavily dependent on fossil fuels, and the technology to sustainably power air transport has not reached a sufficiently mature level to displace current propulsion technologies. Several options are being explored to enable this transition, including using Sustainable Aviation Fuels (SAF) with existing engines and developing hybrid-electric and hydrogen-powered propulsion technologies. Hybrid-electric powertrains, in particular, show promise in the ongoing projects illustrated in Figure 1. Industry investment and academia continue to provide significant backing to these concepts, but their evaluation can become challenging using traditional techniques. Several new processes have been developed by Cinar [9], de Vries [10], and Zamboni [11], concentrating on these various designs.

Most of these projects explored in [12]–[17] fit within the commuter/regional or short-haul category, showing performance and economic benefits with hybrid propulsion architectures. However, hybridization does bring about changes to other aspects of the aircraft, notably to the fuel system, which no longer becomes the most significant energy storage system supplying the propulsion units. The Air Systems Lab at Concordia University aims to implement some of these methods into tools for sizing, analyzing, optimizing various concepts, and performing trade studies. This assessment involves estimating the aircraft's performance and weight as a whole and of individual systems. As part of the Lab's goals, this thesis aims to develop a methodology to estimate the fuel system weight from a system architecture point of view that applies to both conventional and non-conventional (specifically, hybrid-electric) aircraft. In hybrid-electric applications, both the fuel and electrical energy storage systems work together, but the nature and complexity of each are significant enough that they can be treated individually. The methodology also aims to integrate aspects of the regulatory requirements driving the design, which are well understood and have been followed for many years on conventional aircraft but are still in development for electric energy storage and propulsion units.

1.1 Background and Motivation

Raymer [18] provides an overview of the conceptual design process and its context in the overall aircraft design. It begins with the definition of requirements, an initial layout, and a first guess or estimate of the aircraft's overall size, weight, and performance. The process then iterates to explore different configurations and perform trade studies on the design and requirements to establish a 'well-balanced' solution that is economically viable and meets the requirements.

A vital element of this process is aircraft sizing, which includes estimating the weight. Torenbeek [19] and Roskam [20] provide guidance on the design process and a series of tools and guidelines for estimating the weight of aircraft systems. These approaches estimate the weight of systems based on two methods: The first estimates a system's weight as a percentage of the flight design take-off weight using historical aircraft data and similarity. The second method uses equations derived from statistical aircraft data and aircraft-level parameters. The sizing process by De Vries [10] highlights the modification to traditional methods for use on hybrid-electric aircraft because the powertrain configuration and weight are

significantly different from conventional aircraft. For example, the aircraft fuel system weight is part of the fixed equipment and thus part of the Maximum Operating Weight Empty (MOWE); it is estimated based on historical conventional aircraft data or empirical equations. These estimates incorporate assumptions about the architecture without details of the technology or component-level characteristics. Hence, the motivation for developing a physics-based model estimates the system weight.

1.1.1 Aircraft Fuel Systems

Aircraft fuel systems safely store and supply fuel to the propulsion engines under all conditions and aircraft attitudes within the operating envelope. General Aviation (GA) aircraft typically feature fuel systems in their simplest form to accomplish these primary functions in the least complicated manner. Figure 2 compares the fuel system architecture of a 100-series Cessna light aircraft with the Boeing 747, a large multi-engine airliner, highlighting the scale and complexity of the fuel system compiled from various manuals and other literature [21]–[24].

Fuel is stored in the main fuel tanks that supply the engines and are typically located within the wing box cavity but can also be placed in other locations in the aircraft fuselage. The tanks are classified into three types: 1) Integral tanks, which use the wing box structure to create a sealed compartment that holds liquid fuel, 2) Bladder tanks which are fabricated from a thick layer of rubber to create a flexible bag to hold the fuel and can be installed within the wing box or fuselage cavity, and 3) Rigid tanks made from thin-walled metal or composite material that can also be installed within a wing or the fuselage.

Fuel lines connect the main tanks to the engines, fuel pumps, valves, filters, and other fuel system components. Special lines and ducts are also used to exchange the air and flammable fuel vapors between the tank interior and the ambient atmosphere, protecting the tank's integrity from under/overpressure and igniting fumes. Fuel quantity instrumentation components are also installed in the tanks to monitor the amount of fuel onboard at all operating conditions. Some aircraft with large fuel volumes feature additional fuel measurement equipment to account for fuel properties (temperature and density) which can vary from region to region and help reduce the error in fuel quantity measurements.

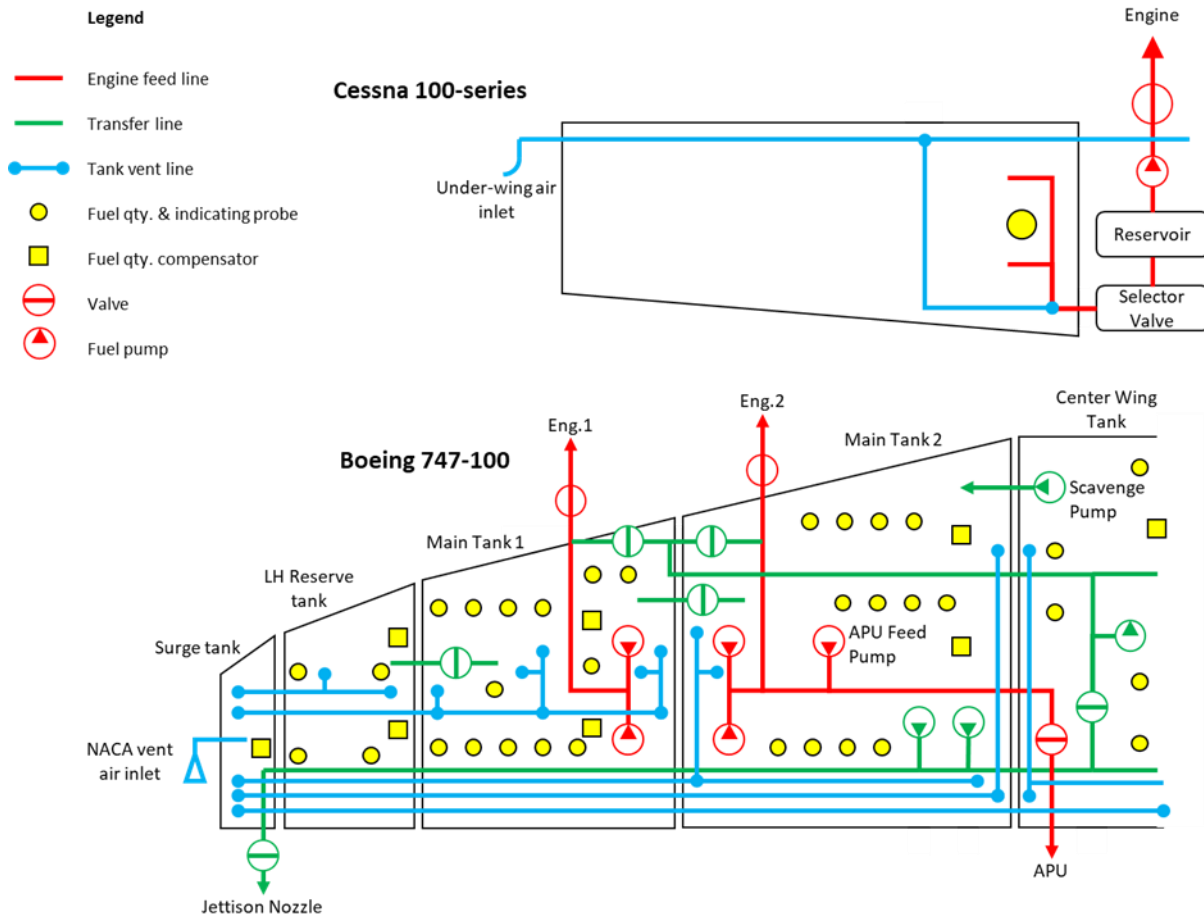


Figure 2: Fuel system comparison between Cessna 100-series and Boeing 747-100

In general, larger aircraft have more fuel storage capacity and complex systems that offer additional functionalities. These extra functions become necessary in commercial transports to accommodate operational and safety requirements such as Center of Gravity control, wing load alleviation, fuel jettison, and fuel quantity gauging. The necessity and trends in implementation in various aircraft types can be assessed by reviewing aircraft schematics to determine their interaction with the main propulsion feed circuitry.

1.1.2 Aircraft Propulsion and the Fuel System

This section highlights the relationship between aircraft fuel and propulsion systems. With conventional aircraft, the fuel system supplies an internal combustion engine that converts the stored chemical energy in the fuel into useful propulsive power, as shown in Figure 3(a). Introducing hybrid-electric propulsion technology adds batteries and power electronics to the architecture, working in concert with the fuel system to supply energy to the propulsion units through the arrangement in Figure 3(b). One benefit is

the reduction of fuel consumption because the electrical energy portion contributes to the overall propulsive power.

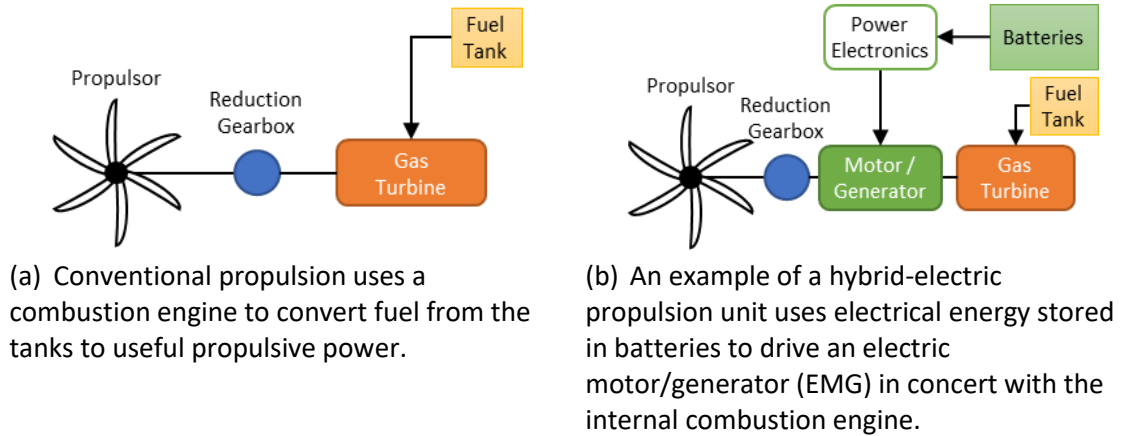


Figure 3: Comparison of conventional and hybrid-electric propulsion architectures

Hybridization logically leads to a smaller fuel mass and reduced fuel tank size. The downside is the increased aircraft mass due to the heavy and bulky battery and the power electronics mass discussed in [10], [14], [17]. The fuel system components in conventional aircraft do not make up a significant portion of the MOWE, so an increasing degree of hybridization does not necessarily result in weight savings in the fuel system. It is reasonable to assume that certain components will need to remain in the system to maintain the critical primary and secondary functions.

1.2 Scope and Objectives of this Thesis

This thesis aims to develop an architecture-based methodology to estimate the weight of an aircraft fuel system suitable for the conceptual design of novel aircraft such as those with hybrid-electric propulsion units. Conventional aircraft fuel systems are studied to identify the type and number of physical components used and establish trends in the layout of the system architecture. The focus is on commuter and regional aircraft, which are likely candidates for hybridization. The methodology is then implemented into a design tool that can be integrated into a multidisciplinary design, analysis, and optimization (MDAO) workspace. However, the scope of this thesis will be limited to fuel systems operating with conventional fossil fuels such as Jet A, Jet A-1, JP-4, etc. Alternative fuels and propulsion systems operating on energy sources such as hydrogen are not considered here because the design requirements are still being developed.

1.3 Organization of this Thesis

This thesis is organized in the following way: Chapter 2 reviews the state-of-the-art weight estimation techniques, specifically for the fuel system, and analyzes the gaps in these methods regarding their applicability to future hybrid-electric aircraft. Chapter 3 introduces an improved empirical model for conventional commuter and regional aircraft fuel systems based on production aircraft data. The findings of the validated model are also presented in this chapter. A new architecture-based weight estimation method is introduced in Chapter 4 and provides an overview of its implementation in an MS Excel workbook. Chapter 5 demonstrates the application of the methodology to two hybrid-electric propulsion case studies for a commuter Dornier 228 and a regional turboprop ATR42 aircraft. These case studies show how the amount of hybridization reduces the maximum fuel capacity, and the placement of system components affects the weight of the fuel system within the airframe. Chapter 1 summarizes the overall work and limitations of the method currently implemented and highlights potential future improvements and next steps. The appendix is organized into five subsections: Appendix A contains details on the aircraft geometrical definitions, equations, and estimation algorithms used in the ASSET estimation method. Appendix B lists the relevant Type Certificate Data Sheets and other sources of information for the aircraft studied as part of this work. Appendix C contains fuel system schematics for a wide range of aircraft spanning from light GA to commuter, regional, and large commercial transport airliners. It aims to show the layout of the four main subsystems and consolidate each aircraft's non-standard system symbols and information into one source. Appendix D summarizes the empirical equations from Roskam and NASA, the current state-of-the-art tools for estimating the fuel system weight.

2 State of the Art Fuel System Weight Estimation Methods

This chapter examines the methods of determining the fuel system weight based on Torenbeek [19] and Roskam [20]. A more recent method from the National Aeronautics and Space Administration (NASA) is the Flight Optimization System (FLOPS) which includes a weight estimation method. These tools are used in traditional conceptual design to evaluate the various concepts and trade-offs that meet the overall aircraft requirements. The preliminary sizing analysis begins from the mission specification of the aircraft and iterates through sensitivity studies to determine the key design parameters shown below. The intent is to demonstrate the overall value of the design against features that can improve safety and enhance performance while reducing weight and cost.

Table 1: Preliminary design parameters at the aircraft level

	Fuel System Weight Estimation Method	Key Variables						Model Type
		Fuel Capacity	Number of Fuel Tanks	Fuel Tank Type	Number of Engines	Fuel Type	Aircraft speed	
General Aviation Aircraft	Cessna	✓		✓		✓		Linear relationship
	USAF	✓	✓	✓	✓	✓		Multi-variable power law
	Torenbeek	✓				✓		Power law
	NASA FLOPS	✓			✓			Multi-variable power law
Commercial Transport Aircraft	General Dynamics (GD)	✓		✓		✓		Single-variable power law
	Torenbeek	✓	✓	✓	✓	✓		Multi-variable power law
	NASA FLOPS	✓			✓		✓	Multi-variable power law

Roskam outlines the process to estimate the key aircraft design weight and is broken down into three major groupings: The aircraft structure, power plant, and fixed equipment. The fuel system is considered part of the propulsion group in this process, and various methods are available to estimate its weight. Table 1 summarizes the equation characteristics and key variables used by each method from Roskam, Torenbeek, and NASA. It is clear that all these methods heavily depend on the fuel capacity but vary on other high-level aircraft parameters such as the number of fuel tanks, type of tank, number of engines, and so on. The following sections discuss the characteristics, usage, and gaps of the methods presented herein.

2.1 Empirical Fuel System Weight Estimation Methods

The methods by Torenbeek and Roskam are a series of empirical equations based on data for aircraft produced between the 1950s to the early 1990s that allow the designer to estimate the weight of various aircraft systems, including the fuel system. Roskam segregates these into two areas: Class I methods estimate the weight of a system as a percentage of the flight design take-off (or gross weight) obtained from historical data. Class II methods use statistically derived equations to estimate the weight of more detailed systems and subsystems. These equations depend strongly on the aircraft fuel mass and other aircraft-level parameters like the number of engines, the number of fuel tanks, and the construction of the fuel tanks. It assumes that the weight of critical components such as the fuel pumps, fuel lines, fuel quantity probes, and ventilation ducts scale with the mission fuel mass. Eq. (1) defines the Cessna method as a linear function of maximum fuel capacity.

$$\text{Cessna Method: } W_{fs} = \begin{cases} 0.40W_F/K_{fsp} & \text{For aircraft with internal fuel systems} \\ 0.70W_F/K_{fsp} & \text{For aircraft with external fuel systems} \end{cases} \quad (1)$$

A fuel density constant, $K_{fsp} = 6.7 \text{ lb/USG}$ takes into account the fuel properties in the weight estimation. Its value is typically 6.7 lb/USG for turbine engines running on Jet A-1 and 5.87 lb/USG for piston-powered engines running on aviation gasoline. The USAF method described by eq. (2) adds the variables N_e and N_t accounting for the number of engines and the total number of fuel tanks fitted. The additional parameter int accounts for the fraction of fuel tanks that are integral-type tanks.

$$\text{USAF } W_{fs} = 2.49 \left[\left(\frac{W_F}{K_{fsp}} \right)^{0.6} \left(\frac{1}{1+int} \right)^{0.3} N_t^{0.20} N_e^{0.13} \right]^{1.21} \quad (2)$$

Torenbeek proposed two methods depending on the type of propulsion engine used on the aircraft: Eq. (3) is specific to piston-engine aircraft and is further differentiated for single and multi-engine applications. This equation shows that the system on multi-engine aircraft is typically heavier for aircraft with similar maximum fuel capacities. However, this equation remains the same for any multi-engine aircraft, irrespective of the number of engines and type of fuel tanks fitted.

$$\text{Torenbeek Piston Propeller Aircraft (PPA) } W_{fs} = \begin{cases} 2 \left(\frac{W_F}{K_{fsp}} \right)^{0.667} & \text{For single-engine piston propeller aircraft} \\ 4.5 \left(\frac{W_F}{K_{fsp}} \right)^{0.60} & \text{For multi-engine piston propeller aircraft} \end{cases} \quad (3)$$

Eq. (4) is specific to commercial transports and differentiates between aircraft using bladder fuel tanks and integral fuel tanks. The equation for bladder tanks on commercial transports ignores any effects on the weight introduced by the number of engines and fuel tanks fitted. As a result, it is difficult to compare with its counterpart for aircraft systems with integral fuel tanks.

Torenbeek
Commercial
Transport Aircraft
(CTA)

$$W_{fs} = \begin{cases} 1.6 \left(\frac{W_F}{K_{fsp}} \right)^{0.727} & \text{For non-self-sealing bladder tanks} \\ 80(N_e + N_t - 1) + 15N_t^{0.5} \left(\frac{W_F}{K_{fsp}} \right)^{0.333} & \text{For Integral tanks} \end{cases} \quad (4)$$

The NASA Flight Optimization System (FLOPS) is a software application used to analyze new aircraft configurations in the conceptual design phase. The program executes eight modules, one of which is the weight estimation module which outputs the fuel system weight. This method has become widely used in various studies and has been adapted for non-conventional conceptual studies such as the one presented by Antcliff [5], [17]. Eq. (5) below is used by the FLOPS algorithm to estimate the fuel system weight of transport aircraft.

NASA FLOPS Fuel
System Weight for
Transport Category
Aircraft

$$WFSYS = 1.07 \times FMXTOT^{0.58} \times FNENG^{0.43} \times VMAX^{0.34} \quad (5)$$

It is a product of the functions for maximum fuel capacity, the number of engines fitted, and the maximum operating Mach number. The FLOPS methodology also has a separate equation, specifically for general aviation aircraft, which takes the same form as the one for transport aircraft but eliminates the VMAX term, as shown in eq. (6).

NASA FLOPS Fuel
System Weight
General Aviation
Aircraft

$$WFSYS = 1.07 \times FMXTOT^{0.58} \times FNENG^{0.43} \quad (6)$$

Table 2: Estimated fuel system weights for light aircraft from Roskam

Aircraft	Fuel Tank Type	N_e	N_t	Actual W_F (lb) [20]	Actual W_{FS} (lb) [20]	Estimated W_{FS} , lb			
						Cessna	USAF	Torenbeek PPA	NASA FLOPS GA
C150	Bladder	1	2	156	17	11 (-35%)	32 (+88%)	18 (+6%)	20 (+18%)
C182	Bladder	1	2	390	26	27 (+4%)	62 (+138%)	33 (+27%)	34 (+31%)
C210J	Integral	1	2	464	24	32 (+33%)	55 (+129%)	37 (+54%)	38 (+57%)
112TCA	Integral	1	2	230	17	16 (-6%)	33 (+94%)	23 (+35%)	25 (+48%)
BE50	Bladder	2	4	1380	137	94 (-31%)	159 (+16%)	119 (-13%)	95 (-30%)
BE95	Bladder	2	4	672	83	46 (-45%)	94 (+13%)	77 (-7%)	63 (-24%)
C310	Tip Tanks	2	2	612	76	42 (-45%)	88 (+16%)	73 (-4%)	60 (-22%)
C414A	Tip, Bladder	2	6	961	96	65 (-32%)	115 (+20%)	96 (0%)	77 (-19%)

Table 2 above shows the estimated fuel system weights for single and twin piston-engine light aircraft from the Roskam [20] database certified to the Normal Category regulations [25]–[27]. The Cessna, USAF,

Torenbeek PPA, and NASA FLOPS GA equations are the most appropriate since they aim to predict the fuel system weight for General Aviation aircraft certified to the Normal, Utility, Acrobatic, and Commuter category regulations [25]–[27]. The Cessna method predicts the fuel system weight for these aircraft within an error range of -45% to +33%, with the best estimates being for the C182 and 112TCA. The USAF method consistently over-predicts the system weight, and the estimation error for single-engine applications is over 80%. The other methods appear to have mixed results, with no clear pattern regarding the effects of key system and aircraft-level variables on the total fuel system weight.

Table 3 below shows the estimated system weights for multi-engine, turbine-powered aircraft, with the smaller aircraft certified to the Commuter category regulations [25]–[27], while the larger ones are certified under the Transport category regulations [28]–[30]. The two main weight estimation methods applicable to these aircraft are the Torenbeek and NASA FLOPS.

Table 3: Estimated fuel system weights for commuter, regional, and commercial aircraft

Aircraft	Fuel Tank Type	Actual W_F (lb) [20]	Actual W_{FS} (lb) [20], [31]	Estimated W_{FS} , lb	
				Torenbeek CTA (% Error)	NASA FLOPS (% Error)
C441	Integral	2446	93	391 (321%)	109 (17%)
AC690B	Bladder	2606	180	122 (-32%)	111 (-39%)
F27	Integral + Bladder	9198	390	475 (22%)	237 (-39%)
ATR42	Integral	10053	196	482 (146%)	247 (26%)
EMB110	Bladder	3062	86	137 (60%)	124 (45%)
LJ25D	Tip + Integral + Bladder	6098	179	804 ¹ (349%)	210 (18%)
LJ28	Integral + Bladder	4684	237	550 (132%)	181 (-23%)
C550	Integral	5009	189	432 (129%)	179 (-5%)
G159	Integral	10447	133	485 (265%)	251 (88%)
B727-1	Integral	48535	1143	901 (-21%)	865 (-24%)
B727-2	Integral	54284	1210	920 (-24%)	923 (-24%)
B737-2	Integral	34718	575	768 (34%)	579 (1%)
A320-2	Integral	42042	659	798 (21%)	648 (-2%)
DC10-1	Integral	146683	2040	1124 (-45%)	1630 (-20%)
DC10-3	Integral	247034	4308	1261 (-71%)	2205 (-49%)
B747-1	Integral	331675	2322	2251 (-3%)	3006 (29%)

As with the light piston-powered aircraft, the Torenbeek equations show significant variability in the predicted fuel system weight for aircraft in the commuter, regional, and business categories. The Torenbeek CTA method predictions for the F27 and AC690B set a reasonable error range between -32% to +22%, with other commuter and regional aircraft (C441, ATR42, EMB110, and G159) very much outside this range. In contrast, more aircraft (C441, AC690B, F27, ATR42, EMB110 LJ25D, LJ28, and C550) fall within the error range of -39% to +45% when the NASA FLOPS method is used. But the best correlations

¹ LJ25D system weight estimated by treating tip, fuselage bladder, and integral wing tanks individually.

for the NASA FLOPS method are with the B737 and A320, which fall within $\pm 2\%$ of the actual system weight. It may be possible to conclude that the NASA FLOPS method is slightly better than the Torenbeek for commuter/regional aircraft. Still, it is difficult to confirm this, given the data available.

2.2 Architecture-based Estimation Techniques

Architecture-based techniques use the number of components and physical characteristics to estimate the weight and performance of aircraft systems. One such approach proposed in 2008 by Liscouët-Hanke [32] estimates the fuel system weight for commercial (Airbus) aircraft that considers key elements such as the fuel pumps, valves, and fuel system-related electronics. The algorithm derives the system mass and power requirements, as illustrated in Figure 4 below, which are then used by the aircraft power system sizing methodology.

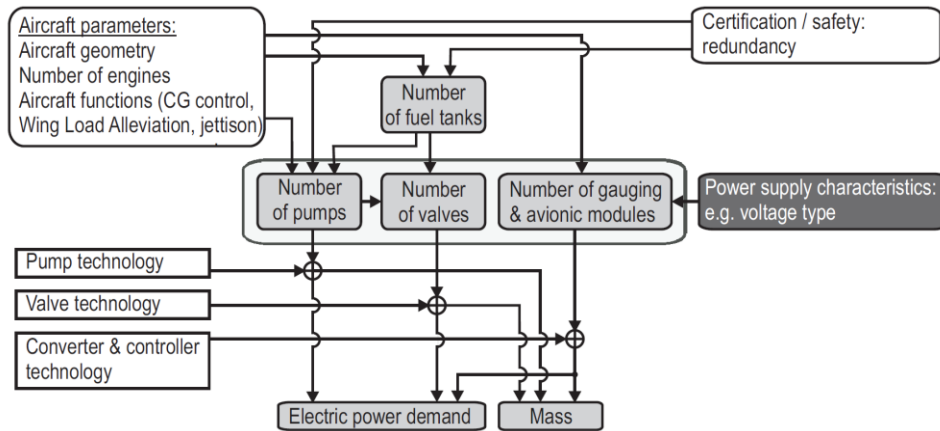


Figure 4: Fuel system logic tree from Liscouët-Hanke [32]

More recently, Olives [33] developed a tool to estimate the weight of fuel and hydraulic systems for large turbofan-powered commercial airliners. This method estimates the system weight by considering the components that make up the system as expressed by eq. (7) below.

$$W_{fuel\ sys} = W_{lines} + W_{pumps} + W_{valves} + W_{sealant} + W_{fuel\ management} + W_{aux} \quad (7)$$

The system schematics are generated using basic rules derived from studying fuel system diagrams that reflect commonly used system layouts. The method also uses manufacturer component specification data to estimate the sizing of the fuel pumps, valves, fuel lines/hoses, and tank sealer material. It accounts for features such as vent surge tanks, refuel/defuel ducts, jettison nozzles, and auxiliary/trim fuel tanks. However, elements like the fuel management system and vent ducts are excluded due to a lack of information. These methods form a starting point for the detailed development of the architecture-based weight estimation method outlined in Chapter 4. This thesis addresses the gap for an architecture-based

method specifically for the commuter/regional aircraft market with conventional and hybrid-electric systems.

2.3 Summary / Gap Analysis

The previous sections review the existing methods available to designers in the aircraft conceptual stage to estimate the fuel system weight. They are based on knowledge of production aircraft since the 1950s and capture the evolution of technologies and design practices over the years. However, the review highlights two observations: The first is the strong relationship to the maximum fuel capacity of the aircraft. Aircraft-level and system-specific variables are considered in the USAF, Torenbeek, and NASA methods but appear to give mixed results with trends that are difficult to identify. The second observation is the uncertainty regarding which of these methods is most applicable to commuter or regional aircraft. The previous section discusses the error margin of the Torenbeek and NASA FLOPS predictions. It shows that the Torenbeek method can predict the fuel system weight within $\pm 30\%$ for two aircraft (AC690B and F27), which are twin-engined turboprops of different sizes and use a mix of integral and bladder fuel tanks. On the other hand, the NASA FLOPS offers a very good correlation for narrowbody airliners. Its error margin is slightly better than the Torenbeek method but is still rather large (-39% to +45%) for commuter and regional aircraft.

Applications with hybrid-electric propulsion systems are expected to be introduced in short-haul commuter and regional categories, and it is expected that hybridization will reduce the maximum fuel capacity but retain most of the components that are already present in conventional fuel systems. Therefore, conceptual designers would benefit from a methodology that can more accurately estimate the fuel system weight in conventional and hybrid-electric aircraft with these considerations in mind. The previously mentioned architecture-based tools by Liscouët-Hanke [32] and Olives [33] can address this gap in the existing state-of-the-art methods. However, these tools focus on fuel systems for large commercial aircraft certified under the Transport category regulations [27]–[29]; the architecture-based models are further discussed in Chapter 4. Commuter and regional aircraft between the Transport category and the Commuter category [25]–[27], and the fuel systems have some differences that need to be considered by the sizing tools. Properly configured tools can then be automated in an MDAO environment for comparing and optimizing different design concepts and trade studies.

3 Improved Empirical Model for Commuter and Regional Aircraft Fuel System Weight Predictions

The previous section examines the state-of-the-art methods designers use to estimate the fuel system weight for conventional aircraft. However, the validation of these methods with data for various short-haul aircraft demonstrates shortcomings, which can negatively affect the estimation of the system weight in aircraft with hybrid-electric propulsion units, where the fuel system capacity is reduced. This section introduces two methods that aim to address the gaps in these existing methods and establish an improved reference for new architecture-based methods. The first method uses historical aircraft data and linear regression analysis to estimate the fuel system weight of conventional aircraft. The second method estimates the weight based on the number of components in a typical aircraft fuel system by analyzing its architecture, the aircraft certification category, regulatory requirements, component technology, and high-level aircraft parameters.

The linear regression model presented here aims to predict the fuel system weight based on historical aircraft data from the Roskam [20] database. Specifically, it focuses on predicting commuter and regional aircraft. Figure 5 shows the non-linear relationship between the fuel system weight and aircraft maximum fuel capacity for light aircraft up to large transport airliners.

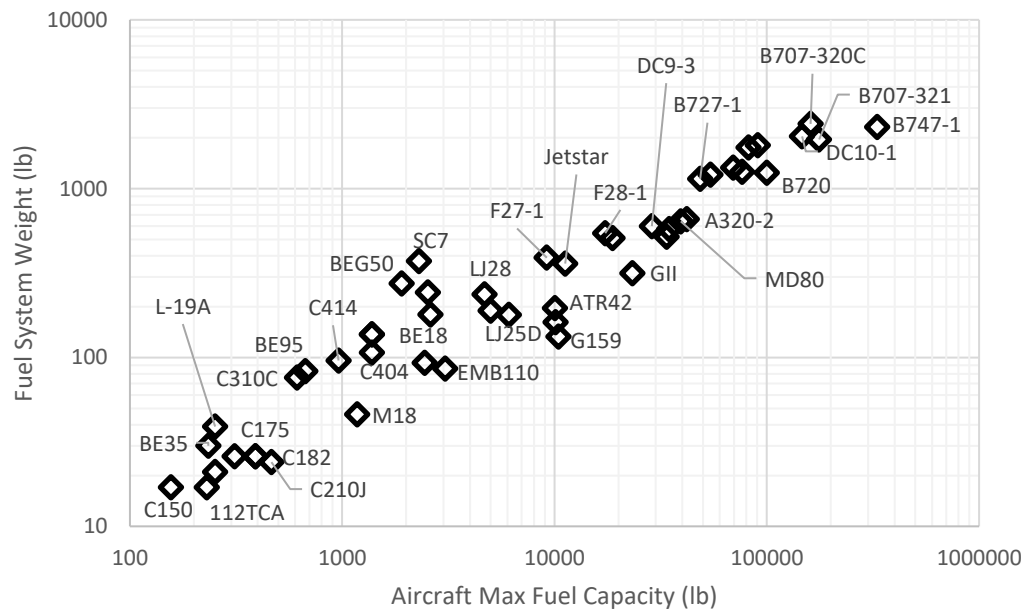


Figure 5: Fuel system weight as a function of maximum fuel capacity

Table 4 shows the data for several commuter-type aircraft and some narrow-body airliners considered at the upper end of the regional aircraft classification. Typically, commuter aircraft are multi-engine, piston, or turbine propeller-driven and have a maximum of 19-passenger (excluding pilot seats) capacity and a

certificated MTOW of less than 19000 lb. Regional and narrow-body airliners are certified under the Transport category [28]–[30] regulations and include aircraft such as the turboprop-powered ATR4, G159, and most business jets, including the LJ28, C550, and GII.

Table 4: Sample of light, commuter, regional, and narrow-body aircraft

Aircraft	MTOW (lb)	Max Fuel Capacity (lb)	Actual W_{FS} (lb) [20], [31]	No. Engines ²	Max Seats	Cert Cat.	TO WF per eng. (pph)	No. Tanks
C414A ^{3,4}	6500	1250	96	2 PP	7	Part 23	280 ⁵	2 tip tanks, 4 aux bladder cells, 2 locker bladder cells
C310C ^{3,4}	4830	612	76	2 PP	5	Part 23	210 ⁵	2 tip tanks
LJ28 ^{3,4}	15000	4684	237	2 TF	10	Part 25	2900	2 wet wing, 1 bladder cell
C550 ^{3,4}	13300	5009	189	2 TF	13	Part 25	1400	2 wet wing
GII ^{3,4}	64800	23400	316	2 TF	19	Part 25	6850	2 wet wing
ATR42 ^{3,4}	34770	10100	196	2 TP	60	Part 25	1100	2 wet wing
A320 ^{3,4}	162000	42100	659	2 TF	195	Part 25	9500	3 integral
B727-1 ^{3,4}	160000	51460	1143	3 TF	130	Part 25	8200	3 integral
B727-2 ^{3,4}	172000	54200	1210	3 TF	189	Part 25	9800	3 integral
G159 ³	35100	10447	133	2 TP	23	Part 25	1150	2 wet wing
AC690B ³	10325	2606	180	2 TP	9	Part 23	500	22 bladder cells
SC7 ³	12500	1400	373	2 TP	20	Part 23	400	4 bladder cells
LJ25D ³	15000	6098	179	2 TF	12	Part 25	2900	2 tip, 2 wet wing, 1 bladder cell
EMB110 ³	12500	3100	86	2 TP	23	Part 23	750	4 bladder cells
F27 ³	37500	9100	390	2 TP	48	Part 25	1000	2 wet wing, 2 bladder cells, 2 discrete

As discussed in the previous chapter, the strong dependency on maximum fuel capacity makes the contributions of other aircraft-level and system-specific parameters difficult to assess. Variables like the number of fuel tanks, the number of engines, and the type of tank are key considerations because they are driven by certification requirements (subsections 953 for fuel system independence, 991 for the number of fuel pumps, and 975 for the fuel tank vents and expansion spaces). The type of engine (piston-propeller, turboprop, or turbofan) and fuel characteristics (aviation gasoline compared to jet fuel) also contribute to the design and weight of the fuel system. The fuel system's tank construction also adds weight if the tanks are made from flexible rubber bladders instead of being integral to the aircraft's structure. These tanks require mounting brackets and related hardware to secure them to the aircraft structure.

Extracting meaningful data for the modeling process presents several problems, the main one being the inconsistency of information available in schematics, type certificate data sheets, and manuals for the aircraft in Table 4. For example, quantifying the added weight from bladder tanks, which are heavier than integral tanks, is difficult to assess and is expected to introduce variability and error in the model. The

² Engine types are PP: piston-propeller, TP: Turbopropeller, TF: Turbofan

³ Aircraft considered as part of the ASSET-FS-L00 model iterations (highlighted in green)

⁴ Aircraft considered as part of the ASSET-FS-L01 model, specifically for integral fuel tank systems

⁵ Fuel flow at take-off estimated based on 'cruise' power (70-75% throttle setting).

AC690B is an example of a small twin-turboprop aircraft used as a utility or business aircraft certified to the Part 23 regulations. Its fuel system comprises 22 interconnected bladder cells that feed a central sump inside the fuselage. According to Roskam [20], eq. (4) in the previous chapter applies to the AC690B fuel system weight. This method predicts the system weight to be 122 lb, approximately 32% less than the actual weight in the Roskam database. Alternatively, if the fuel tanks are treated as two integral wing tanks, the equation will yield a system weight of 361 lb, double the actual system weight. Similarly, the USAF method, which considers non-integral fuel tanks, can overestimate the system weight by 147% if the tanks are treated individually. If the tanks are treated as two individual tanks, the error reduces to 38%. Treating the fuel tanks as a single tank, as described in the maintenance and aircraft flight manual, the error reduces to 50% and 17% for Torenbeek and the USAF methods, respectively. This example demonstrates the ambiguity in applying the state-of-the-art methods and how this variable can introduce uncertainty and error.

Similarities exist for the integral wing tanks in regional and narrow-body airliners, such as the ATR42, ATR72, B727, and A320. Anti-surge baffles are usually installed at approximately mid-span of each wing, dividing each wing tank into two compartments, sometimes termed ‘inner’ and ‘outer’ tanks, to prevent excessive shifts in the center of gravity due to fuel sloshing at different aircraft attitudes. The state-of-the-art methods do not provide a guideline on whether these compartments should be treated separately or as a part of a single tank. For this work, they are treated as part of a single main tank; it is an assumption that seems reasonable based on the data in most type certificate data sheets and aircraft manuals.

Since the raw data against an aircraft-level parameter (max fuel capacity in this case) is non-linear, a new model will need to employ some means of making the weight contributions from these aircraft-level variables more important. A linear approximation can be obtained by applying a logarithmic transform on the fuel system weight (W_{FS}) and the max fuel capacity (W_F) for the aircraft in Table 4. The model is created using the MS Excel regression tool from the data analysis toolpak and takes the form expressed in eq. (8), where the variables N_t and N_e are the number of fuel tanks and engines, respectively, with other variables added to the model as necessary to improve its fit to the data.

$$\log W_{FS} = C_1 \log W_F + C_2 N_t + C_3 N_e + C_4 \dot{W}_{Fe} + C_5(int) + C_6 \quad (8)$$

Various iterations of the linear regression model were created from the data in Table 4, establishing the relationship between $\log(W_F)$, $\log(W_{FS})$, and additional variables, including the number of engines (N_e), the number of fuel tanks (N_t), the fuel flow per engine (\dot{W}_{Feng}), and so on.

Table 5: Summary of variables used in ASSET linear regression modeling

Model	$\log(W_F)$	N_e	N_t	\dot{W}_{Fe}	int^6
ASSET-L00 ⁷	✓				
ASSET-L00 (b)	✓	✓	✓	✓	
ASSET-L00 (c)	✓	✓	✓	✓	✓
ASSET-L01 ⁸	✓	✓	✓		

The ASSET-L00 model considers the relationship of $\log(W_{FS})$ to the $\log(W_F)$ but is not a suitable model since it is based on the maximum fuel capacity. The ASSET-L00 (b) and (c) models introduce the number of engines, number of tanks, fuel flow at take-off, and fraction of tanks that are integral to the structure.

Table 6: Overview of the validation of the improved empirical fuel system weight estimation model

Aircraft	Actual FS Wt.	ASSET-FS-L00		ASSET-FS-L00 (b)		ASSET-FS-L00 (c)		ASSET-FS-L01	
	(lb)	(lb)	(% Error)	(lb)	(% Error)	(lb)	(% Error)	(lb)	(% Error)
Aircraft with integral-type main fuel tanks or a combination of integral/bladder tanks									
C414 ⁹	96	96	0%	65	-32%	72	-25%	107	+12%
G159	133	294	121%	213	+60%	178	+34%	259	+95%
ATR42	196	289	+47%	210	+7%	175	-11%	254	+30%
Aircraft with bladder-type fuel tanks									
SC7 ⁹	373	145	-61%	103	-72%	193	-48%	143	-62%
AC690B ⁹	180	154	-15%	170	-6%	252	+40%	133 ¹⁰	-26%
EMB110 ⁹	86	166	+93%	171 ¹⁰	+98%	119	+38%	144	+67%
F27 ⁹	390	277	-29%	153	-61%	272	-30%	278	-29%

Table 6 shows the performance of each of these models for key commuter and regional aircraft based on the variables from Table 5 above. The initial ASSET-FS-L00 establishes a relationship as a function of max fuel capacity only but predicts extremely large errors for most aircraft in the above table. Iteration (b) gives acceptable errors for the ATR42 and AC690B at the expense of the other aircraft, which fall outside the $\pm 30\%$ range. Iteration (c) improves the error margin for most aircraft, but the magnitudes remain over $\pm 30\%$ in most cases. This error variability may be due to the type of tank used by some of the aircraft in this validation, which in the case of the SC7, AC690B, and EMB110, is an all-bladder-type construction.

In contrast, the F27 combines bladder-integral tanks, and the remaining three aircraft have integral tanks. However, because this information was unavailable for the G159 and the F27, and the effect of the bladder-type tanks could not be assessed properly, the ASSET-FS-L01 model was derived by considering only aircraft known to have integral fuel tanks. The resulting error margin reduces to within $\pm 30\%$ for the

⁶ int is a variable representing the fraction of total fuel tanks that are integral to the aircraft structure, typically in the wing box.

⁷ ASSET is an abbreviation for Aircraft System Sizing Estimation Tool; the L00 and L01 indicate major iterations of the linear regression estimation model, and (b) and (c) represent minor variations of a model.

⁸ The ASSET-L01 model is based on the reduced sample size of the aircraft highlighted in green in Table 4.

⁹ Bladder fuel cells make up a portion of the aircraft fuel tanks.

¹⁰ The interconnected bladder tanks are treated as a single tank per wing instead of individually.

ATR42 and even the F27. These findings relative to the other state-of-the-art estimation tools are presented in Figure 6 below.

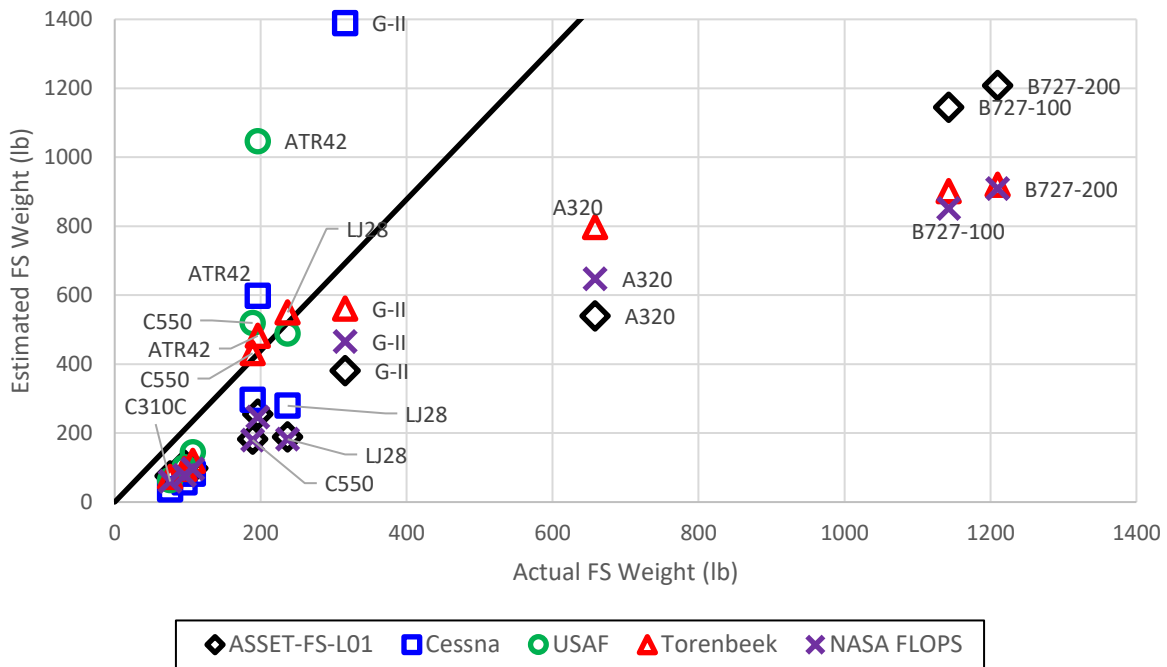


Figure 6: Comparison of ASSET-L01, Roskam, and NASA FLOPS models

Table 7: Linear regression model ASSET-L01 constants

Model Constant	ASSET-L00	ASSET-L00 (b)	ASSET-L00 (c)	ASSET-L01
C_1 for $\log(W_F)$	0.468	0.069	0.376	0.480
C_2 for N_t	0.000	-0.060	-0.190	0.028
C_3 for N_3	0.000	0.464	0.181	0.297
C_4 for W_{Fe}	0.000	0.324	-0.430	0.000
C_5 for int	0.000	0.000	0.150	0.000
C_6	0.588	0.251	0.732	-0.164

The new, improved empirical model reduces the errors in the fuel system weight predictions for commuter and regional aircraft compared to the state-of-the-art weight equations but is specific for regional and commuter-type aircraft with integral fuel tanks with maximum capacities between 700 and 30000 lb. The narrowing of the error range to within $\pm 30\%$ results from focusing on the ATR42 and F27 aircraft and excluding others considered by the methods presented by Roskam and Torenbeek. However, like the existing methods, this new model cannot be universally applied to all aircraft in the commuter/regional category because it does not account for certain architectures. Future aircraft conceptual designs will likely employ integral wing tanks in the fuel system since they are much lighter than bladder tanks. Still, the latter should not be ruled out completely, even in hybrid-electric applications.

4 Architecture-based Weight Estimation Model

The previous section presented an improved empirical method of estimating the weight of aircraft fuel systems using a linear model focusing on published data for typical commuter, regional, and some narrow-body aircraft. It shows an improvement over the existing estimation methods; however, the derived linear model does not consider the system architecture details as an input. Thus, it is still prone to show significant errors for certain aircraft and does not allow investigation of new aircraft architectures featuring hybrid-electric propulsion. Surveys of various aircraft fuel systems across GA, commuter, regional, business, and commercial transport aircraft show the variety of configurations even for similarly-sized aircraft, which may not necessarily be captured in the predictions of empirical models. Architecture-based models can estimate the number of components and the system's overall weight by considering key aircraft-level and system-specific parameters.

This chapter will first present the methodology overview and the detailed estimation models developed for each subsystem weight. Finally, the implementation in an Excel-based tool is presented.

4.1 Methodology Overview

As mentioned in section 2.2, two architecture-based methods have been published by Liscouët-Hanke [32] and Olives [33]. However, since this work focuses on commuter and regional aircraft fuel systems, some concepts from these methods will need to be adapted since they are suited to commercial transport aircraft. For instance, this method is similar to the existing architecture-based methods because it:

- Uses aircraft geometry to define the fuel tanks and the location of system components.
- Identifies and accounts for the number of components used in typical fuel system architectures based on functional and certification/safety requirements.
- Uses component manufacturer specifications and technology levels to estimate the weight of individual components.
- Produces a system schematic (similar to Olives [33]) to estimate the length and weight of the fuel lines.

However, this new method covers additional aspects of the fuel system that are less detailed in the other two methods:

- The component weight data and technology types are specific to most conventional GA, commuter, and regional aircraft components.
- The fuel system is treated as an ensemble of four subsystems (described in detail later) present in all aircraft to facilitate the weight estimation. In contrast, Olives counts the components based on the system's functional capabilities.

- Engine fuel pumps are not treated as part of the fuel system by the methodology described in this section because it facilitates the delineation of components that belong to the airframe and engine, facilitating the weight estimation. It contrasts with Liscouët-Hanke [32] and Olives [33] since fuel pumps are considerably heavier than commercial turbofan engines.
- The new method presented in this thesis adds data relevant to the fuel quantity and tank venting subsystems based on manufacturer data sheets that were not previously available to Olives [33].

A review of various aircraft fuel system schematics across General Aviation, Commuter, Regional, Business, and Commercial Transport aircraft provided a means of comparing the major components, architecture layouts, and system capabilities and requirements. As a result of the review, it is proposed to break down the fuel system into four major subsystems; this is a major difference from Olives' method, which counts the system components by their function and availability on the aircraft.

The **Engine Feed subsystem** is the circuit that supplies fuel from the tanks to the propulsion engines and includes major components such as the fuel feed (or boost) pumps, fuel shut-off valves, and fuel lines. Integral wing tanks are considered part of the wing structure, so the weight does not count towards the feed subsystem weight. In contrast, light GA aircraft manufactured between the 1960s and 1990s typically feature rigid metal or rubber bladder-type tanks that fit inside the wing box but are not a load-bearing structure of the wing; the weight of these tanks must be considered as part of the feed subsystem. The engine-driven fuel pump is not considered in the fuel system weight estimation since its main function is to boost fuel pressure at the engine fuel inlet to prevent cavitation at the high-pressure pump in the engine fuel control.

The **Fuel Transfer subsystem** consists of the following components: transfer and scavenge pumps, cross-feed and transfer valves, and fuel lines connecting these components. Components associated with the fuel jettison and refuel/defuel capabilities of the aircraft are also grouped into this subsystem since they are interconnected to other portions of the transfer subsystem.

The **Fuel Quantity & Indicating subsystem** consists of the fuel quantity probes (also called tank units), fuel quantity management electronics, signal conditioners, fuel quantity displays, and refuel/defuel control panels.

The **Tank Venting subsystem** consists of the vent ducts and float valves that connect the ullage space in the fuel tanks to the surge tank or fuel expansion space and vent inlets that allow the fuel vapors to discharge clear of the aircraft. Most transport category aircraft also feature overpressure and flame arresting devices in the fuel venting subsystem.

Finally, a buffer parameter must be considered to account for the weight of ancillary components consisting of filters, sealing material, mounting brackets, fasteners, and wiring harnesses. The rationale for this factor is that these individual items have unknown weight but collectively can contribute to a considerable amount that contributes to the fuel system. The weight is quantized as a percentage of the weight of the other four subsystems.

The process involves estimating the number and pumps, valves, and length of fuel lines and ducts for each subsystem. The number of fuel quantity gauging probes is then estimated. These numbers are subsequently used to estimate the weight of each subsystem based on typical weight, characteristics, and the technology of the components. The process is illustrated in Figure 7, which is adapted the logic tree for the fuel system by Liscouët-Hanke [32], to show that the focus is solely on the estimation of the mass for each of the four subsystems and the electrical power demand from the aircraft power system for these components is not strictly considered. The rationale is that the estimation for each subsystem contains sufficient detail to determine the number of components and weight based on the inputs.

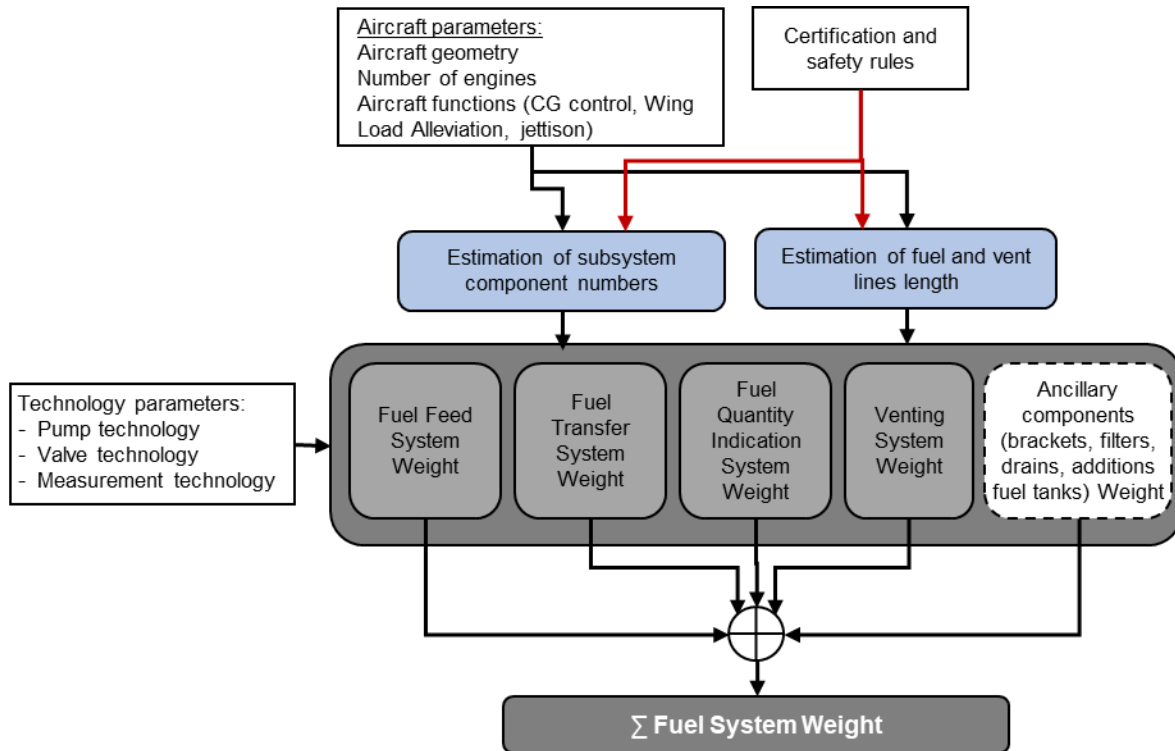


Figure 7: Architecture-based weight estimation process for fuel systems

The specific details of the calculation process for each subsystem are discussed in the next sections; however, it should be noted that the methodology needs to be restricted to fuel systems with tanks that are integral to the aircraft's structure (including wing tanks and center tanks or CWT). The restriction is put in place for two reasons: The first is the lack of available data on bladder tanks, specifically on the weight of the tank itself as a function of the tank volume. The second is that modern aircraft fuel systems seem to be trending towards using integral tanks instead of bladders since it is already known that the installation of bladders incurs additional weight due to brackets and fasteners required to hold them in place. However, bladder tanks should not be completely ruled out since they could still be a viable option for hybrid-electric aircraft concepts, but this is still to be determined.

4.2 Fuel Feed Subsystem

This section outlines the process of estimating the weight of the engine fuel feed subsystem, which implements the fuel system's primary function. A survey of various aircraft architectures shows that a single main tank supplies each engine on multi-engine aircraft, satisfying the safety and regulatory requirements for fuel system independence (FAR Part 23.953 and 25.953, for example). The main fuel tanks on most aircraft are located inside the wing box since it keeps the tanks separated from the passenger cabin and provides wing-load alleviation to benefit the wing structure by reducing the bending moment on the wings for larger aircraft. However, there are exceptions to be aware of, such as on the DHC6, where the fuel tanks are located in the fuselage under the cabin floor. Center tanks, sometimes called center wing tanks (CWT), are common on most low-wing airliners like the A320, B727, B737, and CRJ. Fuel storage is also possible with auxiliary fuel tanks placed in other locations on the aircraft. Examples of auxiliary fuel tanks include the forward, aft, tail cone, and saddle tanks on the Bombardier Challenger 605 business jet in Figure 8 below, which help increase the max fuel capacity in addition to the main tanks. In this particular aircraft, a sump near the aft portion of the aircraft is gravity fed by the saddle tanks and tail cone tanks. The sump contains electrical transfer pumps that can transfer the fuel into the center auxiliary tank. The remaining FWD and AFT auxiliary tanks connect directly to the center auxiliary tank and transfer their fuel by gravity.

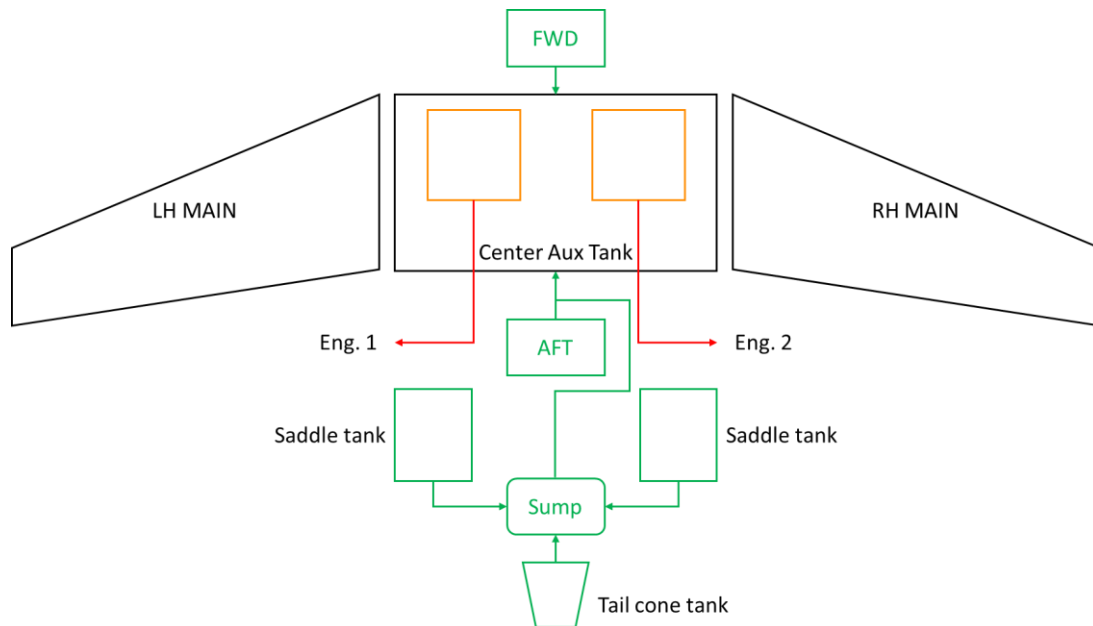


Figure 8: CL605 fuel system with auxiliary fuel tanks

The two feed pumps are installed in a collector compartment or sump of the main tank, which helps to ensure they remain submerged in fuel to mitigate cavitation and fuel starvation. The type of feed pump used varies between aircraft, but in general, most light GA aircraft use 14-28VDC pumps, while business, commuter, and some small regional aircraft only use 28VDC pumps. Larger regional airliners and business

jet aircraft use constant or variable frequency AC fuel pumps. Some commuter, regional, and business jets use jet pumps instead of electrically-driven pumps as the main pump to supply fuel to the engine, for example, in the ATR42, DHC8, C550, and Learjet 28. Jet pumps offer significant weight savings and reliability since they have no moving parts and use the high-pressure fuel return from the engine to maintain positive pressure on the main feed lines.

Olives [33] considers a narrower range of fuel pumps for the engine feed, focusing mainly on commercial 28VDC and 200-400VAC canister-type airframe pumps. The engine fuel pumps are also considered part of the weight because they are part of the fuel system. In this thesis, the following arguments are made to exclude them as part of the airframe fuel system weight: First, the engine fuel pumps are part of the engine itself, and their design, development, and production are overseen by the engine supplier and are not necessarily under the full responsibility of the airframe manufacturer. Secondly, the engine fuel pump is essential to the engine operation, raising the fuel pressure such that it can be properly atomized in the combustion chamber; this is not possible using the airframe fuel pumps alone. Third, the weight analysis becomes much simpler because there is a clear delineation between what components belong to the engine (engine fuel pump, engine fuel control, engine fuel supply lines, fuel filters, heat exchangers, and engine fuel injectors/nozzles). Finally, there is no clarity in the data or the existing state-of-the-art methods about treating the engine fuel pumps as part of the engine or the airframe. In hybrid-electric aircraft applications, the engine fuel system is not expected to change significantly from existing turbine or piston engines. Based on these arguments, the methodology presented in this thesis does not consider the engine fuel system as part of the airframe for either conventional or hybrid-electric applications.

The review of system schematics results in the development of the following proposed rules for the engine feed subsystem weight estimation:

- 1) The number of fuel tanks (N_t) must be equal to or greater than the number of engines to satisfy the requirements for fuel system independence. Auxiliary tanks can be added to accommodate the total mission fuel mass and only connect to the main fuel tanks.

$$N_t \geq \begin{cases} N_e + CWT, & \text{for GA, Commuter, Regional aircraft} \\ N_e + CWT + 1, & \text{for } N_e \geq 4 \end{cases} \quad (9)$$

The max fuel capacity of the aircraft is estimated from the geometry and average wing thickness inputs.

- 2) The number of feed pumps must be two per engine to satisfy the requirements of FAR Part 25.991 and FAR Part 23.991 for turbine-powered aircraft. It is not always the case for piston-engine aircraft since the engine-driven pump can be considered a main pump. Additionally, the type of pump will also affect the weight; jet pumps are much lighter than electrically driven pumps and must be considered. An additional boost pump is also required if the aircraft has an auxiliary power unit (APU) that draws fuel from one of the main tanks. Details on the weight of these pumps are discussed in 4.2.1, but the number of electrically driven pumps is given by:

$$N_{bp} = 2N_e + m - N_{jp} \quad (10)$$

Where $m = 1$ if the aircraft is equipped with an APU and 0 otherwise. The number of jet pumps N_{jp} is equivalent to the number of engines only if the engines have an output for a motive flow return line to power these pumps, and 0 otherwise:

$$N_{jp} = N_e \quad (11)$$

- 3) The fuel line weight depends on its diameter, length, and material characteristics. The details of this calculation process are discussed in section 4.2.2.
- 4) The number of fuel shut-off valves must equal the number of engines, and the individual weight depends on the physical size of the valve, as described in section 4.2.3.

These rules are then combined with the weights of the individual components obtained from various manufacturer data sheets and other sources to obtain the subsystem weight.

4.2.1 Fuel Feed Pumps Weight Estimation

The analysis for the pump rating characteristics, weight, and typical applications is based on manufacturer data sheets [34]–[37], spare parts sold by online vendors [38], and survey data from Weitz [39]. Three observations are made from this data and are summarized here :

- 1) Light, general aviation, and small commuter aircraft (certified to FAR Part 23) usually employ electrical boost pumps operating from a 28VDC power source. These pumps range from 5 to 10 lb, with the heavier pumps used in business and commuter turboprop aircraft.
- 2) The fuel feed circuit is typically implemented in FAR Part 23 certified aircraft using either dual electrically-driven pumps or one ejector and one electrically-driven pump. Examples of this type of arrangement are seen in the Do-228 and PC-12. The alternative option is to use an ejector-type pump as the main pump, driven by a high-pressure fuel output from the engine pump and an electrically-driven stand-by/emergency pump. This second option is often featured on regional aircraft like the DHC8, ATR42/72, and JS4100.
- 3) Transport category airliners almost always implement dual electrically-driven feed/boost pumps in the engine feed circuit; the only exception would be on smaller regional passenger aircraft. Ejectors are not typically used in these applications because, as described by Langton, the motive flow line supplying the ejector pump needs to be impractically large to accommodate the maximum engine fuel flow.

The sizing of the feed pumps requires the engine fuel flow requirements to be known, which can be estimated from the engine power and SFC at takeoff and data from [40], [41]. The approximate pump size can then be interpolated from Table 8, compiled from specifications in [34]–[36], [38], using the engine's fuel flow at takeoff as the input.

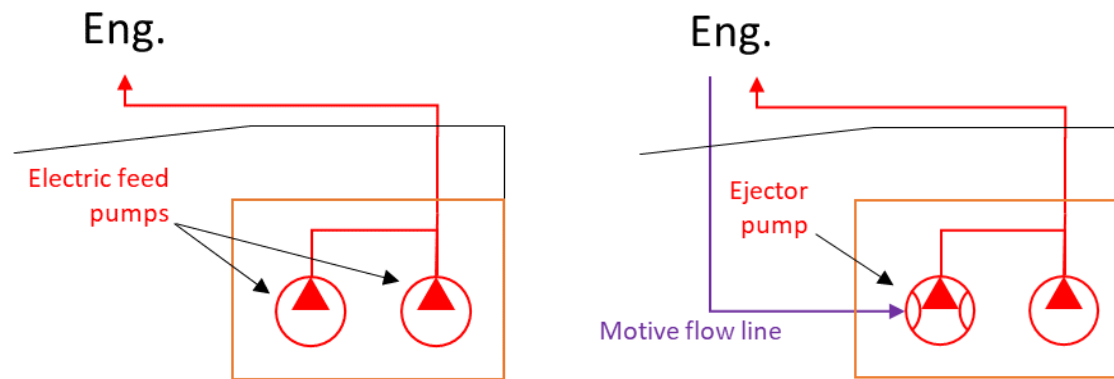
Table 8: Electrical fuel pump data for various aircraft applications

Engine flow (lb/h)	Weight (lb)	Model	Manufacturer [34]–[36]	Pump Type	Typical Application
210	2.712	8150-B	Weldon	24 V.DC	Cessna 340
1508	6.437	20026	EATON	28 V.DC	Auxiliary Power Unit
4004	7.011	1C7-13	AMC	28 V.DC	Cessna 500
8007	7.011	1C00	Parker	28 V.DC	DO228
27778	9.26	20004	EATON	200 V.AC / 400 Hz	B747
11032	11.02	8410	EATON	200 V.AC / 400 Hz	A320
23810	11.35	8810	EATON	200 V.AC / 400 Hz	A330/A340
34921	14.33	9106	EATON	200 V.AC / 400 Hz	B777

An alternative means is from the curve fit for the above data, given by eq. (12).

$$W_{bp} = 0.619(\dot{m}_{Feng})^{0.297} \quad (12)$$

The total number of feed pumps in the subsystem depends on two key safety and certification requirements: 1) A dedicated feed circuit must supply each engine per FAR Part 25.953, and 2) Two pumps are required for each engine feed circuit per FAR 25.991, such that one pump functions as the main pump and the other as the emergency pump shown in see Figure 9. Two feed pumps per engine are used and counted by the $2N_e$ term in eq. (10) of the previous section.



(a) Engine feed circuit using dual electric feed/boost pumps to supply fuel to the engines. Typically seen on most commercial airliners since an ejector feed pump arrangement is not feasible for the fuel flows required in the feed system. Examples include the C414, DO228, EMB110, and F27.

(b) Engine feed circuit using an electric pump (right-side) for engine starting and as an emergency pump. The main feed pump is an ejector driven by a high-pressure 'motive' flow from the engine-driven pump. Typical of most commuter, regional, and business aircraft. Examples include the PC12, C550, ATR42, and DHC8.

Figure 9: Common circuit arrangements for engine feed subsystems

An additional fuel pump must also be considered for aircraft featuring an auxiliary power unit (APU), which usually draws fuel from one of the main fuel tanks. This pump is counted by the parameter m in eq. (10). Finally, some accommodation must be made for aircraft that use ejector pumps as the main feed pump, as shown in Figure 9b). This feed pump arrangement is very common on commuter and regional aircraft. However, many examples of aircraft with the arrangement in Figure 9 (b) exist and must also be considered in the calculations. The number of feed ejector pumps (or jet pumps) is counted by the N_{jp} term in eq. (10) of the previous section. Once the number of pumps in the feed system is determined, the individual weight is estimated from manufacturer data sheets [34], [35], [37]. The pumps form the heart of the feed subsystem and contribute the most weight to the subsystem, especially where electrical pumps are installed.

4.2.2 Fuel Line Weight Estimation

Estimating the weight of fuel lines can be performed by determining the outer diameter (OD, required to support the max fuel flow through the system) and length of segments along the wing structures (forward or aft wing spars) between the fuel pump position and the engine fuel inlet. Typically, the fuel feed compartment is placed at the lowest point of the main fuel tanks so that the fuel can migrate by gravity towards the main fuel pumps. In aircraft with a wing dihedral, the feed compartments are typically nearest to the fuselage (for example, in the B1900D, B737, and A320). In contrast, the feed compartments in anhedral wing aircraft (such as the BAe-146) are closer to the wingtips.

Therefore, the location of the tanks, the feed compartment, and general fuel tank geometry are necessary inputs to determine how the fuel lines are routed to the engines, consequently affecting their length and weight. Appendix section A.1 outlines the process of determining the geometry of wing tanks from key aircraft geometry. The feed compartment is located within the tank, as shown in Figure 10, and is the starting point for the fuel line connecting the feed pumps to the engine it supplies. Routing the line assumes the shortest possible distance between the pumps in the feed compartment and the engine interface, usually along a wing spar to the engine nacelle as proposed by Olives [33]. The sum of the line segments (A, B, and C) provides the total line length, and together with the OD, the weight of the fuel lines can be estimated.

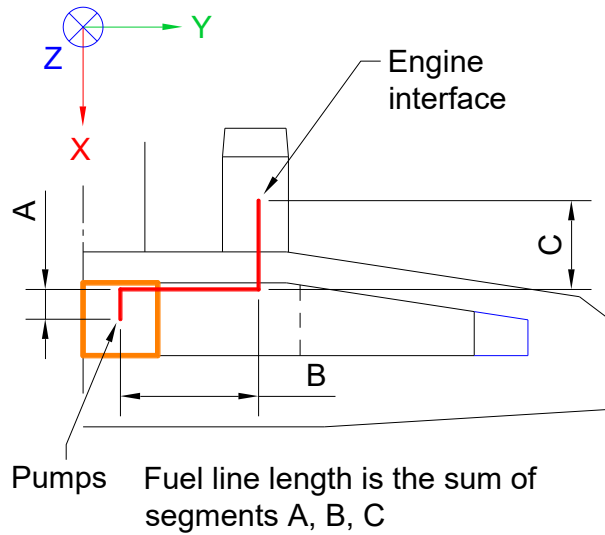


Figure 10: Fuel line length estimation

The following guidelines are proposed and based on the study of system schematics in Appendix C to make the fuel line estimation robust for typical architectures:

- 1) For single-engine aircraft, the fuel supply lines from each wing tank connect to a fuel selector valve located in the fuselage at or near the aircraft centerline. A single line then connects the valve to the engine.
- 2) For multi-engine aircraft with wing-mounted engines, the fuel line routing is along the front spar, similar to Olives [33], then along the nacelle towards the fuel interface point. It also applies to aircraft with engines on the wings mounted closer to the rear spar (ex. Piaggio P.180 Avanti).
- 3) For tail-mounted engines (propulsion and auxiliary power units), the fuel lines are directed towards the aircraft centerline, then towards the rear of the fuselage, and then outward towards the engine nacelle. The approach is similar to the Olives [33] methodology.

The line outer diameter (OD , in) and weight per unit length (W/L) are also required to calculate the overall weight. For the engine feed lines, the OD data compiled by Weitz [39] shows a linear trend against engine thrust for turbofan-powered [40], [41] aircraft in Figure 11.

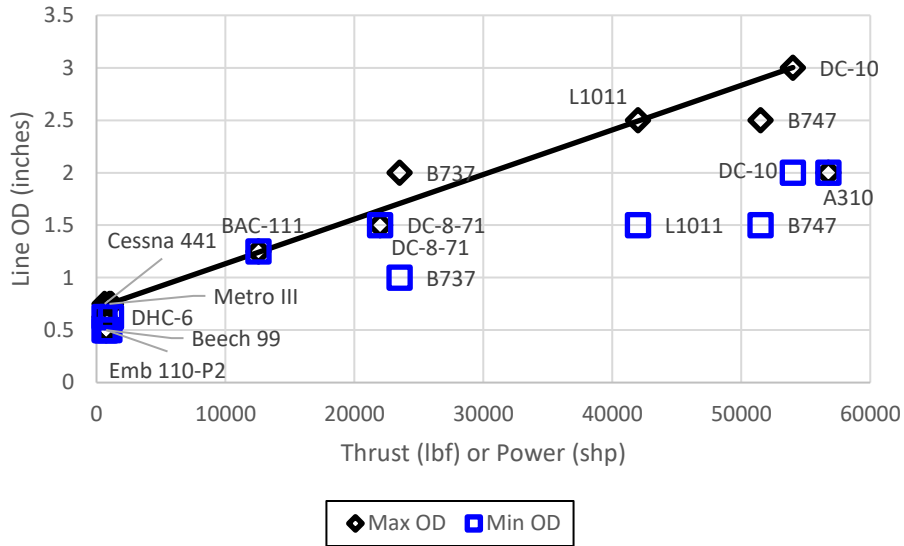


Figure 11: Fuel line OD relationship to engine thrust or power

A single OD is assumed for the feed lines and is calculated by eq. (13) below for turbofan/jet aircraft.

$$OD = 4.25 \times 10^{-5}(F_{thrust}) + 0.708 \quad (13)$$

The relationship also holds for turboprop engines, with the exception that F_{thrust} is simply replaced by the engine take-off power in SHP according to eq. (14) below.

$$OD = 4.25 \times 10^{-5}(SHP) + 0.708 \quad (14)$$

This approach provides a quick means of estimating the approximate fuel line diameter for any aircraft. Still, analysis of the data from Weitz [39] shows that the OD can vary at different locations of the feed circuit: For example, the line OD is usually larger between the feed pumps and firewall, reducing to a smaller OD close to the engine. An alternative approach uses the relationship of OD as a function of rated flow (\dot{W}_F , lb/h) for fuel pumps, again based on the survey data from Weitz [39].

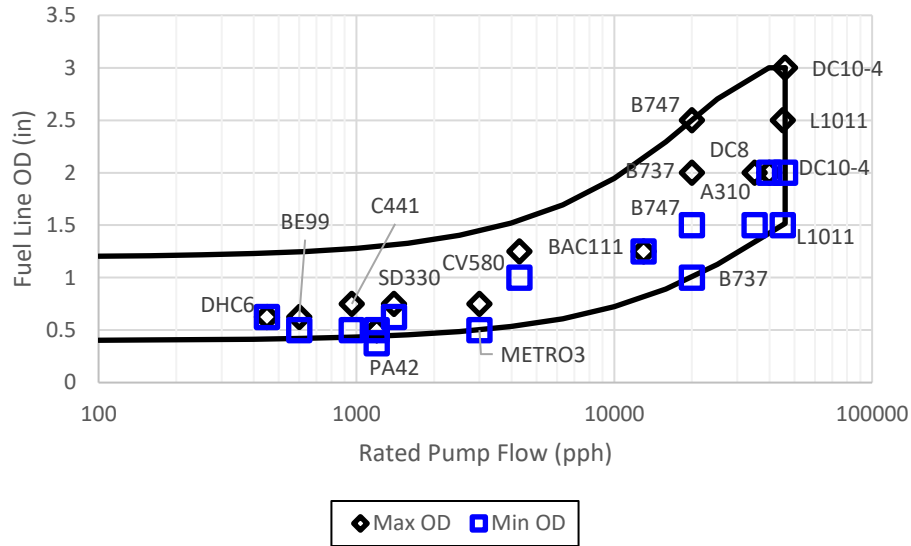


Figure 12: Fuel line OD and rated pump fuel flow

It is a more representative estimation of the diameter since it is based on the max/min OD used in production commercial aircraft. Eqs. (15) forms the upper boundary to the envelope in Figure 12 above for commercial aircraft.

$$OD_{\max} = -9.98 \times 10^{-10}(\dot{m}_F)^2 + 8.51 \times 10^{-5}(\dot{m}_F) + 1.196 \quad (15)$$

Similarly, eq. (16) below forms the lower boundary of the envelope in Figure 12.

$$OD_{\min} = 2.24 \times 10^{-10}(\dot{m}_F)^2 + 3.46 \times 10^{-5}(\dot{m}_F) + 0.40 \quad (16)$$

The min and max OD is then averaged and used with the weight per unit length (W/L) parameter to estimate an 'average' weight of the feed lines. However, the main drawback is that the rated pump flows are unknown at the conceptual design phase. A designer may need to rely on data from existing aircraft with similar fuel system characteristics, which may not always be practical.

Therefore, a third approach is to estimate the max and min OD range from the maximum engine fuel flow (\dot{W}_{Feng} , lb/h) needs; the envelope of possible OD as a function of engine fuel flow is shown in Figure 13 below.

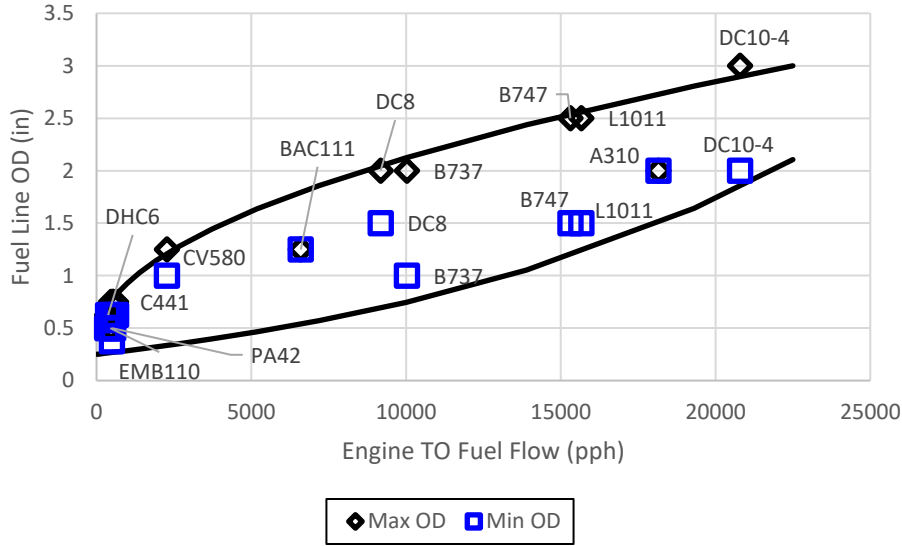


Figure 13: Engine feed line OD envelope as a function of engine fuel flow at take-off

Eq. (17) is the curve fit of the Weitz survey data for max feed line OD against calculated engine fuel flow at take-off.

$$OD_{max} = 0.0175 \sqrt{\dot{m}_{Feng}} + 0.375 \quad (17)$$

Similarly, eq.(18) calculates the min OD using the engine fuel flow, and the average is used with the total line length and the W/L parameter to estimate the weight.

$$OD_{min} = 0.5e^{6.89 \times 10^{-5} \dot{m}_{Feng}} - 0.25 \quad (18)$$

The rigid fuel lines in most aviation applications are made from aluminum alloys according to specifications such as WW-T-787 and WW-T-789. A minimum wall thickness is recommended according to AS18802 [42] (see Appendix section A.3). The OD and wall thickness are needed to obtain the weight per unit length (W/L) from the EMJ Company reference handbook [43] for mechanical tubing of various standard sizes used in aerospace applications. A summary table with the weight per unit length data for fuel lines and vent ducts is available in Appendix A.3.

4.2.3 Fuel Shut-off Valve Weight Estimation

Valves used for fuel shut-off, cross-flow or cross-feed functions, and motive flow returning to the tank are typically electrically actuated and must be sized to accommodate the fuel flows of the system. The study of schematics for various aircraft also shows two main valve technologies are used in the fuel system: Ball valves and solenoids. Ball valves are typically employed for fuel shut-off or cross-feed/flow, while solenoid valves are employed on fuel circuits that handle much smaller fuel flows. For example, the ATR42 low-

pressure valve cuts off the main fuel flow to the engine fuel control and is actuated by two electric motors for redundancy. The motive flow output from the high-pressure pump on the engine passes through a motive flow solenoid valve, which is much smaller and lighter than the low-pressure valve. The weight of these valves will be a function of the technology and the diameter of the fuel line to which the valve connects. For ball valves, the weight is interpolated from Table 9 (compiled from manufacturer data sheets [35], [44]) as a function of the fuel line OD (estimated in the previous section).

Table 9: Lookup table for fuel valve weight estimation

Fuel line OD (in)	FSOV Weight (lb)
0.5	1.5
1.0	1.8
1.5	2.2
2.0	2.3
3.0	4.5

It should be noted that this table only accounts for the weight of the valve without the actuator motors; the absence of motor weight data makes it difficult to establish an accurate estimate of the overall assembly weight. Actuators from Sitec Aerospace [45] range from 0.8 to 2.6 lb, with heavier motors assumed to apply to larger valves for commercial airliners. The total number of fuel shut-off valves in the feed subsystem equals the number of engines on the aircraft.

$$N_{SOV} = N_e \quad (19)$$

In addition, if the aircraft is equipped with an APU, eq. (19) needs to be incremented by 1 to account for the APU shut-off valve.

4.3 Fuel Transfer Subsystem

The fuel transfer subsystem is the most complex of the four subsystems because of the number of secondary functions it serves on some aircraft. Its main function is to transfer fuel between tanks and allow cross-feed functionality. In most cases, the subsystem needs dedicated pumps and valves to fulfill these objectives. The CL605 business jet is an example where the aft auxiliary fuel tanks extend the range but need to be fitted with additional pumps and transfer lines to pump this fuel to the main tanks. Fuel scavenging is another important secondary function of this subsystem since it helps migrate fuel in the tanks toward the engine feed collectors, keeping them full to minimize fuel starvation of the engines. Condensed water is also migrated to the collectors so that it can be mixed by the feed pumps and burned with the fuel supplied to the engines.

In this methodology, the segregation of the four subsystems isolates the components specific to the fuel transfer subsystem such that they can be estimated independently from the other subsystems. It is a

particularly useful approach for aircraft that employ subsystem features such as refuel/defuel circuits and additional auxiliary transfer pumps and tanks. The Olives [33] method considers all of these components by default because they are typically featured in most large commercial aircraft, but this is not always the case for commuter and regional aircraft. Both methods estimate the weight by determining the number of transfer pumps (though the ASSET method considers both electrical and ejector type pumps, while the Olives method considers only electrical pumps), the valves associated with tank transfer lines, refuel/defuel, and engine crossfeed. Finally, the jettison functionality is typically employed on commercial aircraft and is also considered by Olives [33]. However, it is not currently part of the ASSET method since it is unavailable in most commuter and regional aircraft. The following subsections break down the process implemented in the ASSET tool for estimating the weight of this subsystem.

4.3.1 Transfer fuel pumps

The main purpose of the transfer subsystem pumps is to move fuel between and within the tanks. A review of the fuel systems for the aircraft in the Roskam [20] database identifies several trends concerning the implementation of transfer pumps: First, electrical transfer pumps move fuel from auxiliary tanks to the main tanks, as shown in the schematics for the LJ25D, LJ28, A320, A330, A340, and B747-400. However, there are some exceptions, such as with the CL605, which has multiple auxiliary fuel tanks throughout the fuselage and use a combination of gravity and forced flow. Transfer pumps may also perform additional secondary functions in some airliners, specifically facilitating refuel/defuel and jettison capabilities as detailed by the system schematics of the B727 and B747 in Appendix section C.1. The flow demand required for these functions is usually much higher than for engine feed pumps, so they commonly have a higher flow rating and are heavier than engine feed pumps. Scavenge pumps are also part of the transfer subsystem since their purpose fulfills the secondary function of moving fuel within and into the main tanks, helping to migrate fuel and condensed water towards the engine feed collectors. In some cases, these pumps are electrically-driven but employ ejector pump technology for the most part.

The weight estimation process for the transfer subsystem pumps borrows concepts from the weight estimation of fuel feed pumps discussed in previous sections with one major difference: The engine feed pump weight is estimated as a function of the maximum engine fuel flow at take-off conditions, which may not necessarily apply to the transfer pump sizing. An alternative approach is based on a sample of commercial boost and jettison pump weight data [35] in Table 10. The main drawback is that these pumps apply to large commercial airliners fitted with pumps that fulfill jettison or override functions as on the B747 and B777 instead of strictly transferring as in the B737 or A320. Therefore, it may not be particularly useful for smaller aircraft in the commuter and regional class, where the transfer pumps may be similar to those for the fuel feed subsystem.

Table 10: Rated flows and weights for commercial boost and transfer pumps

Aircraft	Boost		Transfer (XFR)		Weight Ratio (XFR/Boost)
	Rated flow (kg/s)	Weight (kg)	Rated Flow	Weight	
B777	4.4	6.5	8.3	8.8	1.35
B777 alternate	4.4	6.5	5.2	7.4	1.14
B747	3.5	4.2	5	6.3	1.50

The weight estimation of ejector-type scavenge pumps is slightly easier. Reviews of the schematics in Appendix C generally show the number and placement of scavenge pumps varies between 1 and 3 from aircraft to aircraft. The weight of the pumps also depends on the induced flow. Datasheets from Cristall [37] and Eaton [35] show the trend against the induced flow in Figure 14. The estimated weight for these pumps is calculated by eq. (20).

$$W_j = 2.87 \times 10^{-3} \dot{W}_F^3 - 9.99 \times 10^{-2} \dot{W}_F + 1.13 \dot{W}_F + 0.271 \quad (20)$$

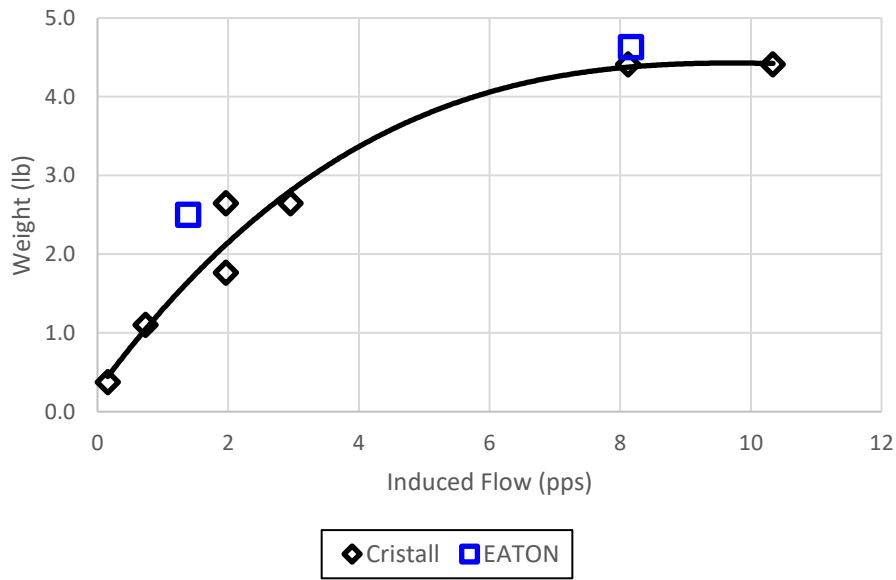


Figure 14: Ejector pump weight as a function of induced flow

As with the electrical transfer pump weight, there is no direct link between the high-level fuel system characteristics (max fuel capacity, max engine fuel flow, number of fuel tanks, etc.) and the ejector pump weight.

Table 11: ASSET tool individual scavenge pump weights

Aircraft classification	Individual Ejector Pump Weight (lb)
Light / commuter	1.0
Regional and Narrow-body	2.0
Wide-body airliners	4.5

However, from Figure 14 and a review of the manufacturer data sheets, induced flows above 6 PPS likely correspond to ejector pumps on large commercial airliners such as the A330, A340, and B747. Flows less than 4 PPS are likely to correspond to narrowbody airliners and regional/commuter aircraft. Therefore, the proposed means of estimating the weight of ejector scavenge pumps for a given aircraft is to use Table 11 as a lookup table.

4.3.2 Transfer lines and valves

The transfer fuel lines and valves permit the auxiliary tanks to be connected to the main tanks and facilitate engine cross-feeding, scavenging, and transferring between tanks, refueling/defueling, and fuel jettison. On multi-engine light and commuter aircraft, the fuel transfer and fuel scavenging functions are of importance, while business, regional, and commercial aircraft may feature all of these functions. Estimating the weight of the transfer fuel lines and valves is similar to that of the engine feed subsystem: The weight of the valves depends on the type (typically ball valve) and the OD of the transfer lines. As a first and simple approximation, the OD for the transfer lines can be made the same as the engine feed subsystem. However, a more detailed review of the data compiled by Weitz [39] shows the trends against maximum aircraft fuel capacity in Figure 15.

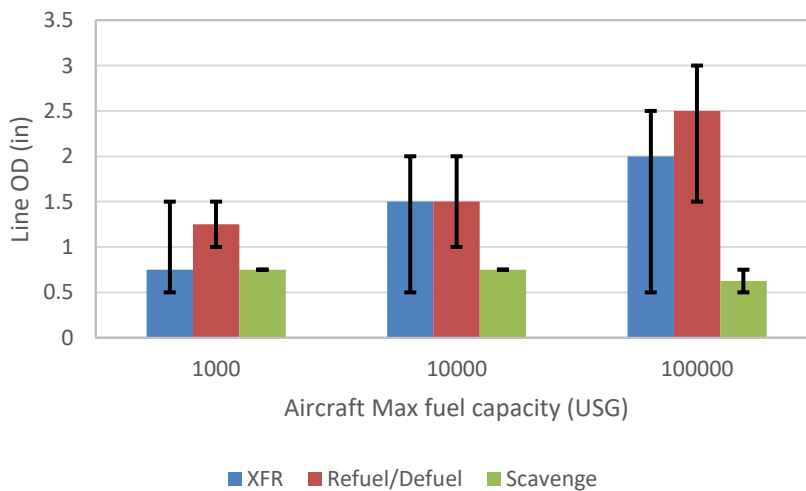


Figure 15: OD size for different fuel transfer subsystem lines

In the plot, XFR designates any fuel lines for transferring fuel between tanks or engine cross-feeding. Once the line OD is determined, the wall thickness and W/L parameter can be determined from the tables in Appendix A.3. The total subsystem weight calculation implemented in the ASSET tool is based on the following proposed rules:

- 1) Electrical fuel pumps: One electrical pump is fitted in each large auxiliary fuel tank of commuter/regional aircraft, similar to the B1900D. All other smaller auxiliary tanks are assumed to transfer fuel by gravity to the larger auxiliary tanks and then pumped into the main tanks. Two electrical pumps are fitted to a center tank or CWT of commercial aircraft.
- 2) Scavenge ejector pumps: Not fitted to light aircraft based on the review of various schematics (for example, Cessna 100-series, C208, and BE33/35/36). Commuter, regional, and commercial aircraft contain 2 scavenge ejector pumps per main tank compartment (a total of 4 pumps in compartmentalized tanks); two pumps are located in the inboard tank compartment containing the collector tanks, and the remaining two are in the outboard-most tank compartment. Airliners with a center tank or CWT contain two (2) additional scavenge ejector pumps in this tank.
- 3) Fuel lines segments and lengths are estimated by establishing that:
 - a. Cross-feed lines connect the engine feed lines at a point on the main wing spar.
 - b. A scavenge fuel line branches off the main feed circuit and connects to all the scavenge pumps. The discharge from the ejector pumps is not considered as part of the length of the fuel lines. Routing of the transfer subsystem fuel lines is assumed such that the line length is kept to a minimum.
 - c. Refuel/defuel lines are fitted to commercial aircraft certified under FAR Part 25 regulations. A large diameter pipe (called a gallery) inside each main fuel tank connects all the tanks together. The gallery is also connected to the refuel/defuel adapters on the aircraft at either one or two locations (single-point or dual-point). As a general rule, single-point refueling is typical for commuter and regional aircraft, and dual-point refueling is typical for wide-body airliners.
 - d. Jettison fuel nozzles must be fitted to satisfy the climb requirements of FAR 25.119 and 25.121(d), and if the MTOW of the aircraft significantly exceeds the MLW. Schematics for aircraft like the A330, A340, B727, and B747 show that the refuel/defuel gallery is connected directly to the jettison nozzles via the jettison valves.

Again, the above rules are based on observations of the trends in various aircraft fuel system schematics and manuals. Implementing these rules in the ASSET tool will lead to deviations and errors in the layout when modeling certain aircraft. One example is the ATR42 aircraft fuel system in Appendix C: The above rules place a total of 4 scavenge pumps in each wing tank of the ATR42, but actual aircraft schematics show only one pump is installed. The difference in actual weight, specifically for this aircraft, would be approximately 5-6 lb, which amounts to about 3% of the actual system weight.

4.4 Fuel Quantity & Indicating Subsystem

The Fuel Quantity and Indicating Subsystem (FQIS) contains fuel quantity sensors (probes or tank units), wiring harnesses, fuel properties measurement devices, and electronic equipment for signal conditioning and fuel management. Olives' method [33] does not cover the weight of FQIS components because of the lack of available data. However, the ASSET method does consolidate some manufacturer data for various components.

The fuel quantity probes are usually resistive or capacitance-type devices (although different technologies, including ultrasound, are now starting to be introduced) intended to help determine the fuel on board. The number of probes in each tank is determined such that the quantity of fuel in the tank can be measured within a reasonable margin and allows for redundancy in case of failure of one or more sensors. The minimum number of probes per tank is typically established by analysis of the interior tank geometry and free surface; however, Langton [46] recommends a minimum of three probes per tank.

The weight of an individual capacitance probe does correlate with its length (as shown in Figure 16) and can be used along with the total number of probes to approximate the weight of the probes in the system. It can be estimated from the curve fit equation in eq. (21) below; the parameter L_{probe} is an average of the length of the FQI probes on the aircraft and can be estimated as 90% of the average wing thickness (t_{wing}) for simplicity.

$$W_{probe} = 0.0981L_{probe} + 0.3284, \text{ assuming } L_{probe} \sim 0.9t_{wing} \text{ [inches]} \quad (21)$$

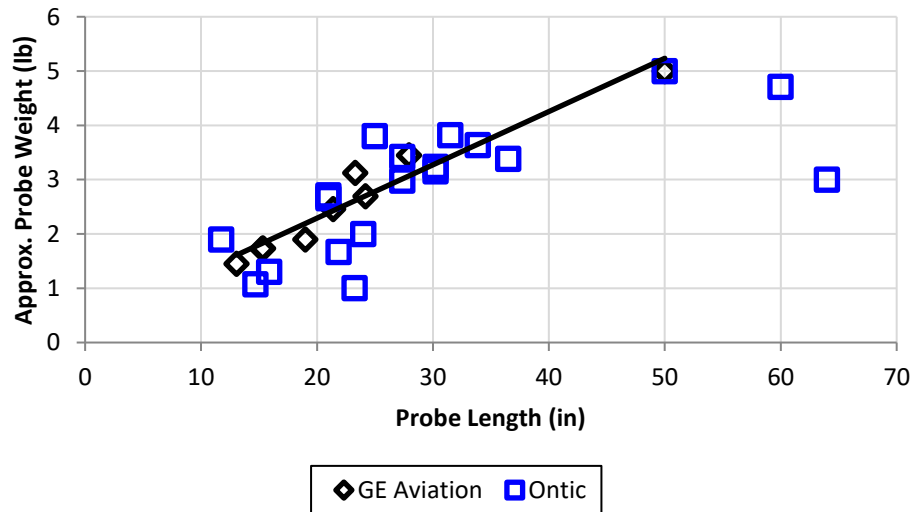


Figure 16: Capacitance-type fuel probe weight as a function of probe length

The bulk of the FQI subsystem weight can be attributed to many probes on some larger aircraft, such as the A380, which has over 150 probes. An analysis of the number of FQI probes used in various aircraft

shows that the wing tanks contain the most FQI probes since the wing tanks usually contain most of the fuel compared to center wing tanks (if fitted). Figure 17 shows the number of wing tank FQI probes trending against aircraft wing span, with the curve fit represented by eq. (22). However, this relationship tends to introduce errors if applied to aircraft with hybrid-electric powertrains because since the wingspan remains larger than the actual tank size, the number of FQI probes will be overestimated. Furthermore, the relative error can be significantly large for some aircraft, which will then affect the weight of the subsystem if the difference between the estimated and actual number of probes is large. An example is the LJ28, which has eight probes in the wing tanks and a wingspan of 43.7 ft. Eq. (22) gives a raw value of 8.58, but it needs to be rounded up to the next even number (for example, 10) to be identical for each wing. The error of the estimated weight can be approximately 25% just by this difference in the number of probes.

$$N = 4.9e^{0.0128 \times S} \quad (22)$$

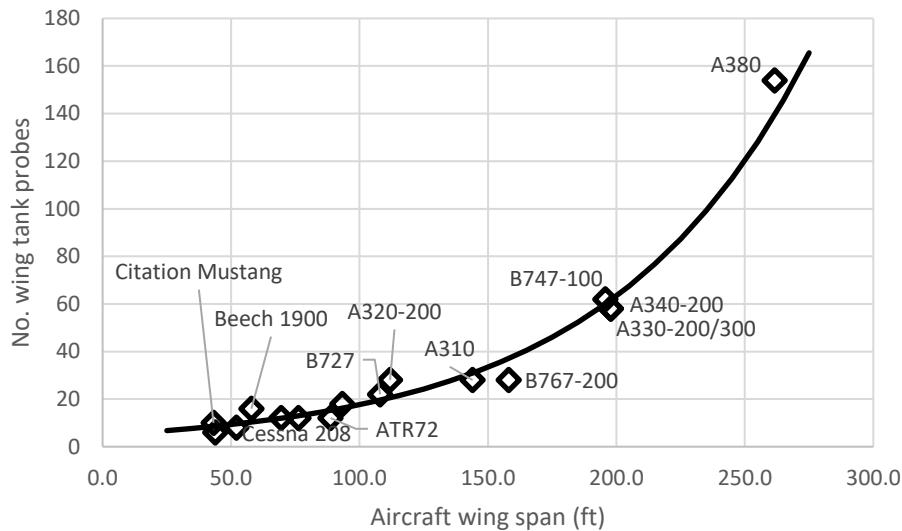


Figure 17: Survey of number of wing tank probes and aircraft wing span

An alternatively proposed estimation is shown in Figure 18 below, which looks at the number of probes per wing tank against the span of the tank. The benefit of this relationship is that the number of wing tank probes can change as a function of how large the tank is and will be more representative of smaller fuel tanks in aircraft with hybrid-electric propulsion systems. The number of wing tank probes can be estimated from eq. (23). The number of probes in this equation needs to be rounded to the nearest integer.

$$N = 0.444 \times L_{tank} - 4.672, N = 3 \text{ for } L_{tank} < 17.28 \text{ ft} \quad (23)$$

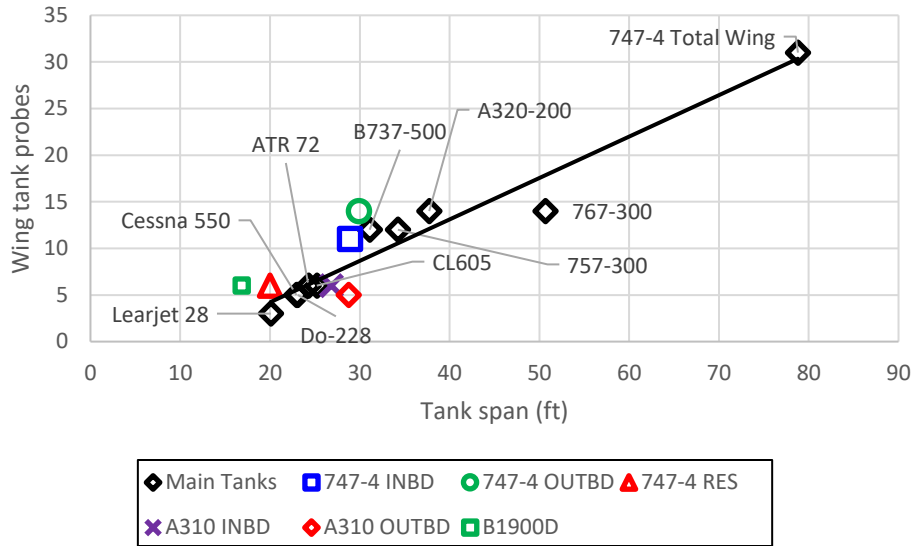


Figure 18: Relationship showing number of wing tank FQI probes against tank span

The remaining components of the FQI subsystem include those listed in Table 12, obtained from Aviall [38]. These may not all be fitted to some aircraft, especially in the case of GA and commuter aircraft, which do not usually have refuel/defuel capabilities and would not be fitted with a refuel/defuel panel, for example. The selection criteria for counting the weight associated with these components follow the rules proposed herein:

- 1) FAR Part 23 general aviation aircraft use float-operated fuel quantity transmitters instead of capacitance-type probes in the fuel tanks. These devices are usually more compact and lighter, but in the absence of verifiable data, a weight of 0.25 lb per transmitter is assumed based on their general size. The weight of the wiring harness, fuel quantity management, and display avionics is neglected since the subsystem is small compared to larger aircraft. This approach supersedes the use of the data in Table 12.
- 2) FAR Part 23 utility and commuter aircraft commonly use capacitance-type FQI probes and include some moderately sized avionics equipment for fuel management and display. Refuel/defuel panels, densitometers, and other related devices are not counted since the schematics review shows these components are not typically fitted. The min weight column from Table 12 is used for these components.
- 3) FAR Part 25 transport category aircraft will include all of the equipment listed in Table 12 because these aircraft normally carry a significant amount of fuel compared to aircraft certified under FAR Part 23. A review of narrow-body schematics and manuals reveals the use of fuel quantity management computers, a fuel densitometer in each main tank, an array of capacitance-type FQI probes, and a refuel/defuel panel, display avionics, and manual fuel measuring sticks. Wide-body aircraft usually have the same equipment but will be much heavier, so the data from the max column of Table 12 is used.

Table 12: Range of weights for various FQIS components

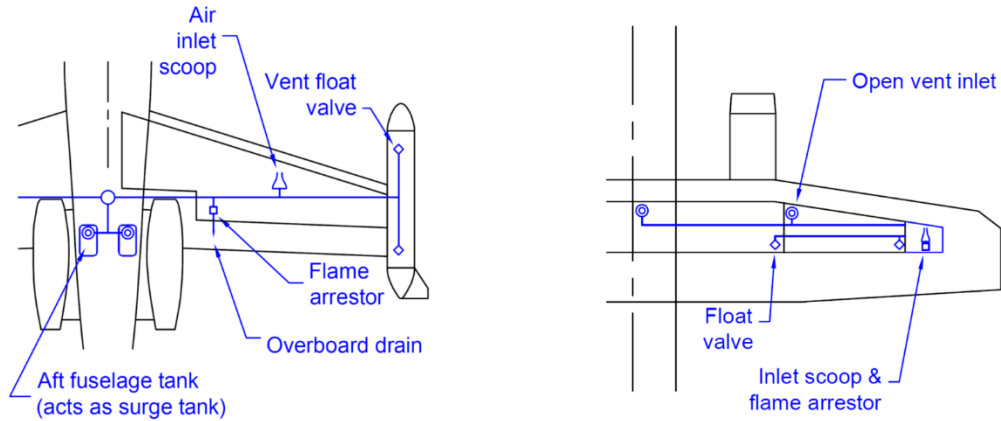
Item	Weight (lb)	
	Min	Max
Capacitive FQI probes	1.0	5.0
Densitometer	1.8	3.6
Fuel Quantity Processing Unit	5.0	21.7
Refuel/defuel panels	7.0	15.0
Fuel measuring stick	0.3	2.0

Strictly speaking, the avionics related to the fuel management, displays, and refuel/defuel subsystems may not necessarily need to be included in the weight breakdown since these components may be counted as part of the electronic and avionics subsystems of the aircraft. However, since there is no clear guideline on this, the methodology does consider them part of the FQI subsystem.

4.5 Fuel Tank Venting Subsystem

The fuel tank venting subsystem consists of a network of lines or ducts connected to the surge tanks (or expansion spaces) that allow air exchange between the tank interior (ullage) and the ambient air according to Parts 23.975 [27] and 25.975 [30]). This duct arrangement prevents the excessive build-up of flammable vapors within the tank and mitigates the over/under-pressure of the tank during altitude changes. Ambient air flows into these surge tanks through NACA air inlet scoops or flush inlets and in-line flame arresting devices that prevent the ignition of flammable vapors in the system (to meet the requirements of Parts 23.954 [27] and 25.954 [30]). Float valves are installed inside the fuel tanks to prevent the ingress of fuel into the vent ducts; however, if this should occur, the ducts are also equipped with one-way drain valves that allow the fuel to drain back into the main tanks.

Figure 19 (a) shows a common vent duct arrangement for business jets like the Bombardier Learjets and Challenger 605 use the expansion space in the fuselage tanks connected to a network of vent lines that span into the wing and tip tanks. The ducts and wing tanks are vented directly to the atmosphere via NACA inlet scoops under the wings. Figure 19 (b) is the second type of vent duct arrangement and is more common in light aircraft, regional, and large commercial airliners. Two separate ducts span nearly the entire wing to vent the inner and outer portions of the main wing tanks. The placement of the vent inlets inside the tank is also important since they need to accommodate venting for attitudes when the aircraft is in a climb or a dive.



- (a) Business jets commonly use fuselage tanks as expansion spaces instead of surge tanks and connect a network of vent ducts and drains to the other tanks. The NACA air inlet scoops are located under the wings.
- (b) Most GA, regional, commuter, and airliner aircraft use hollow stringers as the vent ducts, running nearly the entire span of the wings. The ducts connect to the surge tanks near the wingtips and vent to the ambient air through the NACA scoops.

Figure 19: Assumptions for vent line geometry definitions

Auxiliary tanks are also typically connected to the network of vent ducts, but the methodology discussed herein does not account for these connections because it is difficult to estimate their length in an automated manner. The exception is for center tanks or CWT on airliners because the tank location and boundaries are consistent across aircraft. A single dedicated stringer duct is commonly used to connect the center tank to either the right or left surge tank. Float valves are fitted to the duct openings inside the main tanks to minimize the amount of fuel from entering the ducts and reaching the surge tanks. The process of estimating the weight of the vent subsystem is broken down into two portions: The location of the vent surge tanks and associated component weights and the weight estimation of the network of vent ducts.

4.5.1 Surge Tank and Vent Scoop Location

The surge tanks and vent scoops allow the exchange of air and vapors while mitigating fuel spills from the system under certain conditions. The surge tanks accommodate the fuel's thermal expansion resulting from large temperature changes as it warms up in the tanks while the aircraft sits on the tarmac in hot day conditions. These tanks also collect fuel that may have inadvertently entered the tank through the vent ducts during refueling or high-speed taxiing. The surge tanks and inlet ducts on most commercial aircraft are typically located near the wing tips to allow fuel vapors to discharge clear of the aircraft and maximize the ram air recovery through the inlet scoop, keeping a slightly positive pressure inside the tank.

The surge tank must meet regulatory requirements to accommodate at least 2% of the main tank capacity for commercial transports (14 CFR Part 25.969 [30]). Additionally, flame arrestors are incorporated on most aircraft to meet the safety requirements of 14 CFR Part 25.954 [30] concerning the ignition of flammable vapors leaving the surge tank and propagating the flame into the main tanks. Similar requirements apply to aircraft certified under the Normal, Utility, Aerobatic, and Commuter category [25]–[27]. The only difference is that the expansion space and flame arrestors are not strictly necessary if the tank vent discharges clear of the aircraft. The estimation of the subsystem weight does not count the weight of the surge tank itself since, like the integral wing tanks, it is assumed to be counted as part of the wing structure. However, its placement is critical to defining the discharge outlets of the ventilation ducts.

Table 13: Assumed weight & quantities of vent subsystem components

Component	General Aviation		Regional/Business Aircraft		Commercial Transports	
	Weight (lb)	Typical Qty.	Weight (lb)	Typical Qty.	Weight (lb)	Typical Qty.
Float valves	0.25	2 per duct	0.5	2 per duct	0.5	2 per duct
Flame Arrestors	N/A	1 per wing	0.5	1 per wing	0.5	1 per wing
Air inlet scoop	0.2	1 per wing	2.0	1 per wing	5.0	1 per wing

The weight of the flame arrestors and inlet vent scoops are part of the weight estimation method herein. Based on various aircraft manuals and illustrated parts catalogs, the weight of the inlet vent scoop assembly is estimated to be approximately 5-6 lb for airliners (B737, A320, and B747) and 2 lb for business jets and regional aircraft (LJ28, C550, ATR42). Flame arrestors do not contribute significantly, but Parker Aerospace's specification information [47] suggests they likely do not exceed 1 lb. Table 13 shows the vent subsystem component weights implemented into the ASSET tool.

The weights in the above table may be a source of uncertainty since there is not enough verifiable data to corroborate these numbers. However, the relatively small number of these components used in the subsystem is expected to have no more than a 5% impact on the estimated weight.

4.5.2 Vent Ducts

As previously discussed, the network of vent ducts is usually implemented on aircraft like the arrangements shown in Figure 19. The weight is estimated based on the length of the two (dive and climb) ducts and the diameter, typically about 2 to 4 inches for transport aircraft and about ½ to 1 inch for light and commuter aircraft. Weitz's [39] analysis of commercial aircraft fuel systems contains vent duct OD sizes for five aircraft (BE99, BAC-111, A310, and B747).

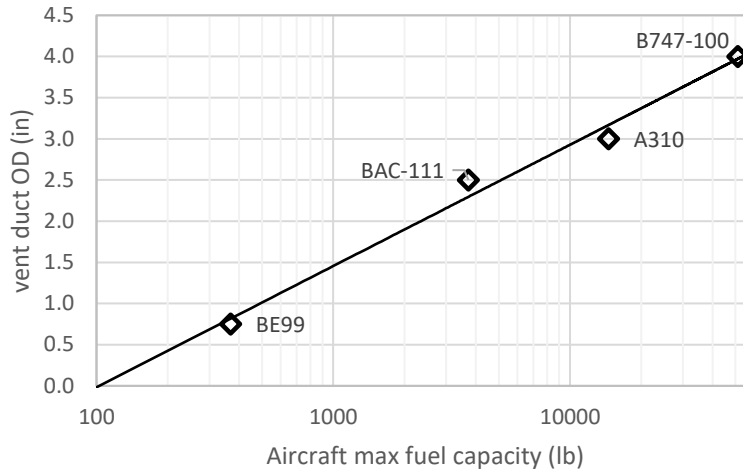


Figure 20: Trend of vent duct OD as a function of max fuel capacity

The trend against fuel capacity is shown in Figure 20, and the curve fit relationship is represented by eq. (24) below.

$$OD(\text{in}) = 0.6396 \ln(W_{F,USG}) - 2.963 \quad (24)$$

A review of the vent schematics in Appendix C yields the following proposed rules to estimate the weight of the vent subsystem and are implemented in the ASSET tool:

- 1) All aircraft are assumed to have an expansion space built into the wing structure near the wing tips, similar to the arrangement shown in Figure 19 (b), including on business aircraft. The ASSET methodology does not count the weight of the surge tanks since it is assumed that they are integral to the wing structure, similar to the wing tanks.
- 2) Two vent ducts per wing tank are defined. One allows for venting while the aircraft is in a dive attitude and the other for when it is in a climb attitude. Both connect to the inboard wall of the surge tank. Connections to auxiliary tanks are not considered since their arrangement configurations vary between aircraft models, and it is difficult to generate a consistent algorithm to account for these connections automatically.
- 3) Each vent duct branches to an opening inside each main tank compartment. This configuration allows for redundant venting passages to meet the safety requirements of Parts 23.975 [27] and Part 25.975 [30].
- 4) Each vent opening is fitted with a float-operated valve to minimize fuel entering the vent ducts. Four float valves per tank are used for a typical arrangement similar to Figure 14.
- 5) The length of each duct is estimated by determining the spanwise distance between the surge tank's inboard corner and the main tank's inboard corner, as shown in Figure 19. Eq.(24) calculates the duct OD from the data collected by Weitz [39]. The duct weight can be estimated by determining the wall thickness using the two tables in Appendix A.3.

- 6) The weight of the float valves, air inlet scoop, and flame arrestor devices is determined in Table 13.

The vent ducts are the most significant component of the subsystem since their length contributes most of the weight.

4.6 Validation of the Proposed Method and Ancillary Components Weight Factor Definition

The previous subsections outline the process for estimating the weight of each of the four fuel subsystems. However, it does not capture the weight of small components, such as filters, check valves, fittings, brackets, and wiring harnesses. The weight of sealer material can also add to the system weight and can be estimated based on the algorithm from Olives [33]. However, for this methodology, a bulk factor may be assumed to be a percentage of the sum of the other four subsystem weights (Feed, Transfer, FQI, and Venting).

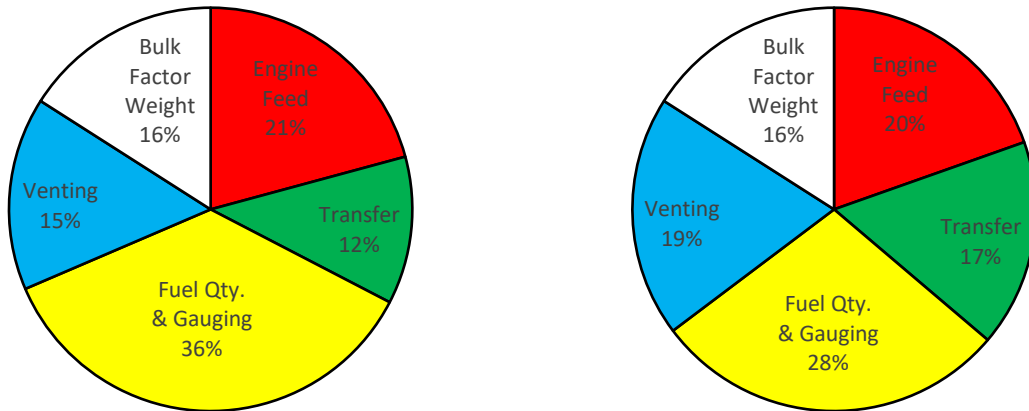
Table 14: Fuel subsystem weight estimation for commuter/regional aircraft

Aircraft	ASSET FS Weight Estimates (lb)					Actual FS Weight (lb)	Delta weight (lb)
	Feed	XFR	FQI	Vent	TOTAL		
A320	147.5	135.3	125.1	215.5	623.5	659.2	-35.7 (-5.4%)
ATR42	41.3	35.0	60.0	40.7	177.0	196	-19 (-9.6%)
A300B2	204.4	200.6	147.1	120.4	672.3	1257	-584.7 (-46.5%)
B737-2	143.6	125.6	87.5	119.9	476.6	575	-98.4 (-17.1%)
F27	60.8	34.6	105	45.2	245.6	390	-144.4 (-37.0%)
C550	39.5	30.9	42.5	36.1	149.0	189	-40.0 (-21.2%)
LJ28	65.0	67.5	40.4	64.3	237.2	237	0.0 (0.0%)

Table 14 shows the weight of each subsystem as estimated by the methodology, which for the aircraft shown is typically below the actual weight published in the literature. The delta weight varies between aircraft without a clear pattern. It may be affected by the construction of materials, the type of technology, and the exact number of small components in each system.

Even so, the relatively large delta weight of the F27 (-37.0%) compared to the delta weight of the ATR42 (-9.6%) may be attributed to the following differences between the two aircraft: A) The F27 features an externally mounted engine feed collector tanks, whereas the ATR42 features collector compartments built into the main wing tanks. Therefore additional mounting hardware such as brackets, fasteners, tubing, and fittings may be required on the F27. B) The F27 uses eight interconnected bladder cells as part of the main wing tanks, requiring mounting brackets, fasteners, tubing, and fittings. In contrast, the main wing tanks on the ATR42 are completely integral, eliminating these extra components. C) Both aircraft feature capacitance-type fuel quantity probes, but the F27 includes a resistance-type probe with an integrated overflow valve in the bladder cells that adds weight. The bladder tanks on the F27 also need tubes that interconnect the ullage spaces in the cells to the main vent lines, which are not required on the integral

wing tanks of the ATR42. The delta weight also shows significant variation between the aircraft in Table 14. It is difficult to make a meaningful assessment of whether larger variations are expected for larger fuel systems. Therefore, the percent difference attributed to ancillary components is averaged and assumed to be approximately 19.5%, but further assessment may be required.



(a) F27 fuel system weight estimated by the ASSET methodology is 292 lb. The actual system weight is 390 lb [20].

(b) ATR42 fuel system weight estimated by the ASSET methodology is 210 lb. The actual system weight is 196 lb [31].

Figure 21: Fokker F27 and ATR42 estimated fuel system weight breakdown

Figure 21 compares the percent weight distributions of the major subsystems for the F27 and ATR42. The ATR42 has a slightly larger fuel capacity (5700 L or 1505 USG) than the F27 (5136 L or 1357 USG), but the distribution among the four subsystems is very similar. The major differences are less than 10% and appear in the fuel quantity & indicating subsystem, the fuel transfer subsystem, and the tank venting subsystem. However, as previously explained, the differences can be explained by the analysis of the components in the system schematics in Appendix C. The additional weight of the F27 system (actual weight of 390 lb) compared to the ATR42 (actual weight of 196 lb) may be attributed to the use of interconnected bladder cells in the F27. Since the estimation method cannot accommodate the use of bladder cells, it predicts a lower weight for the F27, meaning that further investigation would be required to adapt the method for these tanks.

4.7 ASSET Tool Implementation in MS Excel

This section gives a brief overview of the implementation of the tool. MS Excel allows a visual representation of the geometry input required for the weight estimation calculations. However, a future iteration of this tool will likely be done using Python, allowing it to interface with other tools in development by the Air Systems Lab.

The implementation consists of a single Excel workbook with various sheets:

INPUTS	Contains all the input parameters necessary to define the geometry of the aircraft and specific characteristics that will define the fuel system architecture (for example, the number of engines, engine type, engine fuel flow at take-off, etc.)
Aircraft Geometry	This sheet visually outputs the airframe geometry and plots the engine interface points.
Engine Feed	This sheet outputs all the calculations and visual representations associated with the fuel tank boundaries, the location of the engine feed pumps, and the routing of the engine feed lines. It also performs the calculations for the number of engine feed components, such as the number and weight of feed pumps, shut-off valves, fuel lines, etc.
Fuel Transfer	Contains the outputs of the calculations and visual representations of the fuel transfer subsystem and how it interacts with the engine feed circuitry.
FQIS	This sheet outputs the number and weight of fuel quantity probes and associated electronics/avionics equipment.
Vent	Outputs the calculated fuel venting subsystem weight and visualizes the major components of the subsystem.
Dashboard	This sheet summarizes the tool outputs in terms of estimated fuel system weight. The Roskam and Torenbeek calculations are added for comparison. They require a known fuel mass (either total fuel or total usable fuel) and fuel density constant along with other pertinent aircraft data (percent of integral fuel tanks, maximum operating flight speed, number of engines, and number of fuel tanks).

Aircraft Fuel System Weight Estimation - ASSET

Required Inputs

Required Fuel System Input Parameters

Parameter	Units	Description
17	Wingspan [m]	Aircraft wingspan (does not include winglets, sharklets, wing tip fences, etc).
2	N_e [-]	Number of propulsion engines on aircraft
4	Eng [-]	Propulsion Engine type (1 = turbofan, 2 = turboprop, 3 = turboshaft, 4 = fuel flow requirements)
550	WFF [pph]	Propulsion engine fuel flow @ TO setting
0	CWT [-]	1 = Aircraft has a center wing tank (CWT); else set to zero
0	MOTIVE [-]	1 = Engines provide fuel motive flow; else set to zero
0	APU N/A	1 = Aircraft has an APU; else set to zero
0	INBD_FEED N/A	1 = Feed collectors (and pumps) are located in the CWT (ex. CRJ); can only be used with CWT = 1
15.0%	B_XFWD [%]	Defines the location of the front spar based on the WS points as a percentage of the airfoil section chord relative to the wing LE. Default value should be 15%.
25.0%	B_XAFT [%]	Defines the location of the aft spar based on the WS points as a percentage of the airfoil section chord relative to the wing TE. Default value should be 25%.
90.0%	B_YWT [%]	Defines the location of the outboard-most wing tank wall as a percent of the half-wingspan.
0	PRD N/A	Pressure refueling/defueling capability (1 = pressure refueling/defueling available)
0	CGCTRL N/A	Longitudinal CG control capability (1 = cg control capability available)
0	LXFER N/A	1 = Lateral fuel transfer capability
0	RECEPT N/A	0 = gravity refueling, 1 = single point pressure refuel adapter, 2 = dual point pressure refuel adapter; PRD must = 1
2	TCCAT N/A	1 = Normal Category, 2 = Commuter, 3 = Transport
13.5	t_wing in	Average wingbox thickness (height)
0	CWT_FUS N/A	CWT_FUS = 0 indicates fuselage tank, CWT_FUS = 1 indicates a CWT
1	W_FCT lb	Center tank fuel capacity (lb)

Aircraft Geometry Inputs

Fuselage Stations

	Left Side			Right Side		
	X (m)	Y (m)	Z (m)	X (m)	Y (m)	Z (m)
FS01	1.720	0.000	0.000	1.720	0.000	0.000
FS02	4.313	-0.816	0.000	4.313	0.816	0.000
FS03	11.347	-0.816	0.000	11.347	0.816	0.000
FS04	16.757	0.000	0.000	16.757	0.000	0.000

Wing Stations & Engine Interface

Component/Reference	Left Side			Right Side			Component/Reference
	X (m)	Y (m)	Z (m)	X (m)	Y (m)	X (m)	
LH Engine Interface	6.740	-2.363	0.000	6.740	2.363	0.000	RH Engine Interface
APU Interface			0.000	0.000	0.000	0.000	N/A
WS00LE	7.050	0.000	0.000	7.050	0.000	0.000	
WS01LE	7.063	-0.783	0.000	7.063	0.783	0.000	
WS02LE	7.086	-2.116	0.000	7.086	2.116	0.000	
WS03LE	7.086	-2.843	0.000	7.086	2.843	0.000	
WS04LE	7.659	-7.047	0.000	7.659	7.047	0.000	
WS05LE	9.107	-8.485	0.000	9.107	8.485	0.000	
WS05TE	9.268	-8.489	0.000	9.268	8.489	0.000	
WS04TE	9.307	-7.047	0.000	9.307	7.047	0.000	
WS03TE	9.413	-2.843	0.000	9.413	2.843	0.000	
WS02TE	9.413	-2.116	0.000	9.413	2.116	0.000	
WS01TE	9.413	-0.783	0.000	9.413	0.783	0.000	
WS00TE	9.413	0.000	0.000	9.413	0.000	0.000	

Horizontal Stabilizer Geometry

TP00LE	15.459	0.000	0.000	15.459	0.000	0.000
TP01LE	15.498	-2.879	0.000	15.498	2.879	0.000
TP01TE	16.774	-2.879	0.000	16.774	2.879	0.000
TP00TE	16.774	0.000	0.000	16.774	0.000	0.000

Aircraft top view: Twin wing mounted engine aircraft

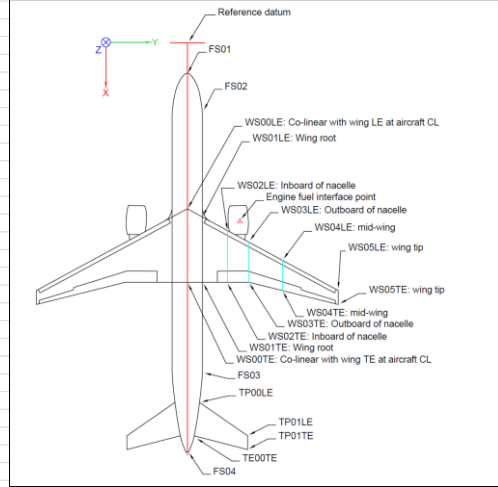


Figure 22: ASSET inputs page

Aircraft Geometry Data

This data is specific to the Twin Commander 690B aircraft

X	Y	Z
(m)	(m)	(m)

Param Units

17.0 Wingspan m

1

- (1) Define the following aircraft parameters:
- Location of reference datum (x,y,z)
 - MAC
 - Wingspan
 - Fuselage width

Fuselage Stations

	Left Side			Right Side		
	X	Y	Z	X	Y	Z
	(m)	(m)	(m)	(m)	(m)	(m)
FS01	1.720	0.000	0.000	1.720	0.000	0.000
FS02	4.313	-0.816	0.000	4.313	0.816	0.000
FS03	11.347	-0.816	0.000	11.347	0.816	0.000
FS04	16.757	0.000	0.000	16.757	0.000	0.000

0

- (0) Optionally, define the boundaries of the fuselage (for visual purposes only). Enter the point coordinates for the LH side; the RH side is the mirror of the LH.

Geometry Points for Wing Stations & Engine Interface

Component/Reference	Left Side			Right Side			Component/Reference
	X	Y	Z	X	Y	X	
	(m)	(m)	(m)	(m)	(m)	(m)	
LH Engine Interface	6.740	-2.363	0.000	6.740	2.363	0.000	RH Engine Interface
APU Interface	0.000	0.000	0.000	0.000	0.000	0.000	N/A
WS00LE	7.050	0.000	0.000	7.050	0.000	0.000	
WS01LE	7.063	-0.783	0.000	7.063	0.783	0.000	
WS02LE	7.086	-2.116	0.000	7.086	2.116	0.000	
WS03LE	7.086	-2.843	0.000	7.086	2.843	0.000	
WS04LE	7.659	-7.047	0.000	7.659	7.047	0.000	
WS05LE	9.107	-8.485	0.000	9.107	8.485	0.000	
WS05TE	9.268	-8.489	0.000	9.268	8.489	0.000	
WS04TE	9.307	-7.047	0.000	9.307	7.047	0.000	
WS03TE	9.413	-2.843	0.000	9.413	2.843	0.000	
WS02TE	9.413	-2.116	0.000	9.413	2.116	0.000	
WS01TE	9.413	-0.783	0.000	9.413	0.783	0.000	
WS00TE	9.413	0.000	0.000	9.413	0.000	0.000	
TP00LE	15.459	0.000	0.000	15.459	0.000	0.000	
TP01LE	15.498	-2.879	0.000	15.498	2.879	0.000	
TP01TE	16.774	-2.879	0.000	16.774	2.879	0.000	
TP00TE	16.774	0.000	0.000	16.774	0.000	0.000	

2

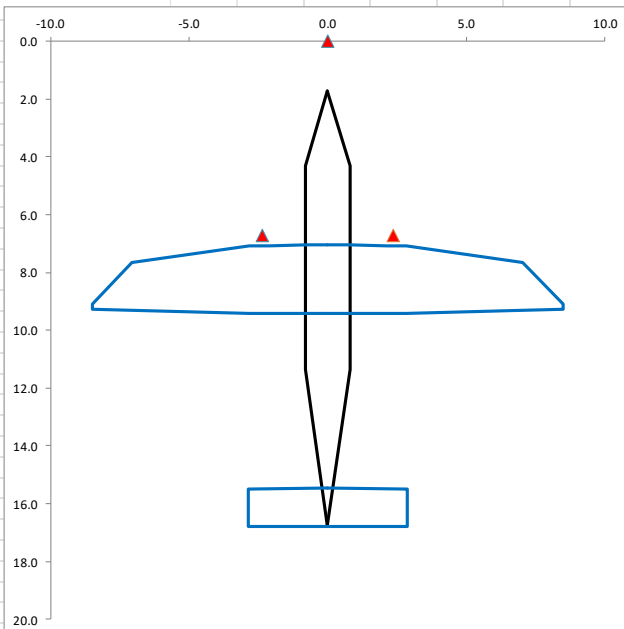
- (2) Define the location of the engine and APU (if any) interfaces; enter the (x,y,z) coordinates on the LH side. If the aircraft does not have an APU, enter zero for the coordinates.

3

- (3) Define the wing station points based on the diagram shown to the right. **NOTE: All WSxxTE points must have the same y-coordinate as their corresponding WSxxLE.**

0

- (0) Optionally, define the horizontal stabilizer (for visual purposes only).



Output

Plot shows the top view of the aircraft geometry. The engine fuel interface is represented by the red triangles.

Once the aircraft geometry is defined, move on to the Engine Feed tab.

Figure 23: ASSET Aircraft Geometry view

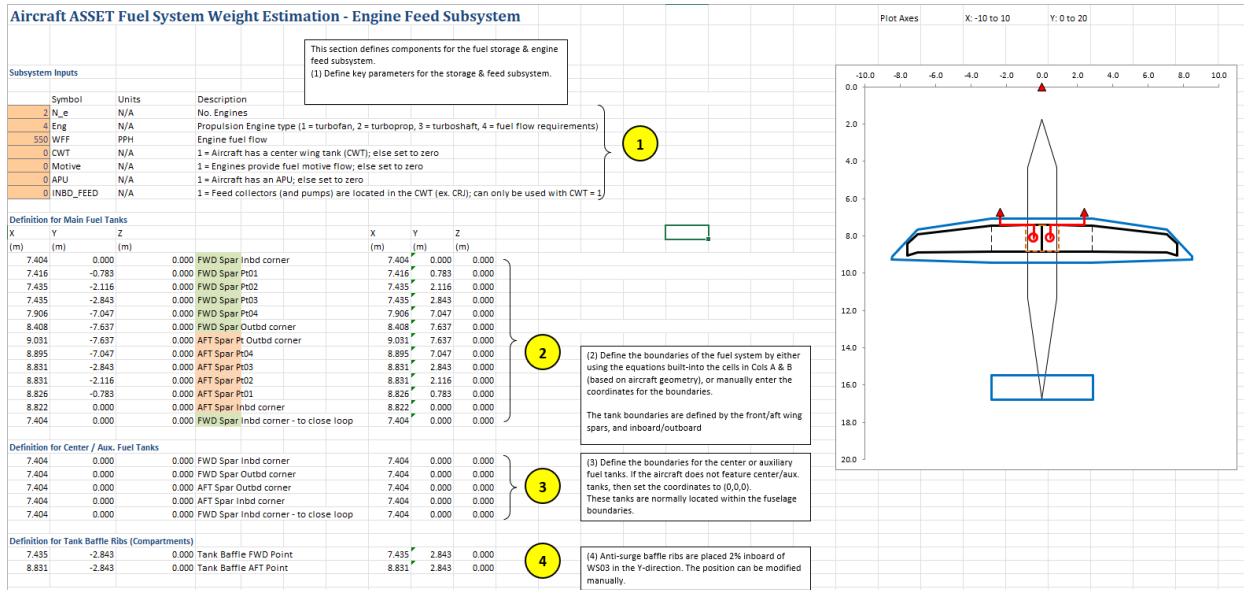


Figure 24: ASSET Engine Feed subsystem view

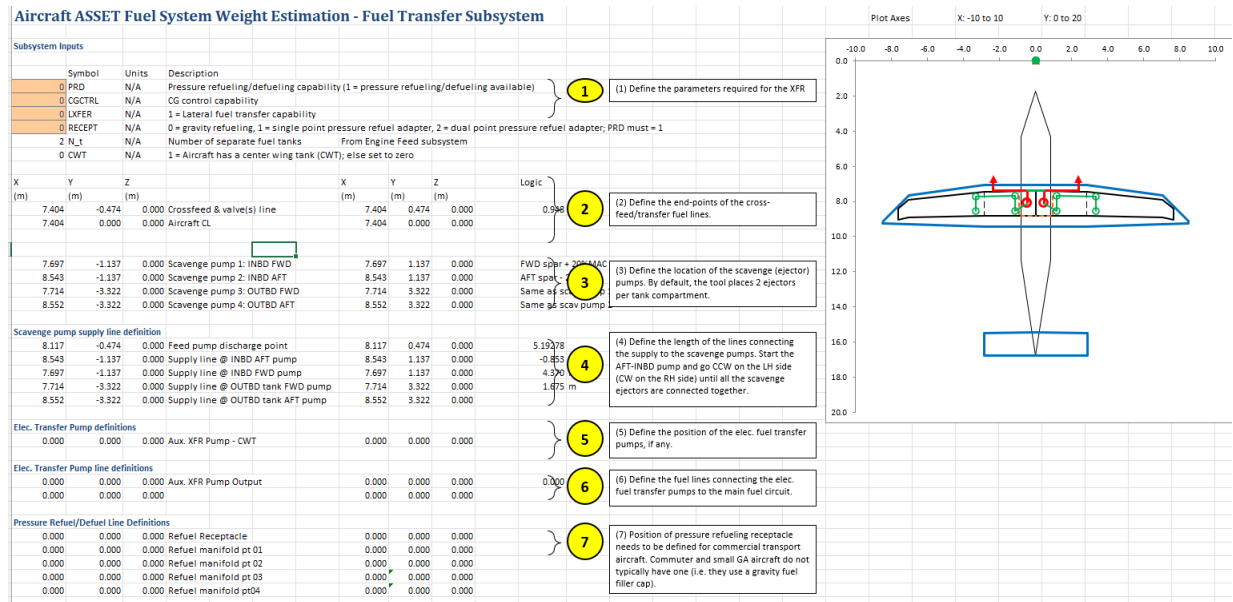


Figure 25: ASSET Fuel Transfer subsystem view

Aircraft ASSET Fuel System Weight Estimation - Fuel Quantity & Indicating			
Subsystem Inputs			
Symbol	Units	Description	
2 TCCAT	N/A	1 = Normal Category, 2 = Commuter, 3 = Transport	1 (1) Define aircraft category, wing thickness.
13.5 t_wing	in	Average wingbox thickness (height)	
0 CWT_FUS	N/A	CWT_FUS = 0 indicates fuselage tank, CWT_FUS = 1 indicates a CWT	
1 W_FCT	lb	Center tank fuel capacity (lb)	
55.760 S	ft	Aircraft wingspan	0 (0) Check these values from other tabs, in particular to num tanks (N_t), CWT availability (CWT), and span of the wing tanks (S_t)
0 PRD	N/A	1 = Pressure refueling/defueling capability available	
2 N_t	N/A	Number of separate fuel tanks From Engine Feed subsystem	
0 CWT	N/A	1 = Aircraft has a center wing tank (CWT); else set to zero	
25.1 S_t	ft	Tank span	
Definition for FQI Probe Locations			
			Major Ribs
Subsystem Outputs			
Symbol	Units	Description	Logic
12 N_wingprobes	N/A	Total number of wing tank FQI probes	Min 3 probes per tank. For conventional propulsions aircraft, number of probes in wing tanks increase as
0 N_cwtprobes	N/A	Total number of CWT FQI probes	Need logic for number of probes in CWT, must have a min of 3
12 L_plavg	in	Average probe length	90% of average wing thickness (height)
18.2 W_probes	lb	Probe weight	
0 W_rdcpl	lb	Weight of refuel/defuel control panel	Assume one panel, weighing
11 W_fcic	lb	Weight of fuel quantity computer/avionics	Assume one unit for transport category
0 W_fpmu	lb	Weight of fuel properties measurement units	Assume one unit per tank, each unit weight 3.5 lb
29.2 W_FQIS	lb	Total weight of FQI subsystem	

Figure 26: ASSET FQIS view

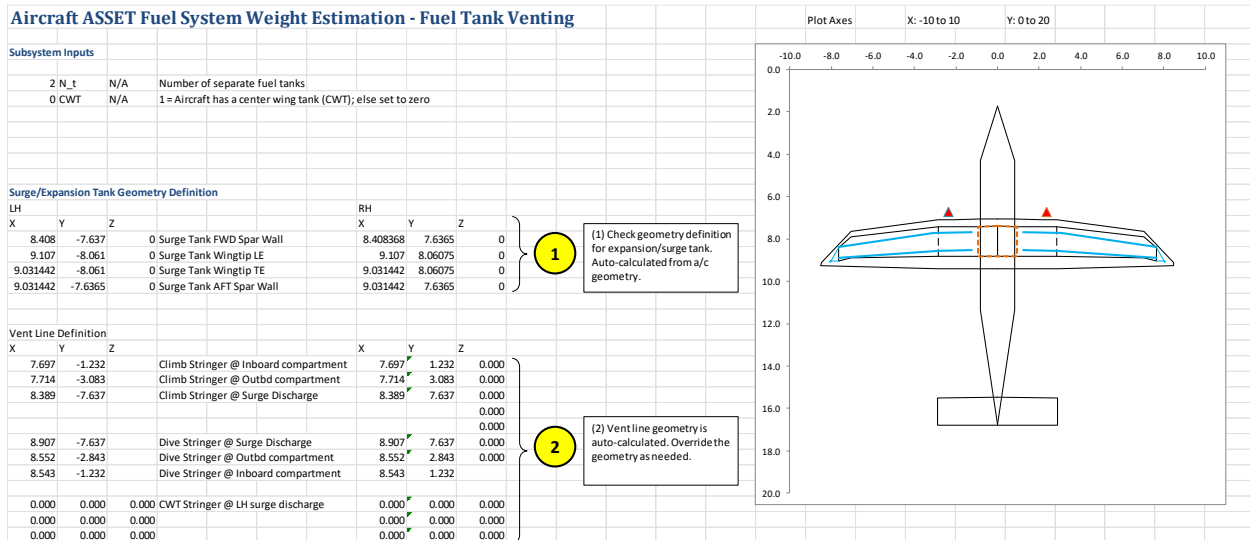


Figure 27: ASSET Vent subsystem view

Aircraft Fuel System Weight Estimation - ASSET

1

Aircraft: Aircraft

207.9 Total Fuel System Weight (lb) 659.1754 Obert FS weight (lb)

Wt. (lb) Subsystem

- 64.6 Engine Feed
- 29.0 Transfer
- 29.2 Fuel Qty. & Gauging
- 37.2 Venting
- 48 Bulk Factor Weight

Fuel System Estimation for Plots

- 207.9 ASSET
- 2521 Cessna
- 1615 USAF
- 631 Torenbeek
- 806 GD
- 650 NASA FLOPS

2

0.3 WFLFactor

0.3 WBulkFactor

This Dashboard provides a summary of the outputs of each of the fuel subsystem tabs (Engine Feed, Fuel FQIS, and Vent).

(1) Ensure the aircraft model/name is defined in cell A2.

(2) For each of the SOA methods, need to enter the following information: total fuel or total usable fuel. S to either 6.71 for jet fuel or 5.78 for Av-Gas.

Begin using the tool by following the instructions on the Aircraft Dimensions tab.

ASSET FS Weight Estimation Breakdown

Subsystem	Weight (lb)	Percentage
Engine Feed	218.1	33%
Bulk Factor Weight	150.0	23%
Venting	106.2	18%
Fuel Qty. & Gauging	95.3	14%
Transfer	75.2	12%

Roskam FS Weight Estimation Methods

Cessna Method

$$W_{fs} = 0.40W_f / K_{fsp}$$

6.71 K_fsp lb/USG

Applicable to DO-228 since it has an internal fuel system

Total fuel (L)

Total usable fuel (L)

6325 Total fuel (USG)

6303 Total usable fuel (USG)

42441 Total fuel mass (lb)

42293 Total usable fuel mass (lb)

2530 W_FS Total

2521 W_FS Usable

Fuel System Weight Estimations

Aircraft	Est. Weight (lb)
ASSET	~200
Cessna	~2500
USAF	~1600
Torenbeek	~600

Engine Feed Subsystem			Fuel Transfer Subsystem				
Value	Parameter	Units	Description	Value	Parameter	Units	Description
2	N_t	N/A	Number of separate fuel tanks	0	N_txpump	N/A	Number of electrical transfer pumps
4	N_bp	N/A	Number of electric boost pumps	8	N_scavpui	N/A	Number of ejector type scavenge pumps
0	N_jp	N/A	Number of feed ejector/jet pumps	0	JETTISON	N/A	Jettison system required
2	N_fsov	N/A	Number of fuel shut-off valves	0	L_jett	N/A	Jettison system line length
0.527361	OD_feed	inches	Engine feed line outer diameter	1.5	OD_xfer	inches	Fuel transfer line OD
21.4	L_feed	ft	Combined engine feed line length	33.7	L_xfer	ft	Combined transfer line length
1.3	W_lines	lb	Combined engine feed line weight	4.5	W_xferlin	lb	Combined fuel transfer line weight
56.0	W_bp	lb	Combined weight of electric boost pumps	20.1	W_scavpu	lb	Combined weight of scavenge pumps (ejector)
7.2	W_fsov	lb	Combined weight of fuel shut-off valves	0	W_xferpu	lb	Combined weight of electric transfer pumps
0	W_jp	lb	Combined weight of ejector/jet pumps	4.4	W_valves	lb	Combined weight of transfer valves
404.5	V_wtank	USG	Estimated wing fuel tank capacity (per wing)				
64.6	W_FEED	lb	Weight of engine feed subsystem	29.0	W_XFR	lb	Weight of fuel transfer subsystem

Figure 28: ASSET Dashboard and weight estimation outputs

This section presents an overview of the tool interface, the required inputs, calculations, and processes that determine the outputs. The tool's implementation subdivides the aircraft fuel system into four major areas whose individual component weights are estimated and summed to determine the overall system weight. The estimation algorithms for each subsystem follow similar methodologies to the work from Olives [33] but with various changes that accommodate the fuel system architectures for commuter and regional aircraft.

5 Validation and Application to Hybrid-Electric Case Studies

The validation and results of the ASSET architecture-based fuel system weight estimation outlined in the previous chapter are presented in this section. Two case studies for hybrid-electric propulsion aircraft based on the existing DO228 and ATR42 airframes are also demonstrated. For each case study, two proposed configurations show possible placement options for the fuel tanks and battery compartments.

The hybrid-electric case studies considered in this section assume that a certain reduction in the usable fuel volume will be achieved due to the degree of hybridization of the aircraft, and any reduction in the fuel storage capacity can be allocated for electrical energy storage. Since most aircraft store the fuel in integral wing tanks, it is logical that batteries can replace any space not used for fuel. Should it be necessary to add more batteries to the configuration, additional space will need to be identified in the fuselage, such as in a cargo bay or near the main cabin.

5.1 ASSET Validation for Conventional Aircraft Fuel Systems

The ASSET methodology developed in the previous chapters takes on an architecture-based approach to estimating the weight of aircraft fuel systems by looking at the architecture and system components. This subsection compares its performance to the existing state-of-the-art methods for a series of aircraft in the Roskam database. Table 15 below compares the ASSET architecture-based model to the Torenbeek, and NASA FLOPS predictions for aircraft ranging from small business jets to regional turboprops and airliners.

Table 15: Torenbeek, NASA FLOPS, and ASSET FS Weight Estimations for commercial aircraft

Aircraft	Aircraft Class	Actual Weight, lb [20], [31]	ASSET Estimation, lb	Torenbeek, lb	NASA FLOPS, lb
A300 B2	Airliner	1257	800 (-36.3%)	1077 (-14.3%)	927 (-26.3%)
A320-200	Airliner	659	742 (+12.6%)	631 (-4.2%)	648 (-1.6%)
ATR42	Regional	196	211 (+7.4%)	483 (+146%)	248 (+26.5%)
B737-200	Airliner	575	558 (-3.0%)	768 (+33.6%)	579 (+0.6%)
F-27/1	Regional	390	292 (-25.1%)	307 (-21.3%)	224 (-42.6%)
C550	Business jet	189	177 (-6.2%)	432 (+129%)	180 (-4.8%)
LJ28	Business jet	237	282 (+19.1%)	550 (+132%)	182 (-23.2%)

The predictions from the FLOPS model align especially well for the A320 and B737 with errors less than $\pm 2\%$. However, the ASSET prediction is a manageable 7.4% for the ATR42, whereas the FLOPS is over 20%, and the Torenbeek is very high at 146%. Finally, the ASSET and FLOPS methods compare reasonably well for the two business jets, the LJ28 and C550, with the differences being less than 15 lb from the published data, equivalent to less than $\pm 10\%$ error.

5.2 Case Study 1: Dornier 228

The DO228 is a 15-19 passenger, twin-turboprop commuter aircraft developed in the 1980s with a range maximum range of 724 NM for the -100 model and a more limited 323 NM for the -200 model. The -100 is the basic with a maximum 15-passenger capacity, while the -200 model features a lengthened fuselage and accommodation for up to 19 passengers and a larger baggage compartment. The DO228 is certified under the Part 23 normal category and is considered a commuter-type aircraft.

5.2.1 Conventional DO228 Fuel System

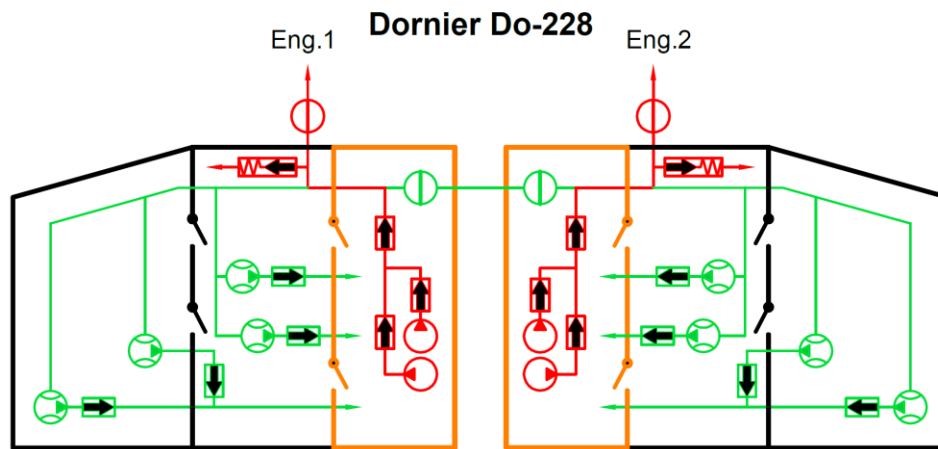


Figure 29: Conventional propulsion DO228-100 fuel system

As shown in Figure 29 above, the fuel system supplies fuel to each engine from a dedicated integral wing tank through two 28VDC boost pumps. These pumps also supply fuel to five scavenge ejector pumps located in each wing tank and through the cross-feed fuel line to the other wing tank. The aircraft does not have an APU or a pressure refueling system (i.e., refueling/defueling is accomplished by gravity).

The relevant specifications [40], [48], [49] of the aircraft and its fuel system are provided in Table 16, and the geometry points are defined in Figure 30 below.

Table 16: DO228-100 conventional aircraft fuel system and geometry parameters

Total fuel	2440 L / 4250 lb [49]
Usable fuel	2386 L / 4155 lb [49]
Estimated fuel tank wing area (per wing)	6.924 m ² / 74.53 ft ²
Estimated average wing thickness	6.78 in
Propulsion engines	TPE331-5-252D [49]
Estimated Propulsion engine fuel flow @ TO power	550 pph (engine data)

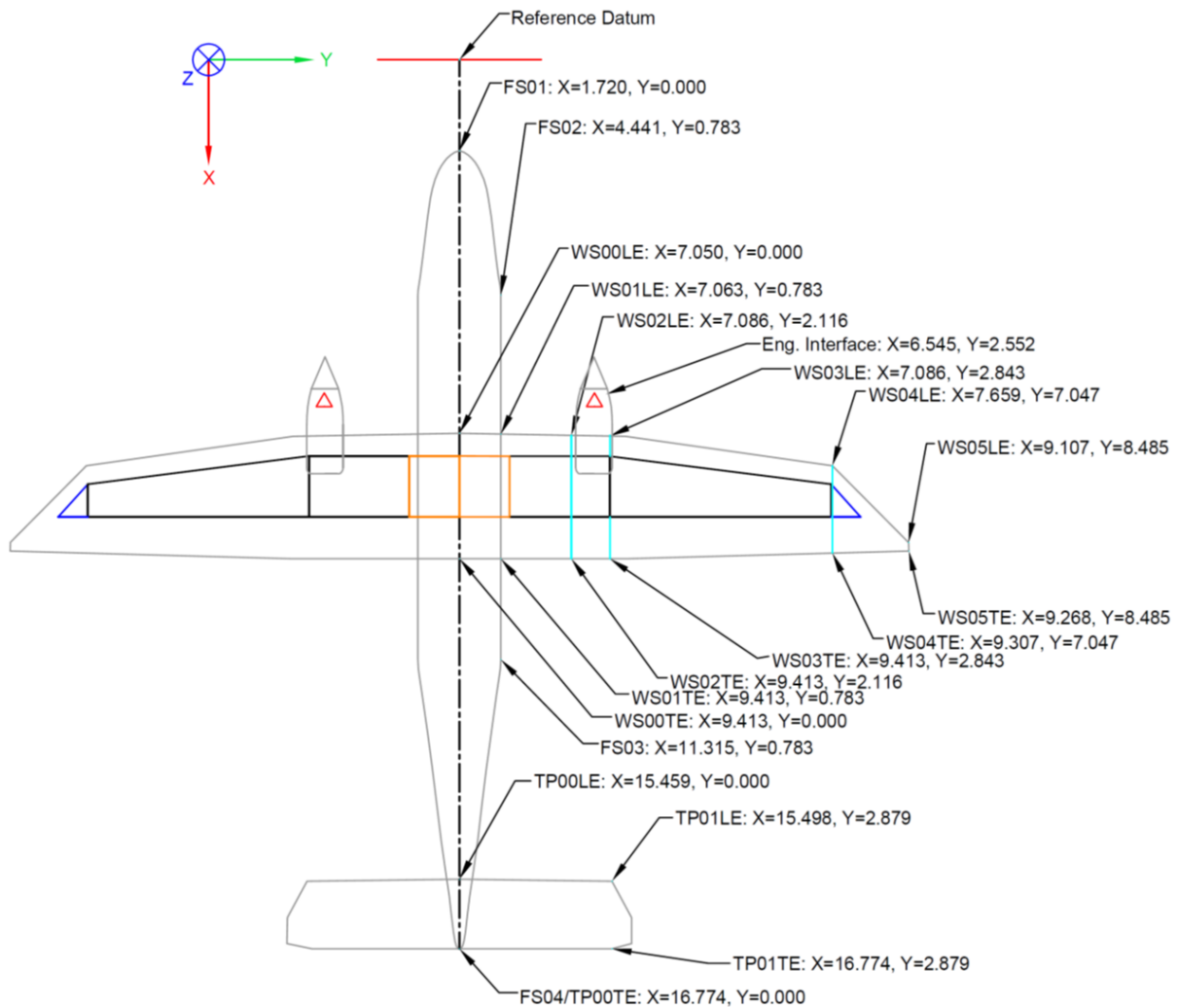


Figure 30: DO228-100 aircraft geometry

This aircraft is not equipped with an APU or a pressure refueling circuit, so these components are excluded from the analysis. The conventional fuel system weight for this aircraft is estimated to be 157.3 lb and is broken down into the various subsystems in Table 17.

Table 17: ASSET estimation weight breakdown for the DO228-100 fuel system

	Actual	ASSET Estimation
Engine Feed Subsystem Weight	N/A	64.7 lb
Number of electrical feed pumps	4	4
Number of ejector feed pumps	0	0
Number of shutoff valves	2	2
Estimated fuel line OD	N/A	0.53 in
Feed line length	N/A	21.4 ft
Fuel Transfer Subsystem Weight	N/A	29.0 lb
Number of scavenge pumps	8	8
Number of electrical transfer pumps	0	0
Estimated transfer fuel line OD	N/A	1.50 in
Transfer fuel system line length	N/A	33.67
Fuel Quantity & Indicating Subsystem Weight	N/A	29.2 lb
Total number of wing tank probes	10	12
Number of center tank probes	0	0
Additional FQI components	Fuel Low-level switch Fuel flow indicators (cockpit) Fuel counter (cockpit) Fuel tank quantity indicator selector switch 28V Turbine fuel flow meter Fuel pressure switches	Fuel quantity & indication management avionics
Fuel Venting Subsystem Weight	N/A	37.2 lb
Estimated vent duct OD	N/A	1.32 in
Estimated vent duct length	N/A	84.5 ft
Ancillary Components Weight	N/A	30 lb

Table 18: Comparison of FS weight estimation methods for conventional DO228-100

FS Weight Estimation Method	Estimated Weight (lb)
ASSET	190
Cessna	252
USAF	275
Torenbeek	420
NASA FLOPS	134

Table 18 above compares the ASSET weight prediction with the state-of-the-art models discussed in chapter 2. The absence of data for this aircraft makes it difficult to compare the models, but the one that stands out is the Torenbeek method showing a weight of 420 lb for this type of aircraft. In the previous chapter, the performance of the ASSET and Torenbeek methods was compared for the ATR42, which is a larger aircraft with a greater fuel capacity and more powerful engines than the DO228. The Torenbeek-

predicted fuel system weight of 483 lb for the ATR42 is only about 15% more than its prediction for the DO228. The published data for the ATR42 also shows that the Torenbeek prediction error is over 140%, meaning that the DO228 prediction is likely over-estimated. The spread of predicted values from the other methods indicates a window of 141 lb, which, relative to the heaviest of these (the USAF method), could mean an error up to 50%.

5.2.2 Hybrid-Electric Configurations 1 & 2

Two hybrid-electric configurations are investigated below, assuming the airframe dimensions and geometrical characteristics are maintained. It is also assumed that reducing the fuel tank volume by 75% of the original capacity will create a space in the wing box. Configuration HE01 is characterized by placing the fuel tanks inboard of the nacelles, close to the aircraft centerline, and the batteries occupying most of the wing box space, as shown in Figure 31. Placing the batteries outboard of the nacelles can benefit wing load alleviation due to the battery weight. However, the centralized location of the fuel tanks requires longer vent ducts passing over the batteries to connect to the surge tanks. Placement of the fuel tanks near the passenger cabin will also need additional consideration from a safety perspective.

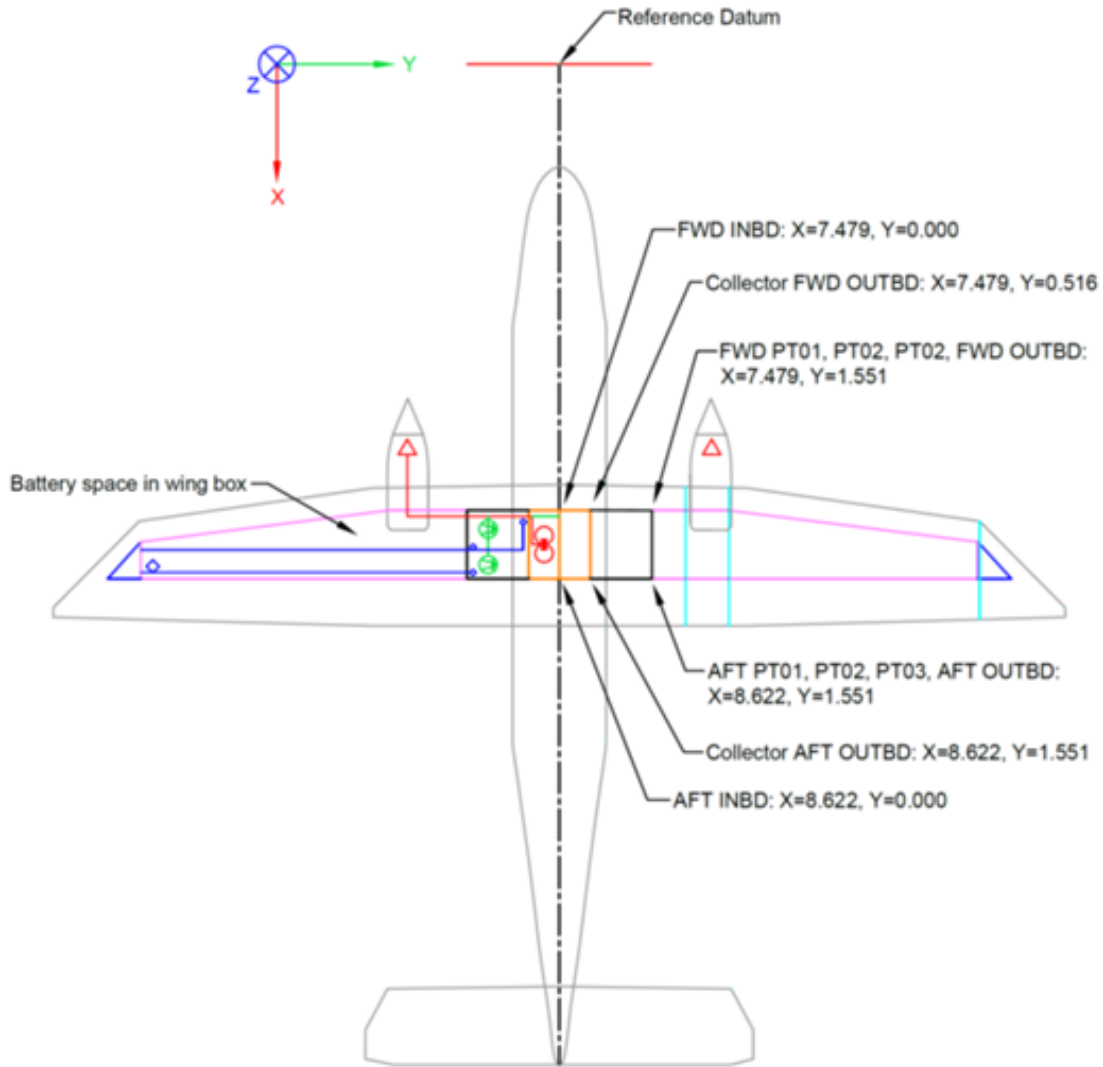


Figure 31: DO228-100 hybrid-electric configuration HE01

Configuration HE02 inverts the placement of the fuel tanks and the batteries such that the fuel tanks are now placed near the wingtips while the batteries occupy the remaining space, as illustrated by Figure 32. Configuration HE02 shortens the length of the ventilation ducting since the main tanks are close to the surge tanks but increases the crossfeed line length.

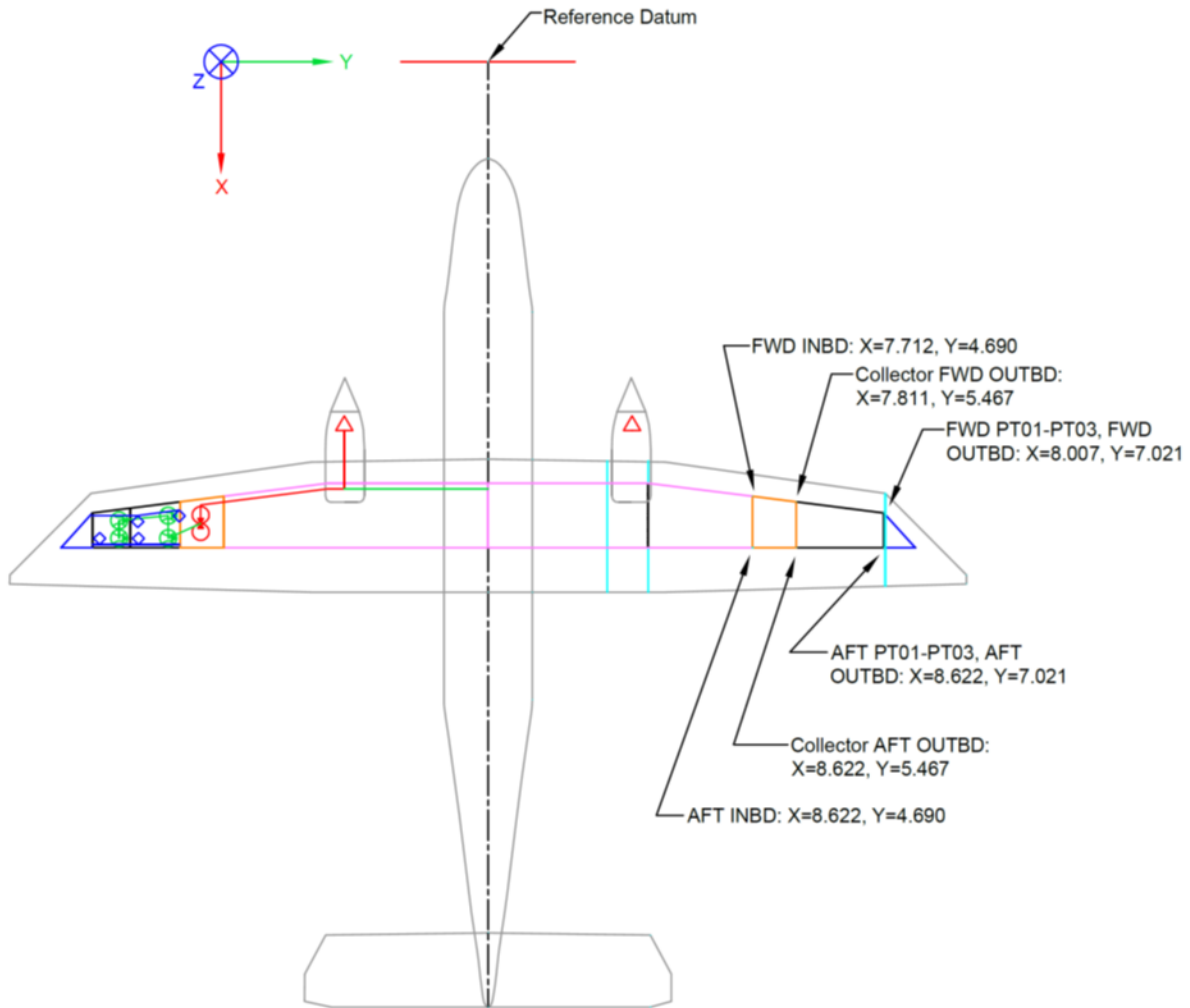


Figure 32: DO228-100 hybrid-electric configuration HE02

The ASSET estimated fuel system weights for the various DO228 configurations are given in Table 19 below.

Table 19: ASSET fuel system analysis for the DO228 configurations

	Actual	ASSET - Conventional	ASSET – HE01	ASSET – HE02
Engine Feed Subsystem Weight	N/A	64.7 lb	64.7 lb	64.9 lb
Number of electrical feed pumps	4	4	4	4
Number of ejector feed pumps	0	0	0	0
Number of shutoff valves	2	2	2	2
Estimated fuel line OD	N/A	0.53 in	0.53 in	0.53 in
Feed line length	N/A	21.4 ft	23.1 ft	26.3 ft
Fuel Transfer Subsystem Weight	N/A	29.0 lb	26.7 lb	30.8 lb
Number of scavenge pumps	8	8	8	8
Number of electrical transfer pumps	0	0	0	0
Estimated transfer fuel line OD	N/A	1.5 in	1.5 in	1.5 in
Transfer fuel system line length	N/A	33.67 ft	16.6 ft	47.5 ft
Fuel Quantity & Indicating Subsystem Weight	N/A	29.2 lb	20.1 lb	20.1 lb
Total number of wing tank probes	10	12	6	6
Number of center tank probes	0	0	0	0
Fuel Venting Subsystem Weight	N/A	37.2 lb	30.9 lb	27.7 lb
Estimated vent duct OD	N/A	1.32 in	0.53 in	0.53 in
Estimated vent duct length	N/A	84.5 ft	88.2 ft	23.8 ft
Ancillary Components Weight	N/A	30 lb	27 lb	27 lb
Total Fuel System Weight	N/A	190.3 lb	169.5 lb	170.7 lb

The estimation results show consistent weight reduction is achieved in the fuel quantity indication subsystem and the fuel tank venting subsystem due to the reduction in fuel volume. A reduced fuel volume means fewer fuel quantity probes are required, hence less wiring and possibly less heavy fuel management electronics. The venting subsystem also takes advantage of the reduced fuel volume because the vent duct diameter can be reduced.

Table 20: Comparing conventional and hybrid-electric DO228 fuel system weight predictions

Estimation Method	Conventional, lb	Hybrid-electric, lb (ΔW_{fs} relative to conventional)
Cessna	252	65 (-74%)
USAF	275	113 (-59%)
Torenbeek	421	355 (-16%)
NASA FLOPS	134	78 (-43%)
ASSET	190	170 (-11%)

Overall, hybridization reduces the capacity of the fuel system, and according to Table 20 above, ASSET predicts a weight savings of approximately 11%. In comparison, all the existing methods tend to predict a significant weight reduction (more than 40% in the case of the Cessna, USAF, and NASA FLOPS models). Additionally, the new ASSET method can capture changes to the system weight (even if they are minor)

because it considers the relative placement of the main system components relative to the engines and fuel tanks, which is a detail that is not captured by the existing methods.

5.3 Case Study 2: ATR 42

The ATR 42 is a regional twin-turboprop aircraft with a 42-50 passenger capacity and range of 950 [48] NM, certified under the Transport category. Its entry into service was with the PW100-series engines and has seen a variety of upgrades and variants to cater to operators' needs worldwide. Its airframe specifications and performance have been the baseline for the concept and performance study by Antcliff [5], [17].

5.3.1 Conventional ATR 42 Fuel System

The ATR 42 fuel system review is based on the ATR 72 fuel system; the ATR72 is a stretched version of the ATR 42 with an increased MTOW, increased range, a 70-80 seat passenger, and a 500 kg additional fuel capacity. This case study assumes that the ATR 42 fuel system is identical to the ATR 72 regarding the number of components used. Compared to the DO228, the ATR fuel system appears to be much simpler regarding the number of components used.

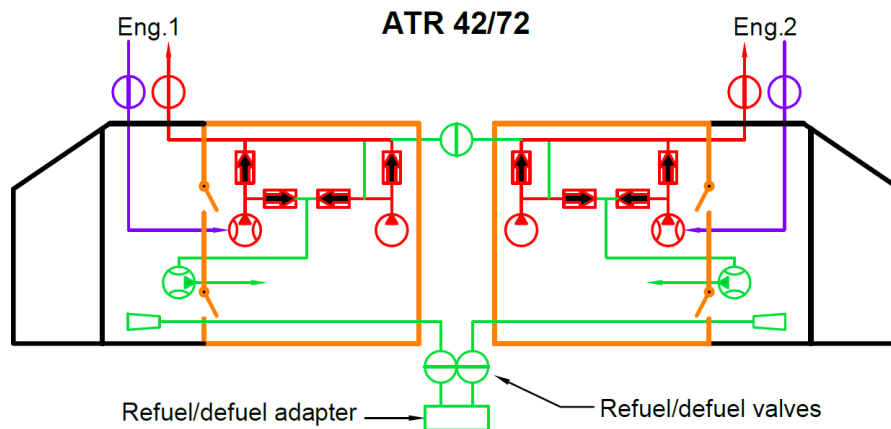


Figure 33: ATR 42/72 fuel system schematic

In this architecture, each integral wing tank uses a single electrically driven feed pump to supply fuel to the engine during the start process and acts as the backup/emergency fuel pump in-flight. The main feed pump is an ejector pump driven by the engine's motive flow, which itself is used to operate the scavenge ejector pumps that maintain the feed collector full. The Bombardier Dash 8 is another twin-turboprop regional airliner comparable to the ATR aircraft and uses a similar engine feed subsystem.

The ATR42 fuel system specifications [50] are provided in Table 21, and the aircraft geometry is shown in Figure 34 below.

Table 21: ATR 42-400 conventional aircraft fuel system and geometry parameters

Total fuel	5727 L / 4571 kg / 10077 lb (see Appendix Appendix B)
Usable fuel	5700 L / 4550 kg / 10031 lb (see Appendix Appendix B)
Estimated fuel tank wing area (per wing)	8.41 m ² / 90.48 ft ²
Wing area (per wing)	27.25 m ² / 293.3 ft ²
Estimated average wing thickness	13.3 in
Propulsion engines	PW127
Estimated Propulsion engine fuel flow @ TO power	1100 lb/h (engine data)

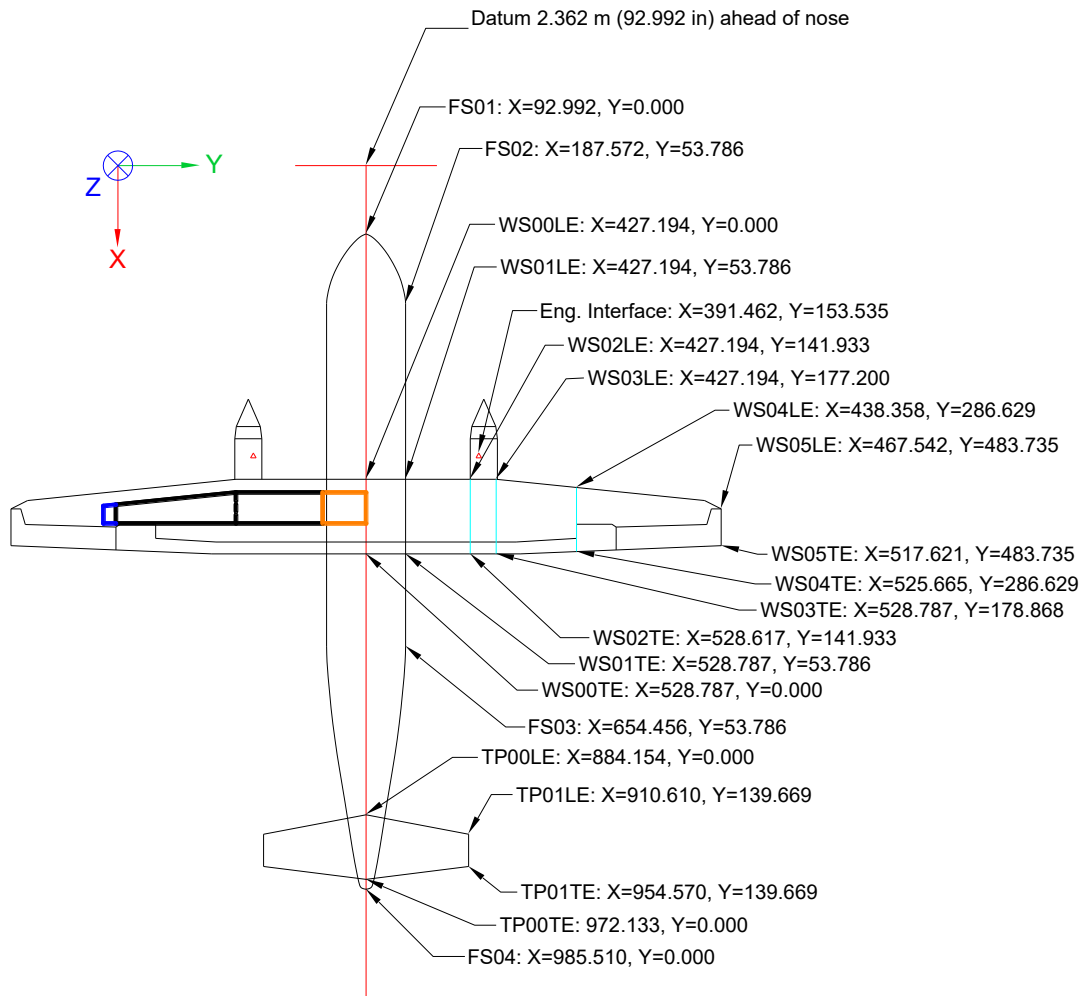


Figure 34: ATR42 aircraft geometry

The ASSET tool estimates the conventional fuel system weight to be 210.6 lb and is broken down into the four subsystems, as shown in Table 22 below.

Table 22: ASSET estimation weight breakdown for the ATR 42 fuel system

	Actual [31]	ASSET Estimation
Engine Feed Subsystem Weight	N/A	41.3 lb
Number of electrical feed pumps	2	2
Number of ejector feed pumps	2	2
Number of shutoff valves	4	2
Estimated fuel line OD	N/A	0.62 in
Feed line length	N/A	68.5 ft
Fuel Transfer Subsystem Weight	N/A	35.0 lb
Number of scavenge pumps	2	8
Number of electrical transfer pumps	0	0
Estimated transfer fuel line OD	N/A	1.5 in
Transfer fuel system line length	N/A	79.3 ft
Fuel Quantity & Indicating Subsystem Weight	N/A	60 lb
Total number of wing tank probes	10 (based on training manual)	16
Number of center tank probes	0	0
Additional FQI components	Refuel/defuel control panel Fuel low-level switch Fuel high-level switch Fuel used/flow indicator (cockpit) Fuel quantity indicator (cockpit) Fuel pressure switches Fuel temperature probe/indicator	Refuel/defuel control panel Fuel quantity avionics Fuel properties devices
Fuel Venting Subsystem Weight	N/A	40.7 lb
Estimated vent duct OD	N/A	1.74 in
Estimated vent duct length	N/A	88 ft
Ancillary Components Weight	N/A	34 lb

Table 23: Comparison of FS weight estimation methods for conventional ATR42-400

FS Weight Estimation Method	Estimated Weight (lb)
ASSET	211
Cessna	602
USAF	518
Torenbeek	483
NASA FLOPS	247
Actual	196

As with the previous case study, the Cessna, USAF, and Torenbeek methods greatly overestimate the system weight for the conventional ATR 42, while the NASA FLOPS and ASSET are much closer to the data in Obert [31].

5.3.2 Hybrid-Electric Configurations 1 & 2

The conceptual aircraft proposed by Antcliff et al. [17] is similar to the ATR42 and forms the basis for the two case studies in this section. The study analyzes the various levels of hybridization and specific energy of the batteries required for a design mission range of 600 NM. It provides figures for the total battery weight, required fuel weight, battery energy, and cost for the various levels of hybridization combined with battery specific energies of 500 Wh/kg to 1000 Wh/kg. However, the conclusions indicate that specific energies of more than 500 Wh/kg are required for the hybrid-electric concept to be comparable or more economically viable relative to the conventional aircraft variant.

In the case study presented here, the lowest level of hybridization (25%), along with a 750 Wh/kg battery specific energy, is considered. According to Antcliff et al., this will result in a total fuel weight of 2910 lb (1320 kg). Based on the properties of Jet A-1 fuel for the ATR 42, the fuel tank volume is estimated to be 1642L or approximately 28.7% of the original fuel tank capacity. Based on the existing geometry of the ATR, the two configurations below are proposed.

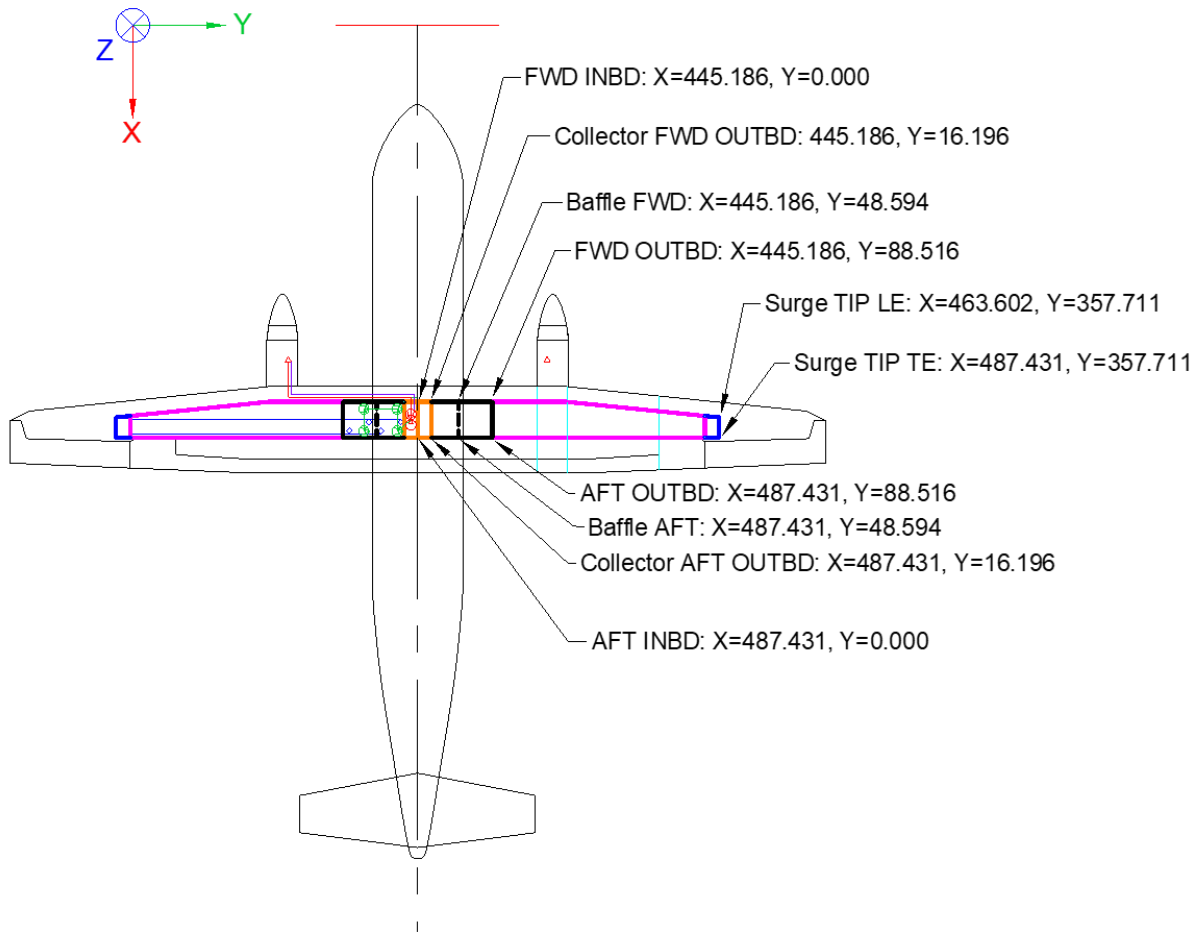


Figure 35: ATR42 hybrid-electric configuration HE01

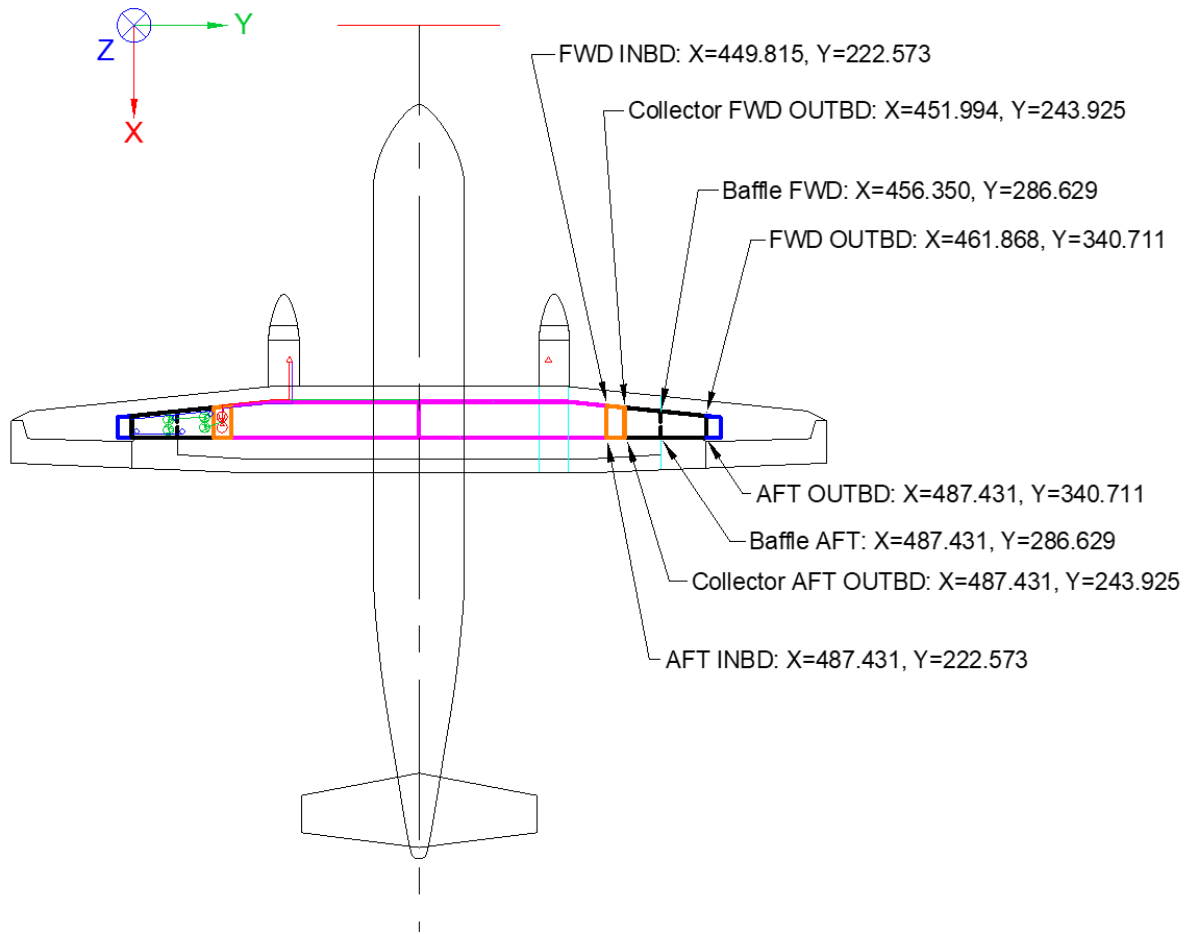


Figure 36: ATR42 hybrid-electric configuration HE02

As with the DO228, configuration 1 places the fuel system inboard of the engine nacelles, closest to the aircraft centerline, while configuration 2 places it closest to the wingtips, with the remainder of the wing box space available for battery storage.

Table 24: Fuel system weight breakdown for conventional and HE ATR42 configurations

	Actual	ASSET - Conventional	ASSET – HE01	ASSET – HE02
Engine Feed Subsystem Weight	N/A	41.3 lb	41.6 lb	40.0 lb
Number of electrical feed pumps	2	2	2	2
Number of ejector feed pumps	2	2	2	2
Number of shutoff valves	4	2	2	2
Estimated fuel line OD	N/A	0.62 in	0.62 in	0.62 in
Feed line length	N/A	68.5 ft	73.4	52.5 ft
Fuel Transfer Subsystem Weight	N/A	35.0 lb	29.3 lb	39.2 lb
Number of scavenge pumps	2	8	8	8
Number of electrical transfer pumps	0	0	0	0
Estimated transfer fuel line OD	N/A	1.5 in	1.5 in	1.5 ft
Transfer fuel system line length	N/A	79.3 ft	36.1 ft	111.3 ft
Fuel Quantity & Indicating Subsystem Weight	N/A	60 lb	45.0 lb	45.0 lb
Total number of wing tank probes	10	16	6	6
Number of center tank probes	0	0	0	0
Fuel Venting Subsystem Weight	N/A	40.7 lb	35.6 lb	28.7 lb
Estimated vent duct OD	N/A	1.74 in	0.75 in	0.75 in
Estimated vent duct length	N/A	88 ft	106.6 ft	30.2 ft
Ancillary Components Weight	N/A	34 lb	29 lb	29 lb
Total Fuel System Weight	196 lb	210.6 lb	180.3 lb	182.0 lb

Once again, inverting the location of the fuel system components (between the inboard and outboard portions of the wing box) has a negligible effect on the order of 2 lb difference between these two configurations. The prediction also shows no significant weight reduction relative to the estimated conventional system weight. It is about 14% and results from smaller FQI and tank venting subsystems impacted by the reduced tank capacity.

Table 25: Comparing conventional and hybrid-electric ATR42 fuel system weights

Estimation Method	Conventional, lb	Predicted Hybrid-electric, lb (ΔW_{fs} relative to conventional)
Cessna	602	173 (-71%)
USAF	518	209 (-60%)
Torenbeek	483	400 (-17%)
NASA FLOPS	247	120 (-51%)
ASSET	211	181 (-14%)
Actual W_{fs}	196	N/A

However, the results for the existing weight equations (Cessna, USAF, and NASA FLOPS in particular) in Table 25 above show much greater weight savings because their dependency on the max fuel capacity is significantly smaller in the hybrid-electric ATR42 compared to its conventional counterpart. As with the DO228 case study, the existing state-of-the-art methods show optimistic weight reductions because of

their strong dependency on the max fuel capacity. The ASSET estimation can capture trends more consistently with the expected weight reductions.

6 Conclusions and Future Work

The research work presented in this thesis highlights and addresses shortcomings of the existing analytical methods to estimate the weight of aircraft fuel systems. Its implementation into a calculation tool can be integrated into an MDAO environment coupled with aircraft-level performance analysis tools that will enable automated optimization and evaluation of different designs and trade studies as part of the conceptual design process.

6.1 Summary and contributions of this thesis

Hybrid-electric may offer the potential to reduce aviation-related greenhouse gas emissions, helping the industry work its way to achieving its climate change targets by the year 2050. Various ongoing projects are currently targetting the regional and commuter aircraft categories since the economics are likely the most viable. Incorporating these new technologies and novel configurations in the conceptual design phase requires new design tools. It is one area of focus of the Air Systems Laboratory at Concordia University.

This thesis has reviewed the existing, traditional methods of estimating the fuel system weight and shows substantial differences between the actual and predicted weights for various aircraft, specifically in the commuter and regional categories, which are best suited for hybrid-electric applications. These errors can lead to an overestimated weight savings of the fuel systems that may not be realistic for hybrid-electric aircraft fuel systems. The segregation of these methods into GA and Commercial Transport categories raises uncertainty regarding the most applicable method for these aircraft categories. These findings motivate a new approach that will close these gaps. Two methods are proposed to address the gaps in the existing estimation techniques.

The first method is an improved empirical model developed from published data for commuter and regional aircraft fuel systems. This model is a good first approximation to baseline the sizing for commuter and regional aircraft fuel systems with integral fuel tanks. However, because the approach to deriving it is similar to the existing weight equations, it will not capture changes in the system architecture components and their layout because it remains strongly dependent on the maximum fuel capacity.

The second method is an extension of the methodology from Liscouët-Hanke [32] and incorporates some elements from the algorithm developed by Olives [33] into the Aircraft System Sizing Estimation Tool (ASSET). It estimates the system weight by counting the number of components in the systems architecture, the individual component weights, and technology and summing them together. This method proposes to break down the system into four subsystems which are common in all aircraft: (1) the engine feed subsystem, (2) the fuel transfer subsystem, (3) the fuel quantity and indicating subsystem, and (4) the tank venting subsystem. The process estimates the weight of key components:

- In general, the fuel tank geometries and placement of components follow a similar concept as in Olives [33], using aircraft geometry to generate the fuel tank boundaries. However, the methodology implemented in the Excel-based tool accommodates some auxiliary fuel tank configurations common to GA, commuter, and regional aircraft.
- The process of determining the number of fuel pumps, valves, and fuel lines is similar to Liscouët-Hanke [32] and Olives [33], except that the engine fuel pumps are not considered part of the airframe system.
- The ASSET estimation incorporates more detailed information for the Fuel Quantity & Indicating subsystem, using weight data for fuel quantity probes and other fuel management devices.

The sum of the weight of these four subsystems then makes up the overall system weight. Furthermore, the method also allows the comparison of systems with different component arrangements to evaluate their effect on the size of the system. This feature can be of particular interest in hybrid-electric applications because the volume required for the batteries will certainly be much larger than the fuel capacity and may require relocation of the system components to fit inside the airframe. Several aircraft from the commuter, regional, and narrow-body airliners were analyzed using this methodology and show that the methodology implemented into a preliminary Excel-based estimation tool predicts the system weight within a range of -25% to + 19% of the published data.

This thesis includes two case studies that illustrate how the new ASSET method can be used to assess the impact of unconventional aircraft, such as those with hybrid-electric powertrains, which impact the size of the fuel system. The preliminary weight estimations for hybrid-electric configurations of the DO228 and ATR42 were presented as part of the AIAA Aviation Forum conference paper titled Architecture-based weight estimation method for conceptual design aircraft fuel systems [51]. The small weight savings predicted by the ASSET method in both studies makes sense because most of the system components in conventional systems will remain present to cover regulatory and safety requirements. Overall weight savings in the fuel system for a hybrid-electric aircraft are negligible because the fuel system only constitutes about 1-3% of the aircraft OEW. This approach offers the advantages of providing a more detailed weight breakdown of the fuel system at the conceptual design stage and tracking changes in the system weight during trade study iterations. The methodology can also offer an alternative to the state-of-the-art empirical equations from Roskam, Torenbeek, and NASA FLOPS, specifically for short-haul conventional and hybrid-electric aircraft.

6.2 Limitations of the Implemented Methodology

The method presented in this thesis is currently implemented in MS Excel since it provides a rudimentary visual representation of inputs and outputs of the tool and performs all the necessary calculations to estimate the weight of the four major subsystems. However, it does have the following limitations:

- 1) A python script file is required to interface between a python-based design system and the Excel-based tool. This script file sets the aircraft geometry points into the Excel workbook and

extracts the relevant data from the tool outputs. The implementation in Microsoft Excel was done to allow a visual result showing the geometry definition and the location of the various subsystems. Iterating through changes to a concept is not very practical with this implementation, requiring copies of the workbooks to be made to track the evolution of the design.

- 2) A 2D top view of the aircraft geometry forms the basis for the fuel tank geometries. It assumes the main fuel tanks are integral to the wing structure, and there is no current provision to model a single fuselage tank for single-engine applications. Similarly, there is no modeling of more than one auxiliary fuel tank; the implementation assumes a center fuselage tank is always located between the two wing tanks and does not extend outside the fuselage. Manual modification of the geometry points is required to achieve a more representative fuel system architecture diagram and weight estimate.
- 3) The tool does not consider the associated weight increment of bladder-type fuel tanks relative to an equivalent integral or rigid tank. In general, the bladder material is much heavier than the material for rigid tanks and typically needs additional fastening hardware to secure them to the aircraft structure.
- 4) Commuter and regional aircraft fuel systems do not typically have fuel jettison circuits, and since the tool focuses on these aircraft, the weight estimation excludes the jettison circuit. Fuel jettison is fitted on most large commercial transports where the MTOW significantly exceeds the MLW.
- 5) The tool has not been validated for aircraft where the number of engines exceeds two because most commuter and regional aircraft are only twin-engined. One exception is the DHC7, but no verifiable fuel system weight data has been obtained for comparison.
- 6) The automation for a hybrid-electric variant of an aircraft defined by the geometry and input parameters is not built into the tool. Currently, the user needs to set the geometry and other input parameters that are representative of a conventional aircraft, then modify the fuel tank geometry to reflect the reduction in fuel capacity for a hybrid-electric variant of the aircraft under study. Additionally, since the tool is currently implemented in MS Excel, the modifications tend to be cumbersome and difficult to manage; it is something to be improved on before integrating into an MDAO environment.

6.3 Future Work

The Aircraft Systems lab at Concordia aims to integrate the methodology and tool as part of a suite of sizing and performance analysis tools for conceptual design in an MDAO framework. The future implementation will likely need to transition from MS Excel to a Python-based script, allowing a more iterative execution to facilitate the analysis of different aircraft concepts and trade studies.

Additional work is required to allow the tool to model non-standard fuel tank configurations, for example, on the CL605 and the DHC-6 aircraft, which have fuel tanks under the cabin floor. The current version of the tool focuses on commuter and regional aircraft, meaning there is no consideration for features such

as a jettison system. Bladder-type fuel tanks are also not modeled because more research is needed to determine the weight penalties associated with these types of tanks.

Finally, the tool can be integrated with a geometrical modeler that will leverage 3D aircraft models to help define a more representative fuel tank geometry and output a 3D placement of the various subsystem components. It is an ongoing project in the Air Systems Lab, and further work is needed to develop the interaction with the modeler.

7 References

- [1] J. E. Penner, D. H. Lister, D. J. Griggs, D. J. Dokken, and M. McFarland, "1.1 Background - Aviation and the Global Atmosphere," 2007. Accessed: Feb. 07, 2022. [Online]. Available: <https://archive.ipcc.ch/ipccreports/sres/aviation/014.htm>
- [2] International Air Transport Association, "Resolution on the Industry's Commitment to Reach Net Zero Carbon Emissions by 2050," Oct. 2021. Accessed: Sep. 04, 2022. [Online]. Available: <https://www.iata.org/contentassets/dcd25da635cd4c3697b5d0d8ae32e159/iata-agm-resolution-on-net-zero-carbon-emissions.pdf>
- [3] NASA Glenn Research Center, "Airplane Concepts," Aug. 2017. Accessed: Feb. 07, 2022. [Online]. Available: <https://www1.grc.nasa.gov/aeronautics/hep/airplane-concepts/>
- [4] Airbus, "E-Fan X Hybrid Electric Flight," 2022. Accessed: Sep. 04, 2022. [Online]. Available: <https://www.aerospace-technology.com/projects/e-fan-x-hybrid-electric-aircraft/>
- [5] K. R. Antcliff and F. M. Capristan, "Conceptual design of the parallel electric-gas architecture with synergistic utilization scheme (PEGASUS) concept," in *2017 18th AIAA/ISSMO Multidisciplinary Analysis and Optimization Conference, AIAA AVIATION Forum*. American Institute of Aeronautics and Astronautics Inc, Denver, Colorado, Jun. 2017. doi: 10.2514/6.2017-4001.
- [6] M. Huber, "UTC Reveals Hybrid-electric Aircraft Demonstrator," Mar. 2019. Accessed: Mar. 18, 2022. [Online]. Available: <https://www.ainonline.com/aviation-news/aerospace/2019-03-26/utc-reveals-hybrid-electric-aircraft-demonstrator>
- [7] W. Kucinski, "UTC's Project 804 hybrid-electric demonstrator may increase regional jet efficiency by 30 percent," Apr. 2019. Accessed: Mar. 18, 2022. [Online]. Available: <https://www.sae.org/news/2019/04/utc%E2%80%99s-project-804-hybrid-electric-demonstrator-may-increase-regional-jet-efficiency-by-30-percent>
- [8] L. Blain, "VoltAero and Kinect hook up for hybrid-electric passenger flights from 2023," May 2021. Accessed: Mar. 18, 2022. [Online]. Available: <https://newatlas.com/aircraft/voltaero-kinect-hybrid-electric-aircraft/>
- [9] G. Cinar *et al.*, "Sizing, integration and performance evaluation of hybrid electric propulsion subsystem architectures," in *55th AIAA Aerospace Sciences Meeting, AIAA SciTech Forum*. American Institute of Aeronautics and Astronautics Inc., Grapevine, Texas, Jan. 2017. doi: 10.2514/6.2017-1183.
- [10] R. de Vries, M. Brown, and R. Vos, "Preliminary sizing method for hybrid-electric distributed-propulsion aircraft," *J Aircraft*, vol. 56, no. 6, pp. 2172–2188, Nov. 2019, doi: 10.2514/1.C035388.

- [11] J. Zamboni, "A method for the conceptual design of hybrid electric aircraft," M.Sc. thesis, Aerospace Engineering, Delft University of Technology, 2018. [Online]. Available: <http://repository.tudelft.nl/>.
- [12] J. van Bogaert, "Assessment of Potential Fuel Saving Benefits of Hybrid-Electric Regional Aircraft," M.Sc. thesis, Aerospace Engineering, Delft University of Technology, 2015. Accessed: Mar. 18, 2022. [Online]. Available: <https://repository.tudelft.nl/islandora/object/uuid:0fc7019f-d988-45c1-a7e2-55825f4f90ca/datastream/OBJ/download>
- [13] M. Voskuijl, J. van Bogaert, and A. G. Rao, "Analysis and design of hybrid electric regional turboprop aircraft," *CEAS Aeronaut J*, vol. 9, no. 1, pp. 15–25, Mar. 2018, doi: 10.1007/s13272-017-0272-1.
- [14] J.-P. Hofmann *et al.*, "A comprehensive Approach to the Assessment of a Hybrid Electric Powertrain for Commuter Aircraft," in *2019 AIAA Aviation Forum*. American Institute of Aeronautics and Astronautics Inc., Dallas, Texas, Jun. 2019. doi: 10.2514/6.2019-3678.
- [15] R. Glasscock, M. Galea, W. Williams, and T. Glesk, "Hybrid electric aircraft propulsion case study for skydiving mission," *Aerospace*, vol. 4, no. 3, Sep. 2017, doi: 10.3390/aerospace4030045.
- [16] P. G. Juretzko, M. Immer, and J. Wildi, "Performance analysis of a hybrid-electric retrofit of a RUAG Dornier Do 228NG," *CEAS Aeronaut J*, vol. 11, no. 1, pp. 263–275, Jan. 2020, doi: 10.1007/s13272-019-00420-2.
- [17] K. R. Antcliff, M. D. Guynn, T. v. Marien, D. P. Wells, S. J. Schneider, and M. T. Tong, "Mission analysis and aircraft sizing of a hybrid-electric regional aircraft," in *54th AIAA Aerospace Sciences Meeting*. American Institute of Aeronautics and Astronautics Inc., San Diego, California, Jan. 2016. doi: 10.2514/6.2016-1028.
- [18] D. P. Raymer, *Aircraft design : A Conceptual Approach*, 6th ed. Reston, VA, USA: American Institute of Aeronautics and Astronautics, Inc., 2018.
- [19] E. Torenbeek, *Synthesis of Subsonic Airplane Design*. Delft, The Netherlands: Delft University Press, 1982.
- [20] J. Roskam, *Airplane Design Part 5: Component Weight Estimation*, 5th ed., vol. Part V. Lawrence, Kansas, USA: DAR corporation, 2018.
- [21] Cessna Aircraft Company, "Maintenance Manual MODEL 172 Series 1996 & On." Cessna Aircraft Company, Wichita, Kansas, USA, 2007.
- [22] Trans World Airlines, "Fuel," in *TWA Boeing 747 Flight Handbook*, Kansas City, Missouri, USA: Flight Operations Training Department, Trans World Airlines, 1997.

- [23] D. L. Jensen, "Analysis of a Boeing 747 Aircraft Fuel Tank Venting System," in *Fluids 2000 Conference and Exhibit*, Jun. 2000, no. 38. doi: 10.2514/6.2000-2454.
- [24] E. D. Ayson, R. R. Dhanani, and G. A. Parker, "The 747 Fuel System," no. 700276. Society of Automotive Engineers, New York, NY, USA, Apr. 1970. doi: <https://doi-org.lib-ezproxy.concordia.ca/10.4271/700276>.
- [25] Transport Canada, "Airworthiness Manual Chapter 523 - Normal Category Aeroplanes," Sep. 2021. Accessed: Jun. 22, 2022. [Online]. Available: <https://tc.canada.ca/en/corporate-services/acts-regulations/list-regulations/canadian-aviation-regulations-sor-96-433/standards/airworthiness-manual-chapter-523-normal-category-aeroplanes-canadian-aviation-regulations-cars>
- [26] European Union Aviation Safety Agency, "Certification Specifications and Acceptable Means of Compliance for Normal, Utility, Aerobatic, and Commuter Category Aeroplanes," Jun. 2015. Accessed: Sep. 04, 2022. [Online]. Available: <https://www.easa.europa.eu/sites/default/files/dfu/CS-23%20Amendment%204.pdf>
- [27] U.S. Government Publishing Office, "Airworthiness Standards: Normal, Utility, Acrobatic, and Commuter Category Airplanes," 2016. Accessed: Sep. 03, 2022. [Online]. Available: <https://www.govinfo.gov/content/pkg/CFR-2016-title14-vol1/pdf/CFR-2016-title14-vol1-part23.pdf>
- [28] European Union Aviation Safety Agency, "Certification Specifications and Acceptable Means of Compliance for Large Aeroplanes," 2020. Accessed: Sep. 04, 2022. [Online]. Available: <https://www.easa.europa.eu/downloads/108354/en>
- [29] Transport Canada, "Airworthiness Chapter 525 - Transport Category Aeroplanes," Aug. 2021. Accessed: Jun. 22, 2022. [Online]. Available: <https://tc.canada.ca/en/corporate-services/acts-regulations/list-regulations/canadian-aviation-regulations-sor-96-433/standards/airworthiness-chapter-525-transport-category-aeroplanes-canadian-aviation-regulations-cars>
- [30] U.S. Government Publishing Office, "Airworthiness Standards: Transport Category Airplanes," 2016. Accessed: Sep. 03, 2022. [Online]. Available: <https://www.govinfo.gov/content/pkg/CFR-2016-title14-vol1/pdf/CFR-2016-title14-vol1-part25.pdf>
- [31] E. Obert, *AERODYNAMIC DESIGN OF TRANSPORT AIRCRAFT*. Amsterdam, The Netherlands: IOS Press, 2009.
- [32] S. Liscouët-Hanke, "A model-based methodology for integrated preliminary sizing and analysis of aircraft power system architectures," PhD dissertation, Université de Toulouse, Laboratoire de Génie Mécanique de Toulouse, Toulouse, France, 2008.

- [33] F. Olives, "Weight estimation of parametrically design of fuel and hydraulic systems of a commercial airplane," M.Sc thesis, Department of Aeronautics, Imperial College of Science, Technology and Medicine, 2019.
- [34] Parker Canada Division, "Aerospace Axial, Cooling and Fluid Pumps | ParkerCA," 2020. Accessed: Mar. 28, 2020. [Online]. Available: <https://ph.parker.com/ca/en/aerospace-axial-cooling-and-fluid-pumps>
- [35] EATON, "Literature Library." Accessed: Jun. 02, 2020. [Online]. Available: <https://www.eaton.com/Eaton/ProductsServices/Aerospace/LiteratureLibrary/index.htm>
- [36] Weldon, "Pumps." Accessed: May 31, 2020. [Online]. Available: <https://www.weldonpumps.com/weldon-pumps>
- [37] Cristall Corporation, "Product Catalog," 2021. Accessed: Nov. 11, 2021. [Online]. Available: <http://okb-kristall.ru/en/>
- [38] Boeing, "Homepage | Boeing (formerly Aviall) - Aircraft Parts, Supplies, Chemicals, Tools and Repair Services | Boeing Distribution." Accessed: Oct. 10, 2020. [Online]. Available: <https://shop.boeing.com/aviation-supply/>
- [39] Weitz P.G., "Commercial Aircraft Airframe Fuel Systems Survey and Analysis," NJ, USA, DOT/FAA/CT-82/80, 1982. Accessed: Oct. 04, 2020. [Online]. Available: <https://apps.dtic.mil/sti/pdfs/ADA119572.pdf>
- [40] Nathan Meier, "Jet Engine Specification Database," 2005. Accessed: Apr. 19, 2020. [Online]. Available: <https://www.jet-engine.net/>
- [41] Élodie Roux, "Turbofan and Turbojet Engines Database Handbook," Blagnac, France: Ed. Elodie Roux, 2007.
- [42] "Fuel and Oil Lines, Aircraft, Installation of," *Aerospace Standard AS18802* . SAE International, Aug. 2013. Accessed: Sep. 28, 2021. [Online]. Available: <http://www.sae.org/technical/standards/AS18802AEROSPACE>
- [43] Earle M. Jorgensen Company, *Reference Book Section K TUBING and PIPE*. Earle M. Jorgensen Company, 2007. Accessed: Jun. 06, 2020. [Online]. Available: https://www.emjmetals.com/site/blue_book
- [44] Parker Canada Division, "Aerospace Valves | ParkerCA." Accessed: Mar. 05, 2022. [Online]. Available: <https://ph.parker.com/ca/en/aerospace-valves>
- [45] Sitec Aerospace GmbH, "Actuators," 2022. Accessed: Sep. 16, 2022. [Online]. Available: <https://www.sitec-aerospace.com/products/actuators.html>

- [46] R. Langton, C. Clark, M. Hewitt, and L. Richards, "4.5 Fuel Quantity Gauging," in *Aircraft Fuel Systems*, John Wiley & Sons, 2009, pp. 76–77.
- [47] Parker Aerospace Fluid Systems Division, "Off the Shelf Flame Arrestor." Accessed: Jun. 12, 2022. [Online]. Available: https://www.parker.com/literature/Fluid%20Systems%20Division/FSD_Flame%20Arrestor.pdf
- [48] J. W. Taylor, Ed., *Jane's All the World's Aircraft*, 75th ed. London: Jane's Publishing, 1984.
- [49] *Pilot's Operating Handbook and LBA Approved Airplane Flight Manual, Dornier 228-100*. Munich: Dornier GmbH, Logistic, 1983.
- [50] AVIONS DE TRANSPORT REGIONAL, "Airplane Flight Manual, ATR42 MODELS 400-500," Blagnac, FRANCE, 1995.
- [51] C. D. Rodriguez and S. Liscouët-Hanke, "Architecture-based fuel system conceptual design tool for hybrid-electric aircraft," in *2021 AIAA Aviation Forum*. American Institute of Aeronautics and Astronautics (AIAA), Aug. 02, 2021. doi: 10.2514/6.2021-2408.
- [52] U.S. Department of Transportation, "Dynamic Regulatory System." Accessed: Feb. 09, 2022. [Online]. Available: <https://drs.faa.gov/browse/doctypeDetails>
- [53] European Union Aviation Safety Agency, "Type Certificate Data Sheets (TCDS)," 2022. Accessed: Feb. 09, 2022. [Online]. Available: <https://www.easa.europa.eu/document-library/type-certificates>
- [54] Transport Canada, "NAPA Issued Certificates Online." Accessed: Feb. 09, 2022. [Online]. Available: https://www.wapps.tc.gc.ca/saf-sec-sur/2/nico-cel/c_s.aspx?lang=eng

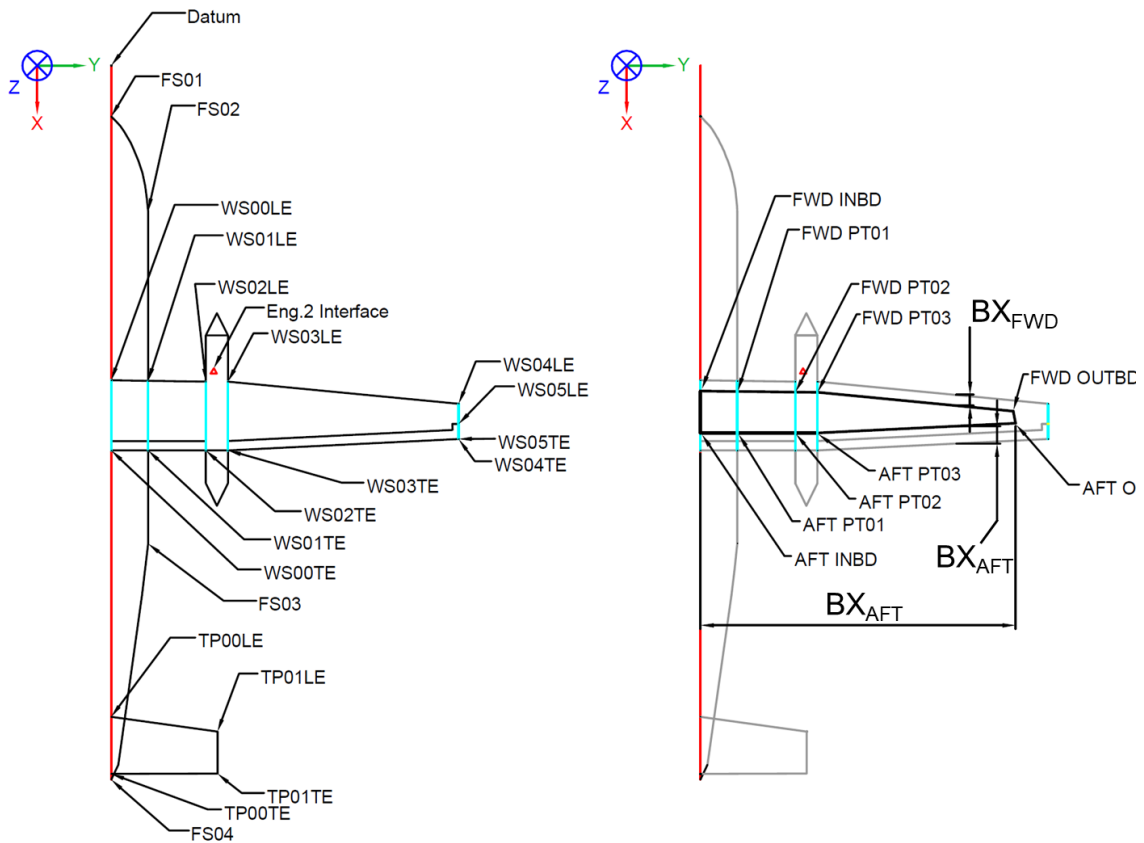
Appendix A ASSET Fuel System Weight Estimation Conventions, Algorithm Logic, and Equations

Detailed information on the defining geometry, related calculations, plots, and look-up tables used in the ASSET estimation tool are presented in these appendix sections.

A.1 Fuel Tank Geometry

The estimation tool requires some form of fuel tank geometry to establish the placement of various fuel system components before estimating their weights. In its current implementation, the tool assumes a planform view of the aircraft and the fuel tanks, neglecting the placement components in the z-direction for simplicity. This section describes the current method by which the tank geometry is generated.

The overall aircraft geometry can be derived from any orthographic projection drawing of an existing aircraft or a 3D model.



(a) Aircraft geometry definition points

(b) Fuel tank geometry based on aircraft geometry

Figure 37: Estimating fuel tank boundaries (right-side) from aircraft geometry

The various key geometrical points are extracted from the aircraft top view, as shown in Figure 37, and are defined below.

Table 26: ASSET aircraft and fuel tank geometry parameters

<i>FS01</i>	Fuselage Station 1 defines the nose of the aircraft.
<i>FS02</i>	Fuselage Station 2 defines the front portion of the fuselage.
<i>FS03</i>	Fuselage Station 3 defines the aft portion of the fuselage.
<i>FS04</i>	Fuselage Station 4 defines the tail cone tip at the back of the aircraft.
<i>WS01</i>	Identifies the wing root and is used to locate the inboard wall of the wing tank.
<i>WS02</i>	Located inboard of the engine nacelle on twin, wing-mounted engine aircraft. This point defines the ends of the engine feed collector cells. For aircraft with tail-mounted engines or single-engine aircraft, the placement of these points only requires to be between <i>WS01</i> and <i>WS03</i> .
<i>WS03</i>	Located outside of the engine nacelle on twin, wing-mounted engine aircraft. For multi-engine aircraft, <i>WS03</i> is placed between the two engines on a four-engine aircraft and drives the division of the wing to create two separate main tanks, one per engine.
<i>WS04</i>	Located outboard of <i>WS03</i> , mid-way between <i>WS03</i> and <i>WS05</i> . This pair of points may drive the placement of another anti-surge rib for 4-engine aircraft. It also drives the placement of the outboard tank wall and can't be less than $B_{Y\ wingtip} \times (0.5Wingspan)$.
<i>WS05</i>	Defines the outboard end of the wing tank and locates the surge tank near the wing tip on most aircraft. From a geometry point of view, it represents the actual wingtip of the aircraft and does not include winglets, tip fences, raked wingtips, etc.
$B_{X\ FWD}$	Defines the front wall (location of the front wing spar) of the wing tank as a percentage offset of the wing chord relative to the wing LE. A value of 15% is used by default and seems typical for most aircraft.
$B_{X\ AFT}$	Defines the back wall (location of the aft wing spar) of the wing tank as a percentage of the wing chord relative to the wing TE. A value of 25% is used as a default.
B_{YWT}	Represents the percent span of the outboard-most wing tank wall as a percent of the half-wing span.
<i>CWT</i>	A boolean variable, where a value of 1 indicates that the aircraft has a center wing tank. When the value is set to 0, the wing tanks are extended towards the centerline, assuming the space is available for fuel storage.
<i>Motive</i>	A boolean variable, where '1' indicates that the engine supplies a motive flow back to the fuel tanks to power feed ejector pumps.
<i>APU</i>	A boolean variable, where '1' indicates that the aircraft is equipped with an APU and requires an independent fuel line and boost pump to run from one of the main wing tanks to the APU fuel interface.

The wing fuel tank geometry in the top view projection is then generated by the tool using the following series of equations:

Point Name	Location	Calculations
FWD INBD	FWD inboard corner of the wing tank	$X_{FWD INBD} = \begin{cases} X_{WS00LE} + B_{X FWD}(X_{WS00TE} - X_{WS00LE}), & \text{if } CWT = 0 \\ X_{WS01LE} + B_{X FWD}(X_{WS01TE} - X_{WS01LE}), & \text{if } CWT = 1 \end{cases}$ $Y_{FWD INBD} = \begin{cases} Y_{WS01LE}, & \text{if } CWT = 0 \\ Y_{WS01LE}, & \text{if } CWT = 1 \end{cases}$
FWD PT01	Colinear to WS01	$X_{FWD PT01} = X_{WS01LE} + B_{X FWD}(X_{WS01TE} - X_{WS01LE})$ $Y_{FWD PT01} = Y_{WS01LE}$
FWD PT02	Colinear to WS02	$X_{FWD PT02} = X_{WS02LE} + B_{X FWD}(X_{WS02TE} - X_{WS02LE})$ $Y_{FWD PT02} = Y_{WS02LE}$
FWD PT03	Colinear to WS03	$X_{FWD PT03} = X_{WS03LE} + B_{X FWD}(X_{WS03TE} - X_{WS03LE})$ $Y_{FWD PT03} = Y_{WS03LE}$
FWD OUTBD	FWD outboard corner of the wing tank	$X_{FWD OUTBD} = \left[(X_{WS05LE} - X_{WS04LE}) \frac{Y_{FWD OUTBD} - Y_{WS04LE}}{Y_{WS05LE} - Y_{WS04LE}} + X_{WS04LE} \right] +$ $\left(\left[(X_{WS05TE} - X_{WS04TE}) \frac{Y_{AFT OUTBD} - Y_{WS04TE}}{Y_{WS05TE} - Y_{WS04TE}} + X_{WS04TE} \right] - \right.$ $\left. \left[(X_{WS05LE} - X_{WS04LE}) \frac{Y_{FWD OUTBD} - Y_{WS04LE}}{Y_{WS05LE} - Y_{WS04LE}} + X_{WS04LE} \right] \right) B_{X FWD}$ $Y_{FWD OUTBD} = B_{Y wingtip} Y_{WS05LE}$
AFT OUTBD	AFT outboard corner of the wing tank	$X_{AFT OUTBD} = \left[(X_{WS05TE} - X_{WS04TE}) \frac{Y_{AFT OUTBD} - Y_{WS04TE}}{Y_{WS05TE} - Y_{WS04TE}} + X_{WS04TE} \right] -$ $\left(\left[(X_{WS05TE} - X_{WS04TE}) \frac{Y_{AFT OUTBD} - Y_{WS04TE}}{Y_{WS05TE} - Y_{WS04TE}} + X_{WS04TE} \right] - \right.$ $\left. \left[(X_{WS05LE} - X_{WS04LE}) \frac{Y_{FWD OUTBD} - Y_{WS04LE}}{Y_{WS05LE} - Y_{WS04LE}} + X_{WS04LE} \right] \right) B_{X AFT}$ $Y_{AFT OUTBD} = B_{Y wingtip} Y_{WS05TE}$
AFT PT03	Colinear to WS01	$X_{AFT PT03} = X_{WS03TE} + B_{X AFT}(X_{WS03TE} - X_{WS03LE})$ $Y_{AFT PT03} = Y_{WS03TE}$

Point Name	Location	Calculations
AFT PT02	Colinear to WS02	$X_{AFT\ PT02} = X_{WS02TE} + B_{X\ AFT}(X_{WS02TE} - X_{WS02LE})$ $Y_{AFT\ PT02} = Y_{WS02TE}$
AFT PT01	Colinear to WS01	$X_{AFT\ PT01} = X_{WS01LE} + B_{X\ FWD}(X_{WS01TE} - X_{WS01LE})$ $Y_{FWD\ PT01} = Y_{WS01TE}$
AFT INBD	AFT inboard corner of the wing tank	$X_{FWD\ INBD} = \begin{cases} X_{WS00TE} + B_{X\ FWD}(X_{WS00TE} - X_{WS00LE}), & \text{if } CWT = 0 \\ X_{WS01TE} + B_{X\ FWD}(X_{WS01TE} - X_{WS01LE}), & \text{if } CWT = 1 \end{cases}$ $Y_{FWD\ INBD} = \begin{cases} Y_{WS01TE}, & \text{if } CWT = 0 \\ Y_{WS01TE}, & \text{if } CWT = 1 \end{cases}$

The number of fuel tanks is also determined by the tool based on the following logic:

- 1) For single-engine aircraft ($N_e = 1$), two wing tanks are assumed.
- 2) For multi-engine aircraft ($N_e > 1$), one tank per engine is assumed.
- 3) The center wing tank (CWT) is counted as an additional tank.

Engine feed pumps are placed at the approximate center of the feed collector compartments. The APU boost pump is located in the left main wing tank near the AFT inboard corner, offset by 15% of the feed compartment walls in the longitudinal and lateral directions.

A.2 ASSET Equations and Logic

This section details the equations used to estimate the number of components in each subsystem and their associated cumulative weight.

Table 27: ASSET fuel system calculated parameters

Description	Eq.	Units
Engine Feed		
Number of tanks	$N_t = 2[OR(N_e = 1, N_e = 4)] + (N_e > 1)N_e + CWT$	N/A
Number of elec. Boost pumps	$N_{bp} = N_e(1 + [Motive = 0]) + APU$	N/A
Number of feed ejector pumps	$N_{jp} = (Motive = 1)N_e$	N/A
Fuel XFR		
Number of elec. XFR pumps	$N_{TXP} = 2CWT$	N/A
Number of scavenge ejector pumps	$N_{scav} = 4(N_t - CWT)$	N/A
Number of Jettison pumps	Not modeled; useful for B747 so far.	N/A
FQI Subsystem		
Number of CWT FQI probes	$N_{CWT FQIP} = \begin{cases} [4.35 \times 10^{-5} W_{FCT} + 2.78], & \text{for CWT confined to fuselage} \\ [1.93(\ln W_{FCT}) - 12.2], & \text{for CWT protruding into wings} \end{cases}$	
Avg. FQI Probe length	$L_{FQIPavg} = 0.9t_{wing}$	In.
FQI Probe Weight	$W_{FQIP} = (N_{FQIP} + N_{CWT FQIP})(0.0981L_{FQIPavg} + 0.3284)$	Lb.
Refuel/defuel panel weight	$W_{RDGP} = 7.0PRD$	Lb.
FQI Computer Weight	$W_{FQIC} = 22.0(1 - 0.5[TCCAT \leq 2])$	Lb.
FPMU Component Weight	$W_{FPMU} = 3.5N_t([TCCAT = 3])$	Lb.
Vent Subsystem		
Vent duct OD	$OD_{vents} = 0.6396 \ln(W_{F,USG}) - 2.963$	In.

A.3 Fuel Line & Vent Duct Wall Thickness and Weight per Unit Length

The approach for estimating the weight of the fuel lines and vent ducts is based on physical characteristics (material, OD, length, and so on) and is discussed in chapter 3 of this thesis. This section provides detailed tables to estimate the wall thickness and weight per unit length (W/L) parameter, both of which are based on the line or duct OD. Fuel lines and ducts are assumed to be made from circular tubes; however, in some aircraft, such as the B747, stringer ducts in the vent subsystem can have a ‘hat’ or rectangular cross-section.

Table 28: Aircraft Tubing Wall Thickness from AS18802

OD (in)	Alu Fuel Line Wall Thickness (in)	Drain & Vent Line Wall Thickness (in)
0.25	0.028	0.022
0.375	0.028	0.022
0.5	0.038	0.022
0.625	0.042	0.028
0.75	0.042	0.028
1	0.049	0.035
1.25	0.049	0.035
1.5	0.049	0.035
2	0.049	0.035
2.25	0.055	0.035
3	0.060	0.035

Table 29: Aircraft Tubing W/L parameter for fuel lines and vent ducts

0.028" Wall		0.035" Wall		0.049" Wall		0.065" Wall	
OD (in)	W/L (lb/ft)	OD (in)	W/L (lb/ft)	OD (in)	W/L (lb/ft)	OD (in)	W/L (lb/ft)
1/8	0.0101	1/8	0.0115	1/8	0.014	1/4	0.0453
1/4	0.0235	1/4	0.0281	1/4	0.0371	3/8	0.0755
3/8	0.0366	3/8	0.0449	3/8	0.0602	1/2	0.1061
1/2	0.0496	1/2	0.0612	1/2	0.0829	5/8	0.1367
5/8	0.0627	5/8	0.0775	5/8	0.106	3/4	0.167
3/4	0.068	3/4	0.0938	3/4	0.1288	7/8	0.1979
7/8	0.089	7/8	0.1112	7/8	0.153	1	0.2295
1	0.1021	1	0.1275	1	0.1754	1 1/8	0.2601
1 1/8	0.1152	1 1/8	0.1438	1 1/8	0.1989	1 1/4	0.2907
1 1/4	0.1149	1 1/4	0.1601	1 1/4	0.2213	1 3/8	0.3213
1 3/8	0.1415	1 3/8	0.1759	1 3/8	0.2448	1 1/2	0.3519
1 1/2	0.1546	1 1/2	0.1928	1 1/2	0.2683	1 5/8	0.3825
1 7/8	0.194	1 5/8	0.2101	1 5/8	0.2907	1 3/4	0.4131
2	0.2097	1 3/4	0.2264	1 3/4	0.3142	1 7/8	0.4415
2 1/2	0.2596	1 7/8	0.2416	1 7/8	0.3356	2	0.4743
3	0.3121	2	0.2591	2	0.3601	2 1/8	0.5022
		2 1/8	0.27	2 1/8	0.3814	2 1/4	0.5328
		2 1/4	0.2917	2 1/4	0.406	2 3/8	0.5633
		2 1/2	0.3254	2 3/8	0.4274	2 1/2	0.5916
		3	0.3891	2 1/2	0.5916	2 5/8	0.6241
		3 1/2	0.4548	2 5/8	0.4734	2 3/4	0.6528
		4	0.5205	2 3/4	0.4962	2 7/8	0.6852
		4 1/2	0.5862	3	0.5423	3	0.714
		5	0.6518	3 1/2	0.6343	3 1/8	0.7459
				3 3/4	0.6803	3 1/4	0.7765
				4	0.7263	3 3/8	0.8071
				4 1/2	0.8179	3 1/2	0.8364
				5	0.91	3 5/8	0.8678
						3 3/4	0.8984
						4	0.9595
						4 1/4	1.004
						4 1/2	1.081
						5	1.203

Appendix B List of Type Certificate Datasheets

Type certificate datasheets (TCDS) are an excellent source of information on the airframe, often providing information like the MTOW, MLW, airspeed limits, engine specifications, limitations, and type category (Normal, Utility, Commuter, Transport), etc. The usable and either unusable or total fuel capacities are also customarily provided. Type certificate datasheets for airframes, engines, and propellers can be obtained online from:

FAA Dynamic Regulatory System (search for Type Certificate Data Sheets) [52]

EASA Type Certificate Datasheets [53]

Transport Canada NAPA Issue Certificates Online: Certificate Search [54]

Aircraft	Cert Category	Propulsion Engines	TO Thrust, Power, Torque	VMO or MMO	Usable Fuel	Total Fuel	Type Certificate Data Sheets
A330-200	Large Aeroplanes Performance Category A	CF6-80E1A	64530-68530 lb	N/A	Wing tanks = 91300 L Center Tank = 41560 L Trim Tank = 6230 L	139527 L	A330-200 Series TCDS EASA.A.004 Issue 56 basic without MOD 205749
A330-200	Large Aeroplanes Performance Category A	PW4168	68600 lb	N/A	Wing tanks = 91300 L Center Tank = 41560 L Trim Tank = 6230 L	139527 L	A330-200 Series TCDS EASA.A.004 Issue 56 basic without MOD 205749
A330-200	Large Aeroplanes Performance Category A	PW4170	70000 lb	N/A	Wing tanks = 91300 L Center Tank = 41560 L Trim Tank = 6230 L	139527 L	A330-200 Series TCDS EASA.A.004 Issue 56 basic without MOD 205749
A330-200	Large Aeroplanes Performance Category A	Trent 772	71100 lb	N/A	Wing tanks = 91300 L Center Tank = 41560 L Trim Tank = 6230 L	139527 L	A330-200 Series TCDS EASA.A.004 Issue 56 basic without MOD 205749
A340-200	Large Aeroplanes Performance Category A	CFM56-5C	13878-15124 daN	N/A	Wing tanks = 91056 L Center Tank = 41468 L Trim Tank = 6114 L	138972 L	A340-200 Series TCDS EASA.A.015 Issue 25 basic without MOD 46761
A300 B2-100	Large Aeroplanes Performance Category A	CF6-50	21500-23050 daN	0.86	Outer Tanks = 9230 L Inner Tanks = 34770	44066 L	A300, A310, A300-600 TCDS EASA.A.172 Issue 04 basic without Mods 01569, 01357, 06696
A300 B2-200	Large Aeroplanes Performance Category A	CF6-50	21500-23050 daN	0.86	Outer Tanks = 9230 L Inner Tanks = 34770	44066 L	A300, A310, A300-600 TCDS EASA.A.172 Issue 04 basic without Mods 01569, 01357, 06696
A320-200	Large Aeroplanes Performance Category A	CFM56-5	22000-27000 lb	0.82	Wing tanks = 15609 L Center Tank = 8250 L	23941 L	A318, A319, A320, A321 TCDS EASA.A.064 Issue 46 for A320-200 3 tank airplane without MOD 160001
ATR42-200	Transport Category	PW120	1491 kW	0.55	Wing tanks = 5700 L Center Tank = N/A	5727 L	ATR42, ATR72 TCDS FAA A53EU ATR42, ATR72 TCDS EASA.A084

Aircraft	Cert Category	Propulsion Engines	TO Thrust, Power, Torque	VMO or MMO	Usable Fuel	Total Fuel	Type Certificate Data Sheets
ATR42-200	Transport Category	PW127E	1790 kW	0.55	Wing tanks = 5700 L Center Tank = N/A	5727 L	ATR42, ATR72 TCDS FAA A53EU ATR42, ATR72 TCDS EASA.A084
DO228-100	Normal Category - Commuter	TPE331-5-252 D	533 kW	0.40	Wing tanks = 2386 L Center Tank = N/A	2440 L	Dornier 228 Series TCDS EASA.A.359 for Do228-100
690B	Normal Category	TPE331-5-251 K	717.5 hp	0.52	Wing tanks = 1454 L Center Tank = N/A	1472 L	Twin Commander TCDS FAA 2A4 Rev. 49
DHC6	Normal Category	PT6A-20	550 hp	202 kts	FWD Tank = 176 USG AFT Tank = 182 USG	365 USG	DHC-6 TCDS FAA A9EA
B727	Transport Category	JT8D	14000-14500 lb	0.90	Wing Tanks = 3636 USG Center Tank = 4550 USG	N/A	B727 TCDS FAA A3WE
B747-100	Transport Category	JT9D	43500-48650 lb	0.92	Total usable fuel = 47210 USG	Reserve Tanks = 500 USG No. 1 & 4 Tanks = 4420 USG No. 2 & 3 Tanks = 12240 USG Center Tank = 12890 USG	B747 TCDS FAA A20WE Rev. 58
B767-200/300	Transport Category	JT9D-7R4	45800-47500 lb	0.86	Wing Tanks = 12140 USG Center Tank = 12000 USG	24157 USG	B767 TCDS FAA A1NM Rev. 39 B767 TCDS EASA.IM.A.035 Issue 09 JT9D Engine TCDS FAA E3NE Rev. 16
B757-200/300	Transport Category	PW2000	37530-40900 lb	0.86	Wing Tanks = 4352 USG Center Tank = 6924 USG	N/A	B757 TCDS FAA A2NM Rev. 32
B757-200/300	Transport Category	RB211-535	36720-42540 lb	0.86			
C550	Transport Category	JT15D-4	2500 lb	0.70	Wing Tanks = 742 USG Center Tank = N/A	752 USG	C550 TCDS FAA A22CE Rev. 44 C550 TCDS EASA.IM.A.207 Issue 07
C208	Normal Category	PT6A-114	600-675 shp	175 KIAS	Wing Tanks = 332 USG Center Tanks = N/A	335 USG	C208 TCDS FAA A37CE Rev. 16 C208 TCDS EASA.IM.A.226 Issue 10
C441	Normal Category	TPE331-8-400	635 shp	0.55	Wing Tanks = 475 USG Center Tanks = N/A	482 USG	C441 TCDS FAA A28CE Rev. 12
C414	Normal Category	GTSIO-520-C	340 hp	156 KCAS	Tip Tanks = 100 USG Wing Tanks = 70 USG Center Tanks = N/A	175 USG	C414 TCDS FAA A7CE Rev. 50
C210J	Normal Category	IO-520-J	285 bhp	196 KCAS	Wing Tanks = 89 USG Center Tanks = N/A	90 USG	C210 TCDS FAA 3A21 Rev. 49
C172	Normal Category	O-300	145 hp	122 KCAS	Wing Tanks = 37 Center Tanks = N/A	42 USG	C172 TCDS FAA 3A12 Rev. 86
C310C	Normal Category	IO-470-D	260 hp	215 KTIAS	Tip Tanks = 102 USG Center Tanks = N/A	102 USG	C310 TCDS FAA 3A10 Rev. 61
F27	Large Aeroplanes Performance Category A	RR Dart 511	1570 shp	224 KIAS	Wing Tanks = 1357 USG Center Tanks = N/A	1380 USG	F27 TCDS FAA A-817 Rev. 22 F27 TCDS EASA.A.036 Issue 07

Aircraft	Cert Category	Propulsion Engines	TO Thrust, Power, Torque	VMO or MMO	Usable Fuel	Total Fuel	Type Certificate Data Sheets
G159	Transport Category	RR Dart 529-8	1950-1990 shp	0.54	Wing Tanks = 1550 USG Center Tanks = N/A	1561 USG	G-159 TCDS FAA 1A17 Rev. 19 for basic aircraft
EMB110P2	Normal Category	PT6A-34	750 shp	230 KIAS	Wing Tanks = 447 USG Center Tanks = N/A	454 USG	EMB110 TCDS FAA A21SO Rev. 8 EMB110 TCDS EASA.IM.A.229 Issue 01
LJ25D	Transport Category	CJ-610-8A	2950 lb	0.80	Tip Tanks = 368 USG Wing Tanks = 347 USG Fuselage Tank = 195 USG	933 USG	Learjet TCDS FAA A10CE Rev. 47
LJ28	Transport Category	CJ-610-8A	2950 lb	0.82	Wing Tanks = 430 USG Fuselage Tank = 269 USG	711 USG	Learjet TCDS FAA A10CE Rev. 47
DC-10-10	Transport Category	CF6-6D	39300-40900 lb	0.88	Wing Tanks = 11975 USG Center Tank = 9697 USG	21765 USG	DC-10/MD-10 TCDS FAA A22WE Rev. 13 for Model DC-10-10
DC-10-30	Transport Category	CF6-50	48400-53200 lb	0.88	Wing Tanks = 12000 USG Center Tank = 14539 USG	36426 USG	DC-10/MD-10 TCDS FAA A22WE Rev. 13 for Model DC-10-30

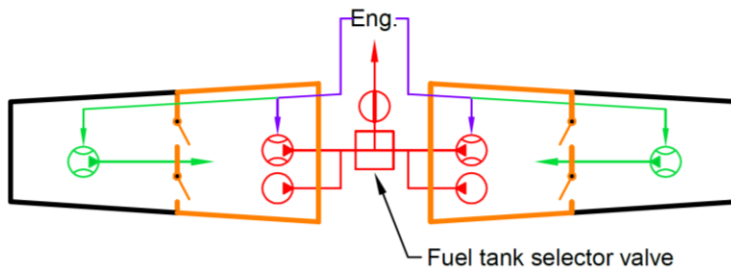
Appendix C Aircraft Fuel System Schematics

The following section provides a series of fuel system schematics for various aircraft as part of the research in this thesis.

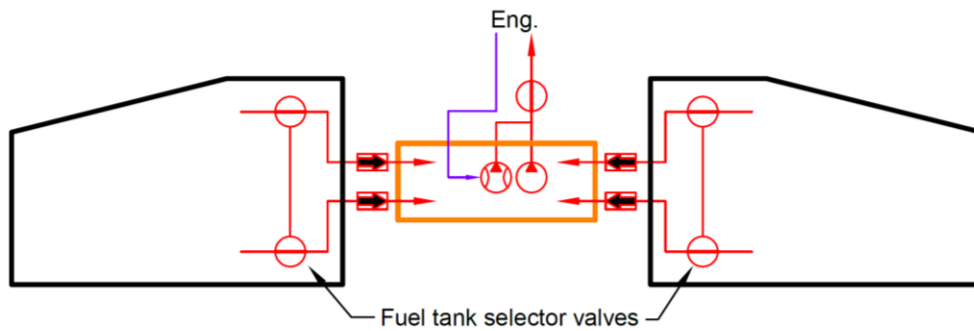
C.1 Feed and Transfer Subsystem Schematics

The engine feed and fuel transfer schematics in this section demonstrate the diversity and complexity of aircraft fuel systems. The schematics range from single-engine, light GA aircraft to large, multi-engine, and wide-body transport airliners. An effort was made to standardize the symbols for the components used from the various manuals available to highlight the most pertinent information. Note that filters, heat exchangers, engine-driven pumps, and other small-element components (pressure reducing/regulating valves) have been omitted since the weight and size data were unavailable or their placement in the schematic could not be determined.

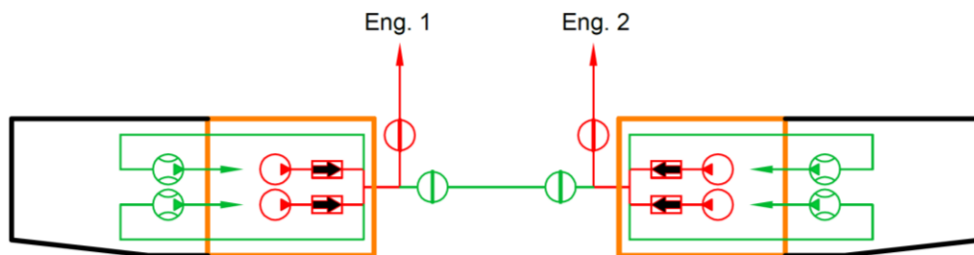
Pilatus PC-12



Cessna 208



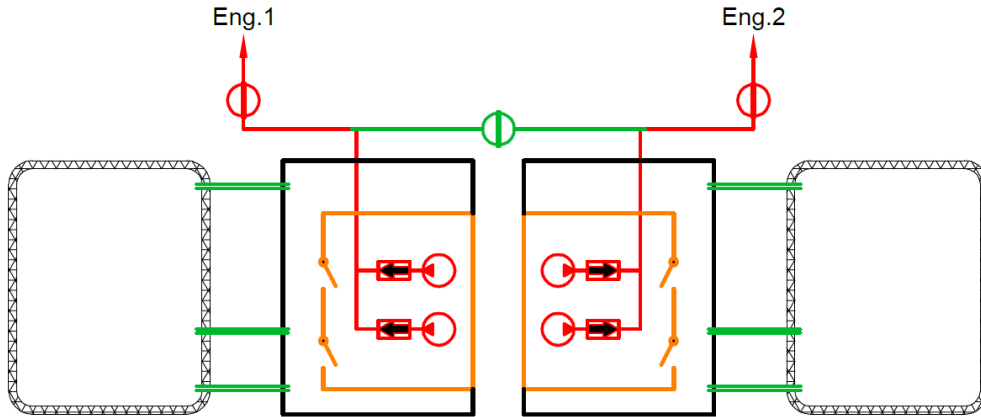
Cessna 414



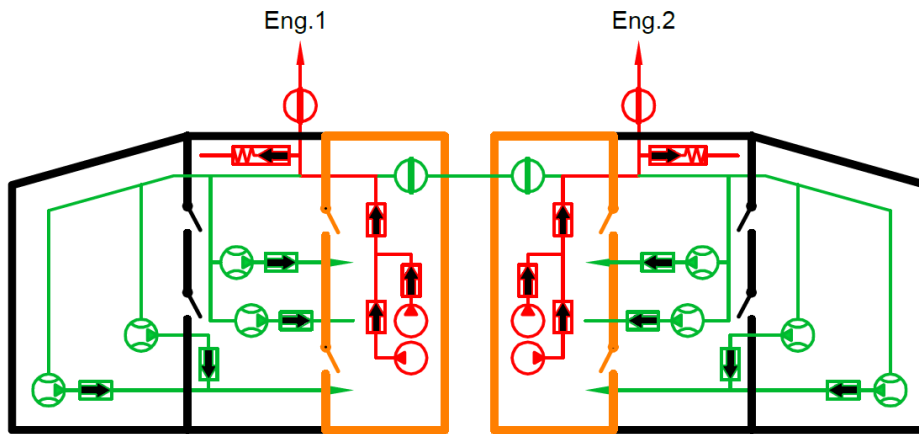
LEGEND

Elec. pump	Float valve	Integral tank boundary
Ejector pump	Engine feed line	Feed compartment boundary
Elec. valve (NO)	Engine motive flow line	Bladder tank boundary
Elec. valve (NC)	Fuel transfer line	Vented rib
Check (non-return) valve	Vent duct/line	Rib with flapper valve
Pressure relief valve	Tank inter-connect line	Diffuser

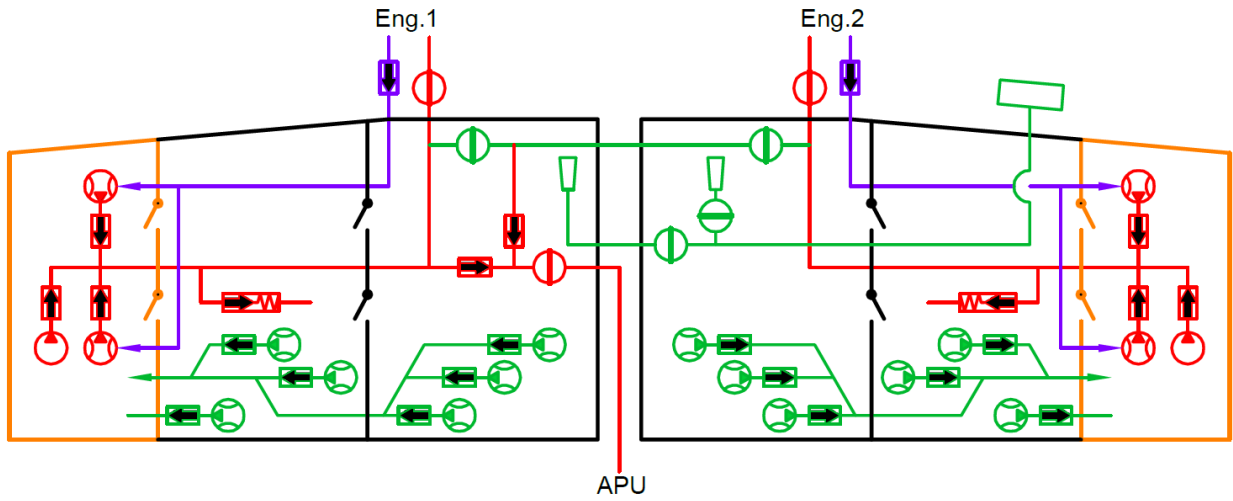
Embraer 110 P2

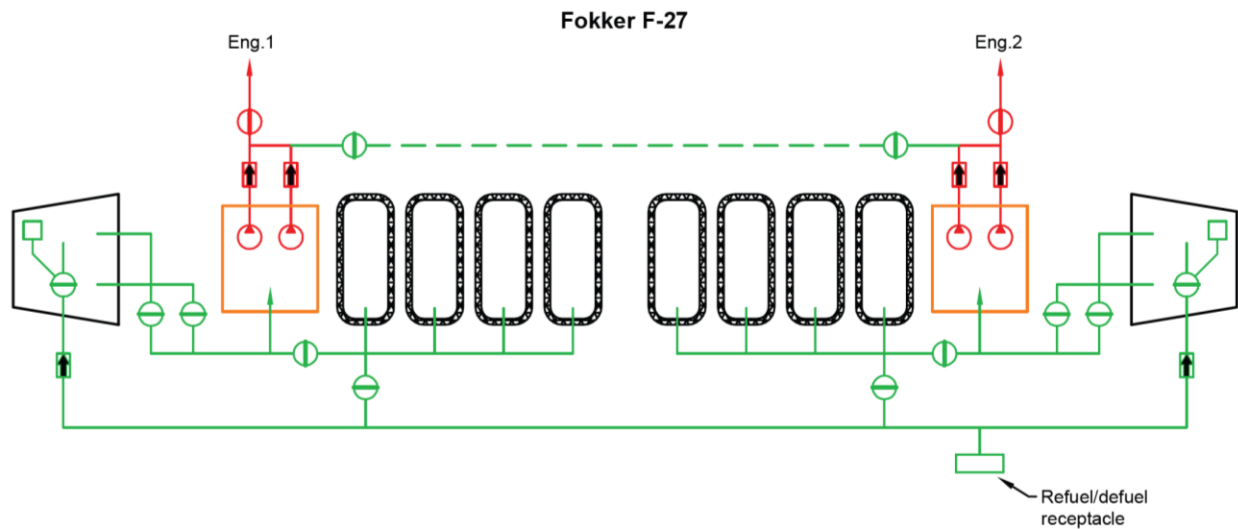
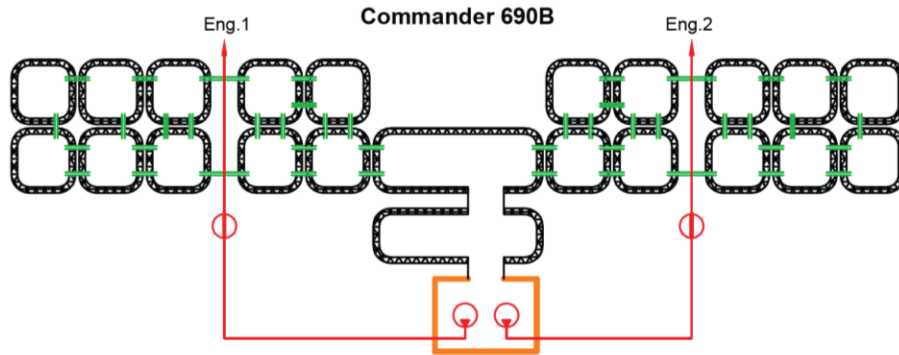
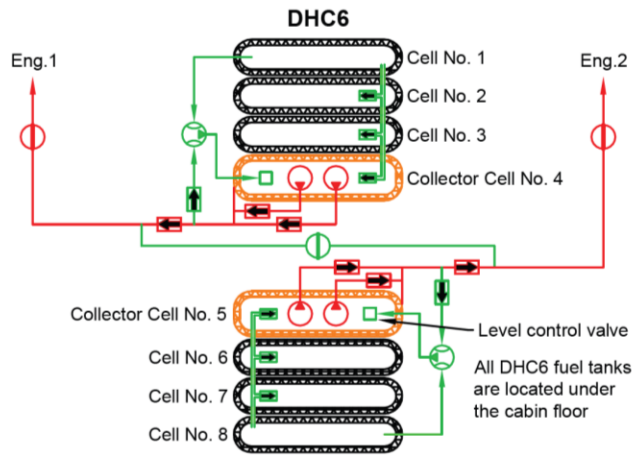


Dornier Do-228

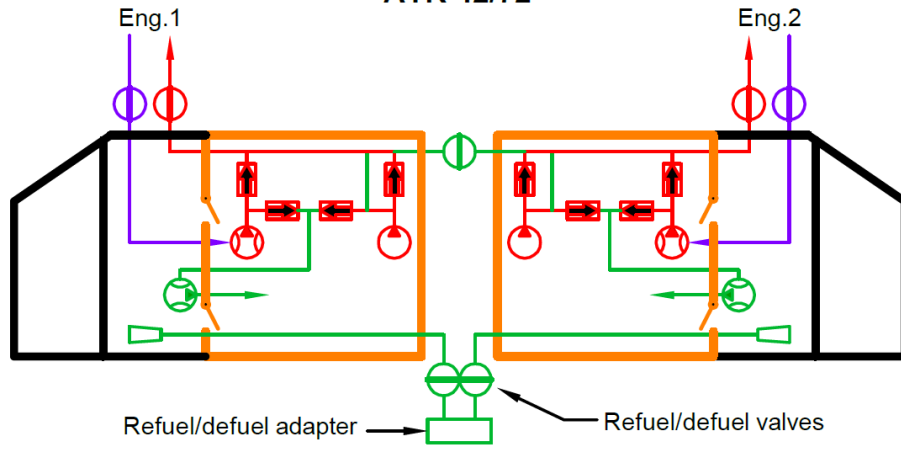


DO328 Jet

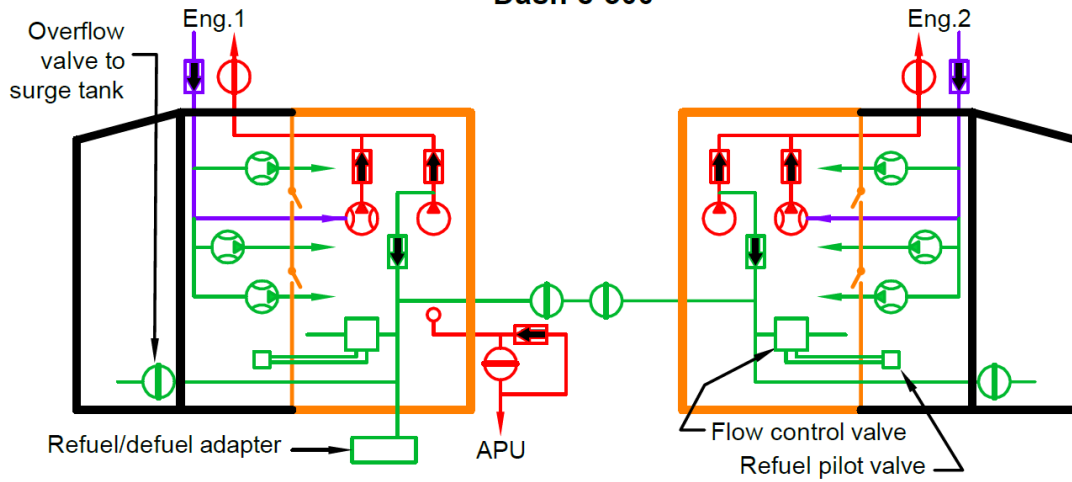




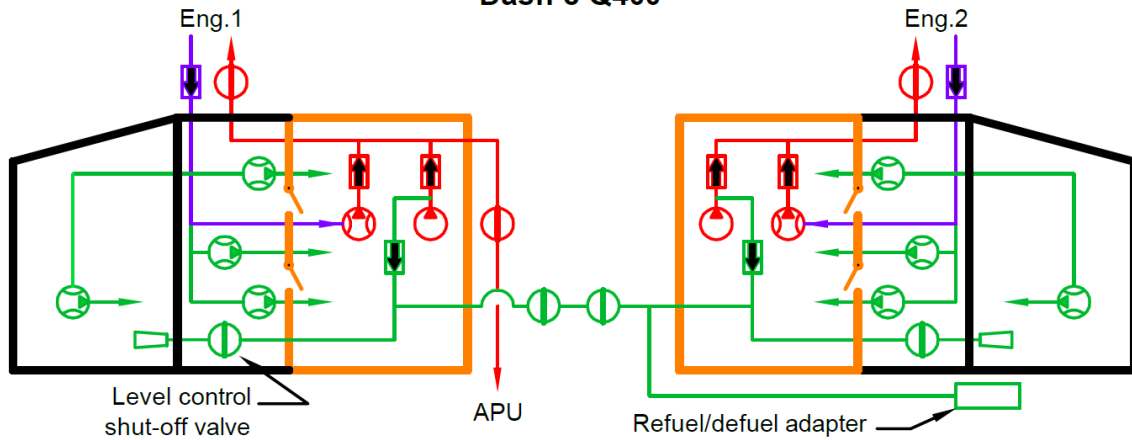
ATR 42/72



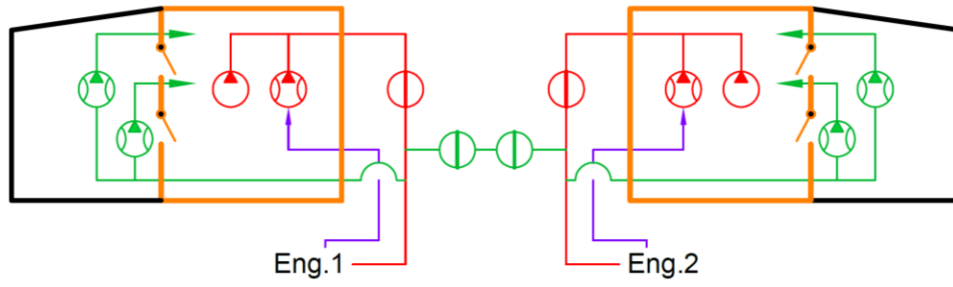
Dash 8-300



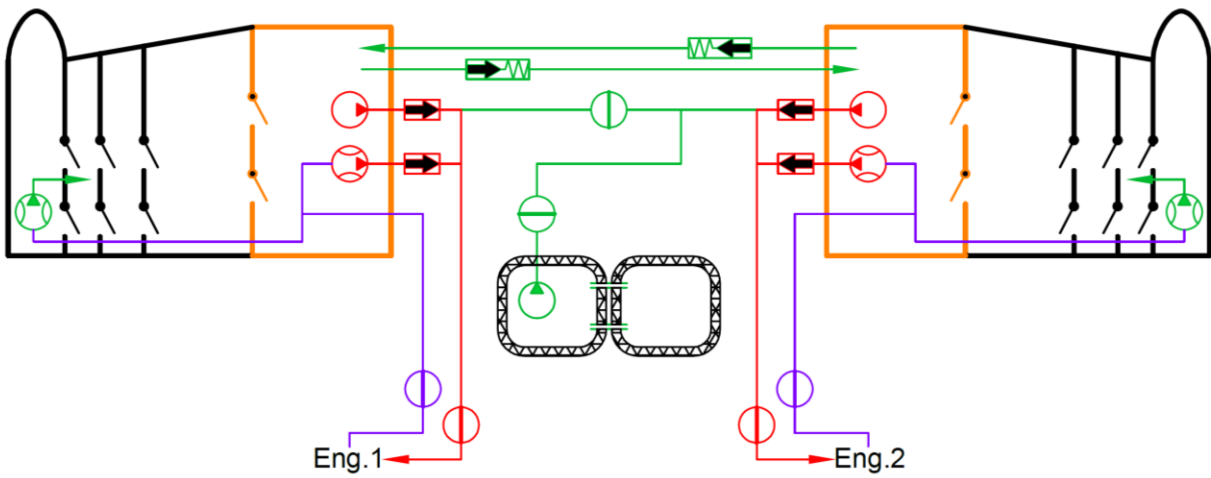
Dash 8 Q400



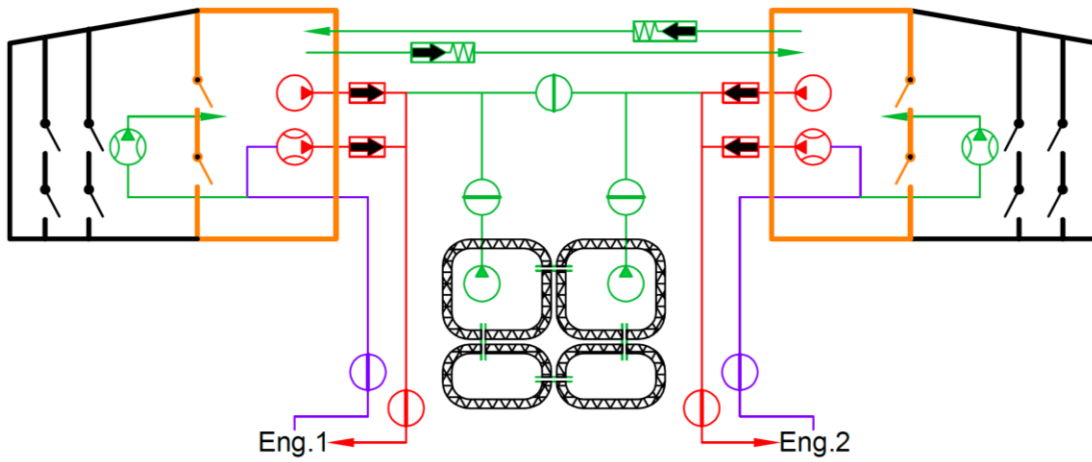
Cessna 550 Citation II



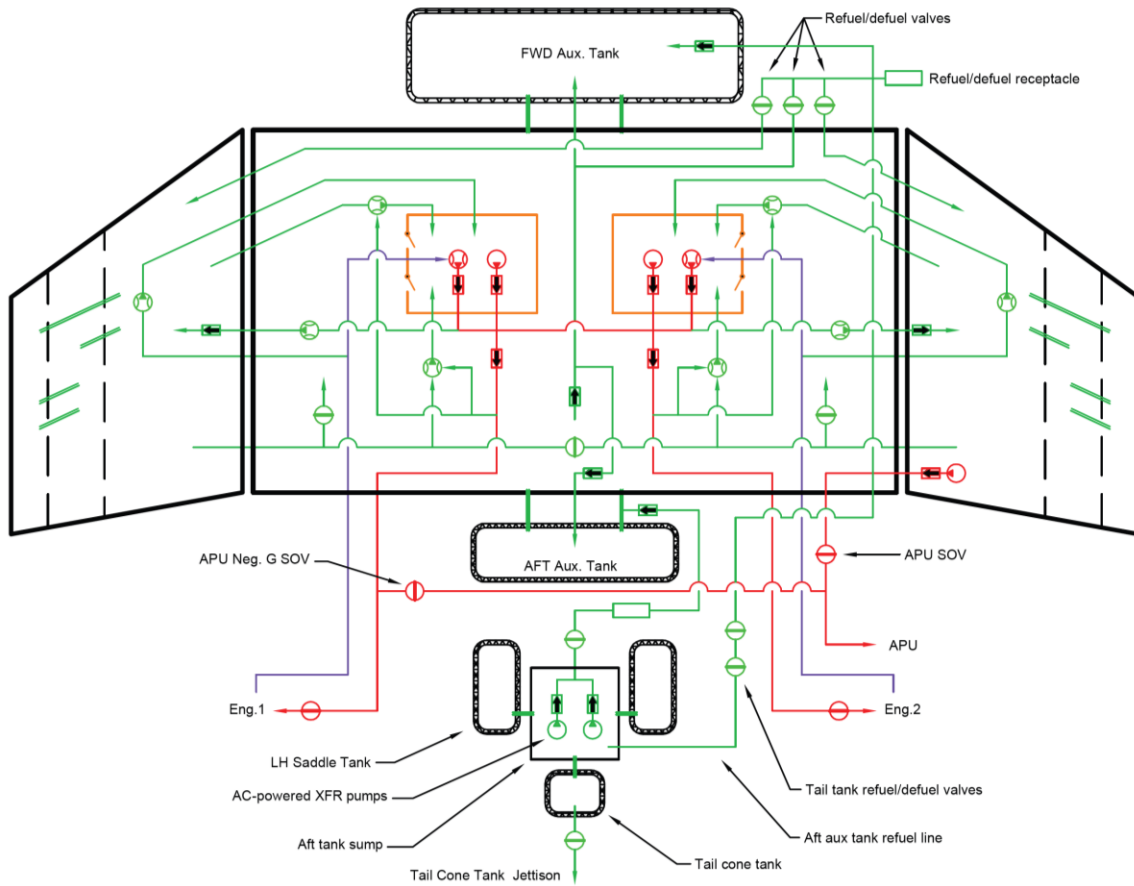
Learjet 25D



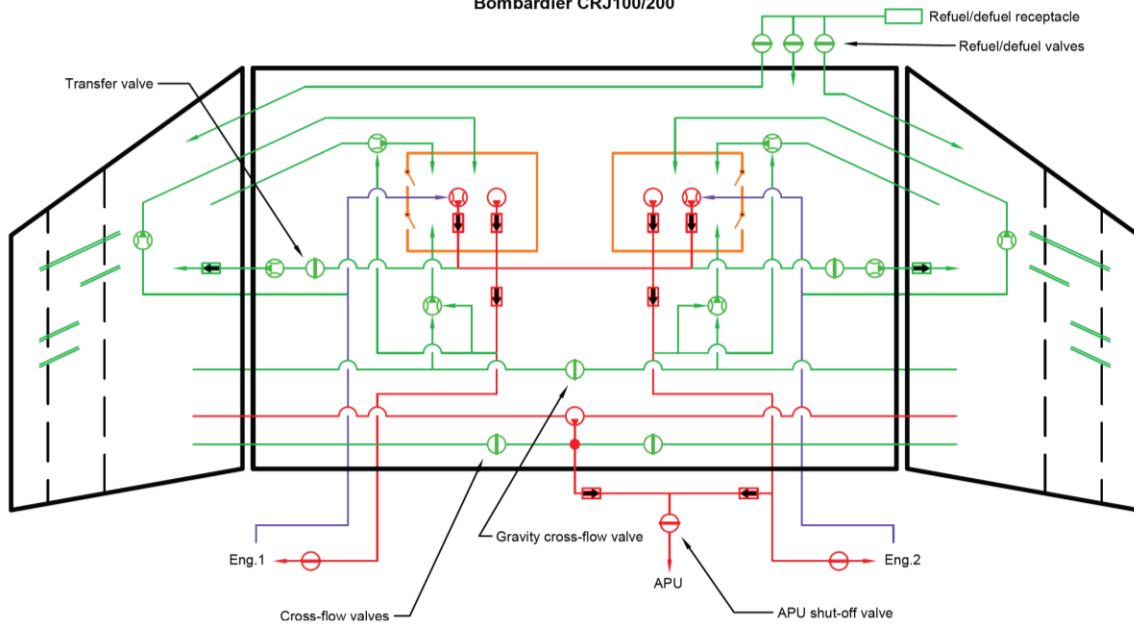
Learjet 28



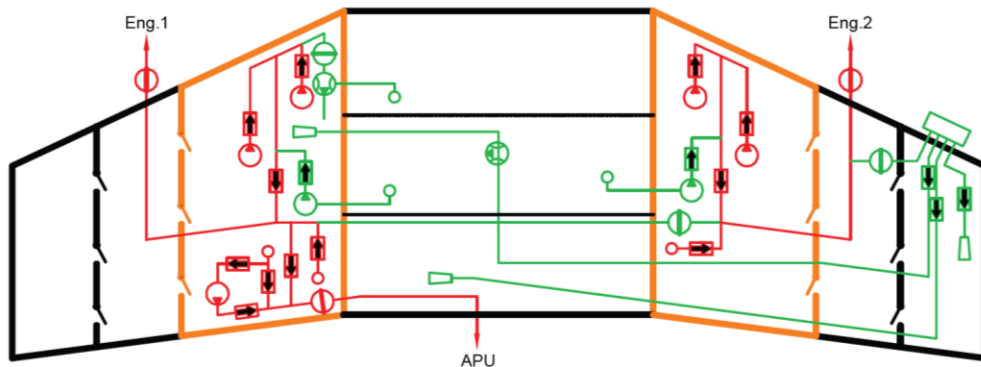
Bombardier CL605



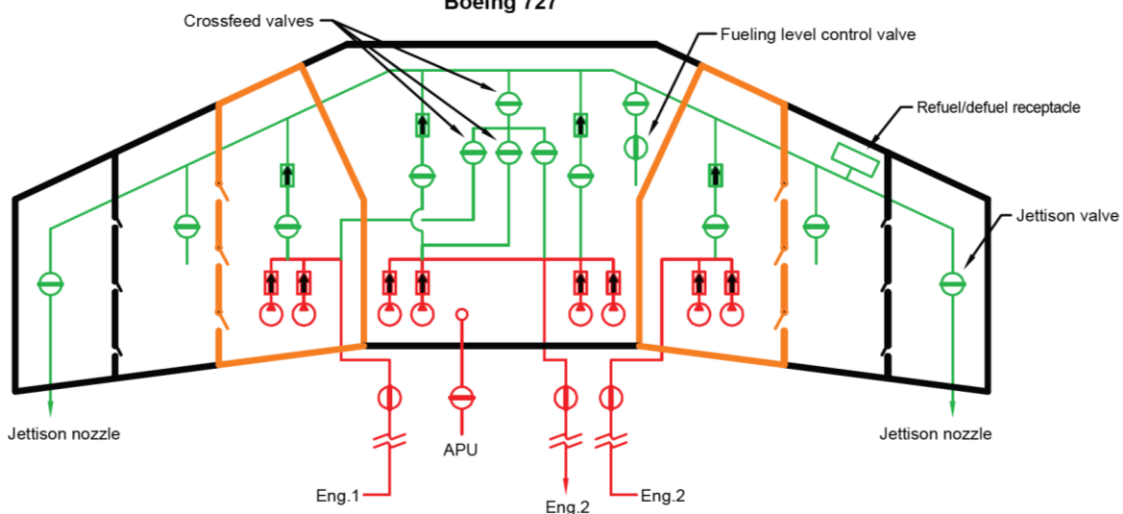
Bombardier CRJ100/200



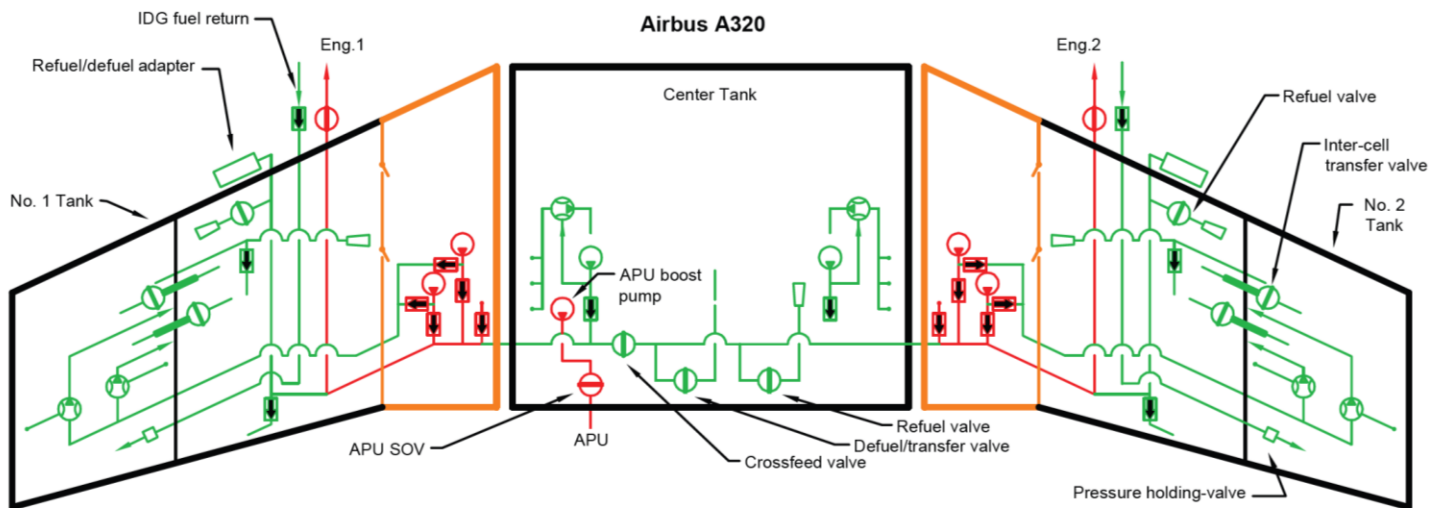
Boeing 737-3/4/5



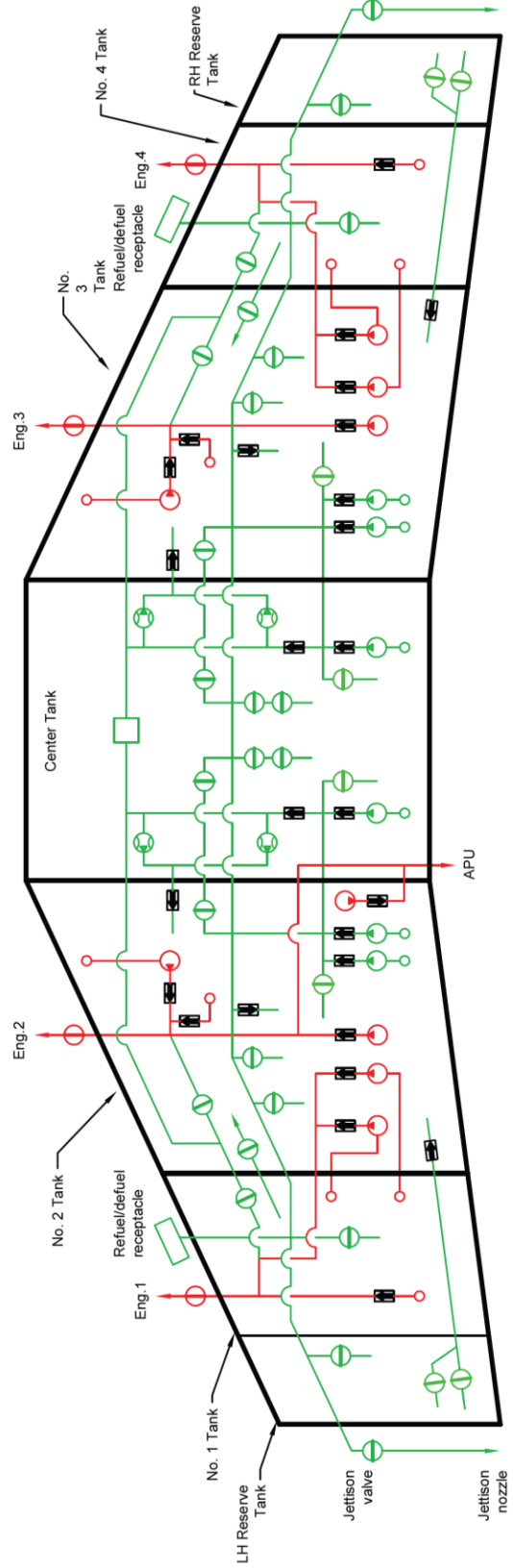
Boeing 727



Airbus A320



Boeing 747-100

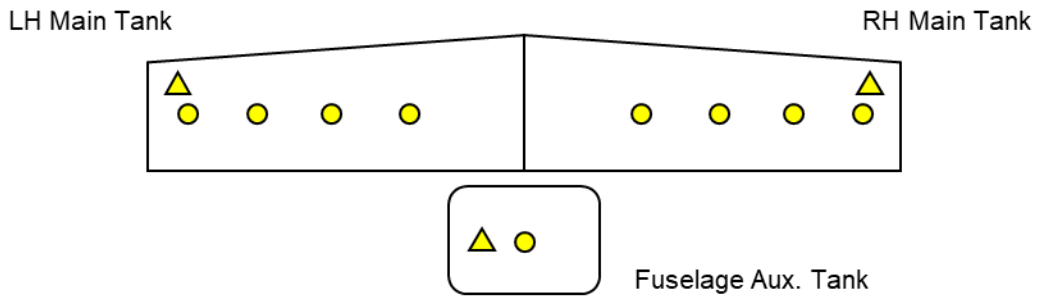


C.2 Fuel Quantity & Indicating Schematics

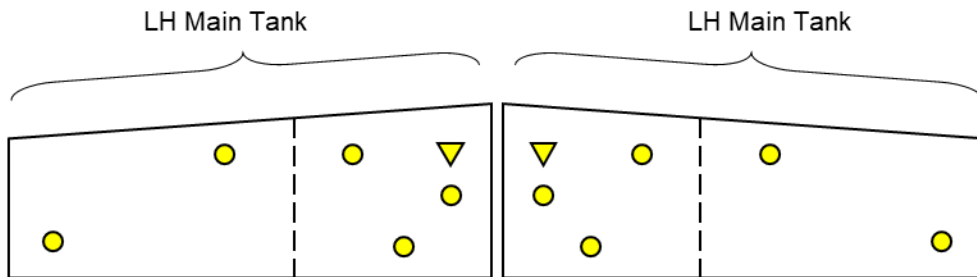
Legend

- Fuel Quantity Probe
- ▲ High-level switch
- ▼ Low-level switch
- ⏏ Fuel measuring stick
- Compensator

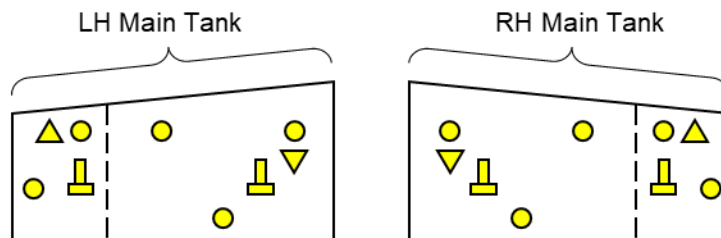
Learjet 28



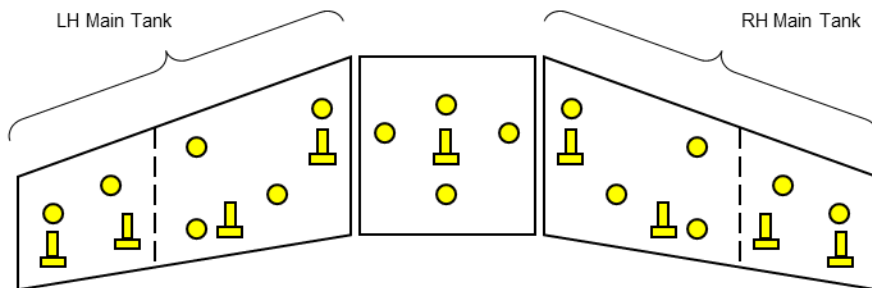
DO228



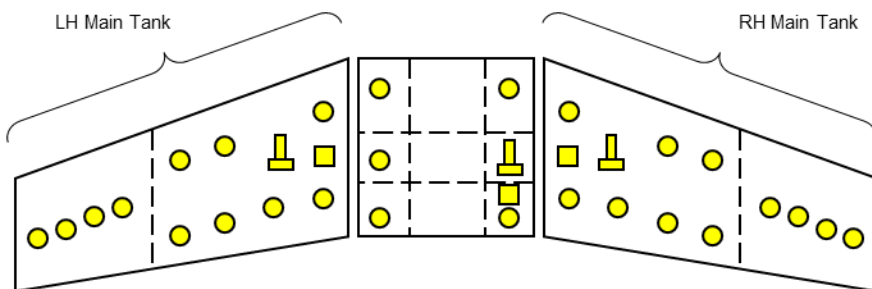
ATR42 / 72



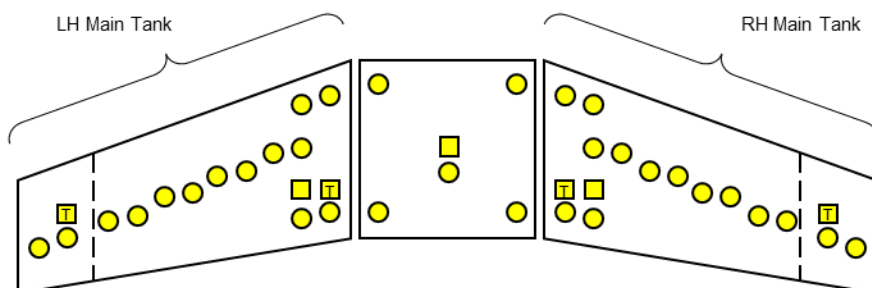
BAC-111



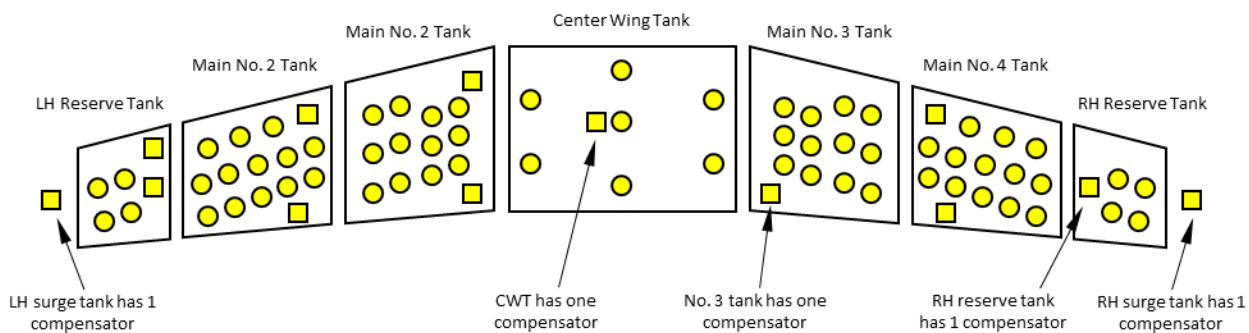
B727



A320








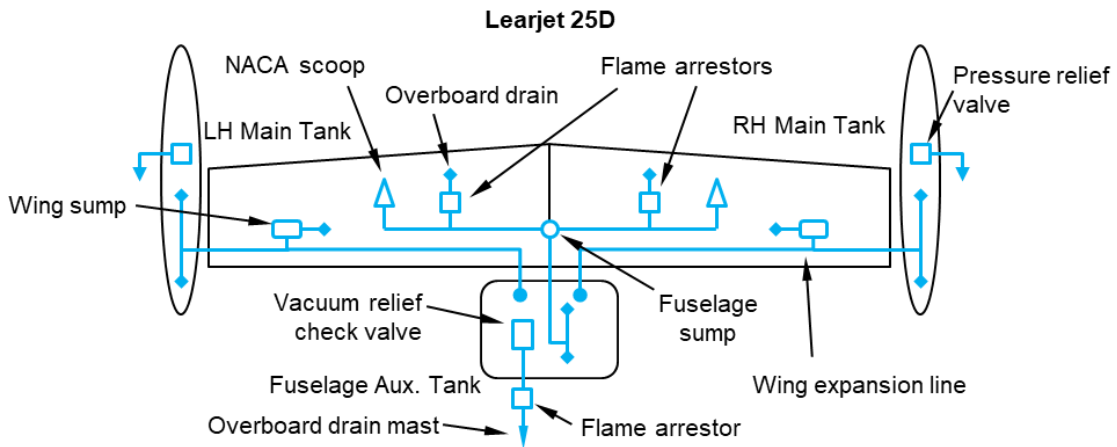
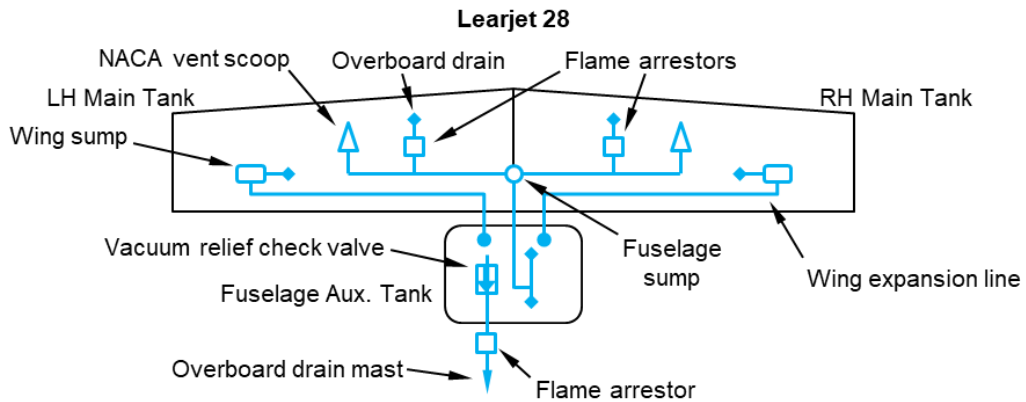
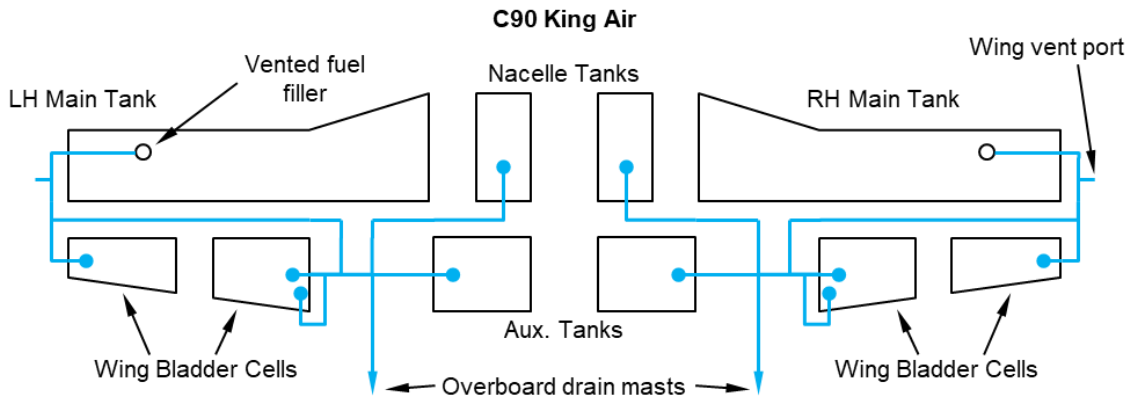
B747-100

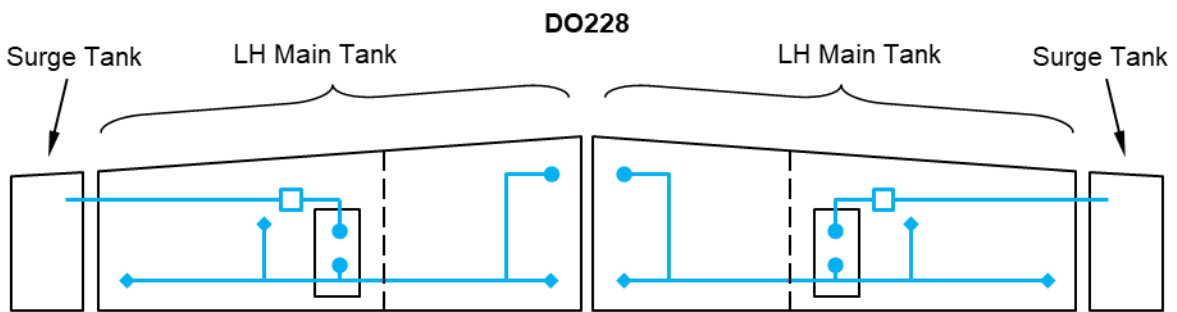
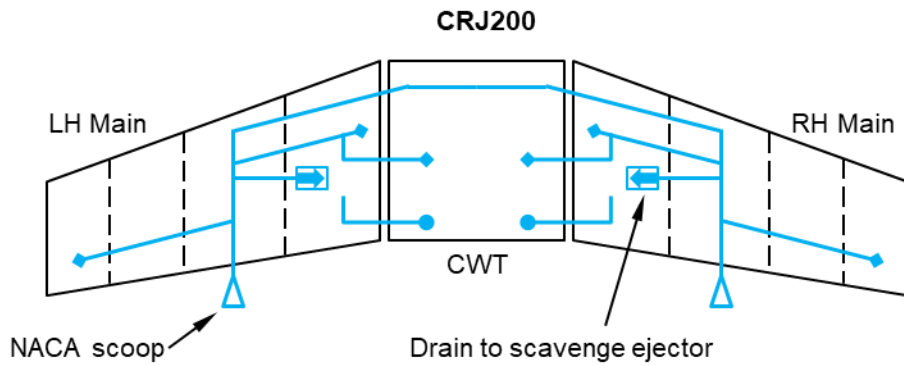
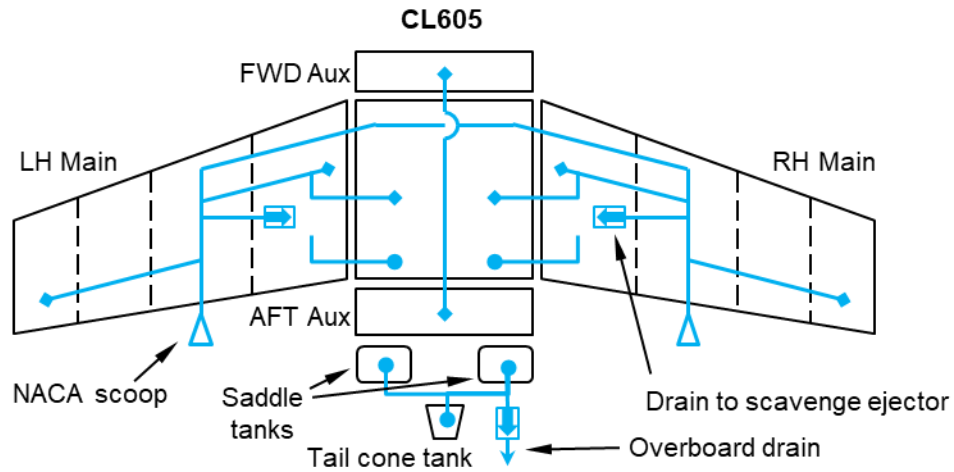


C.3 Fuel Tank Venting Schematics

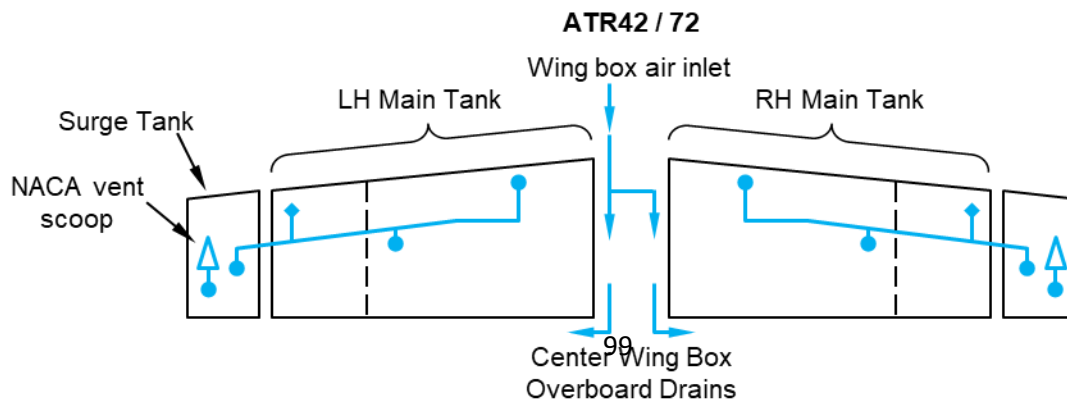
Legend

-  Vent line/duct with float valve
-  Vent line/duct with upturned opening
-  Vent line/duct
-  NACA Duct
-  Check valve

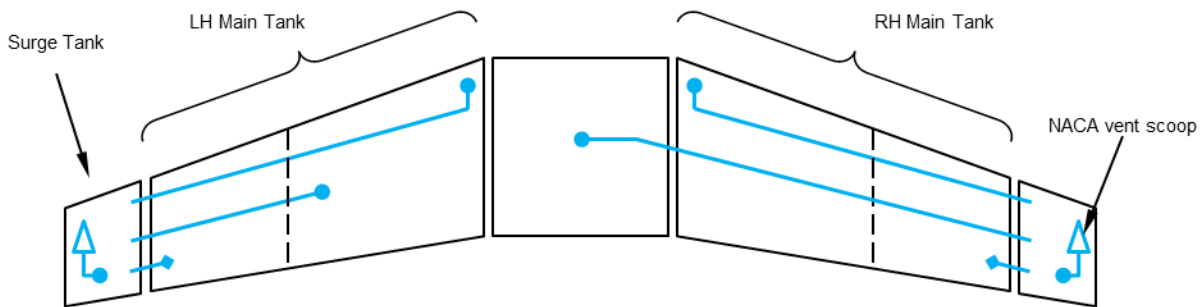




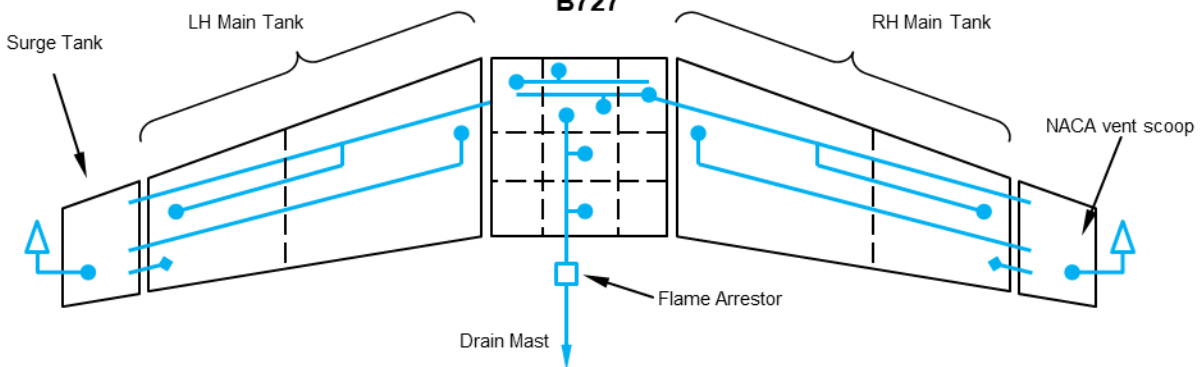
Unable to determine air inlet placement from available sources



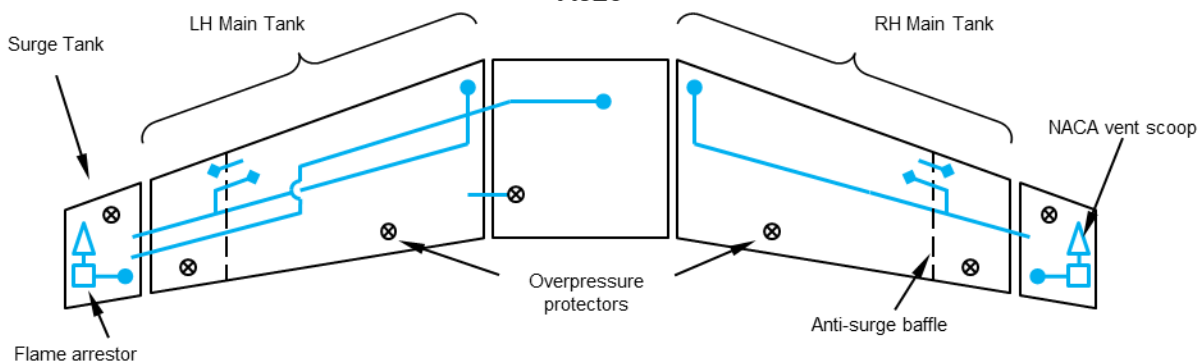
BAC-111



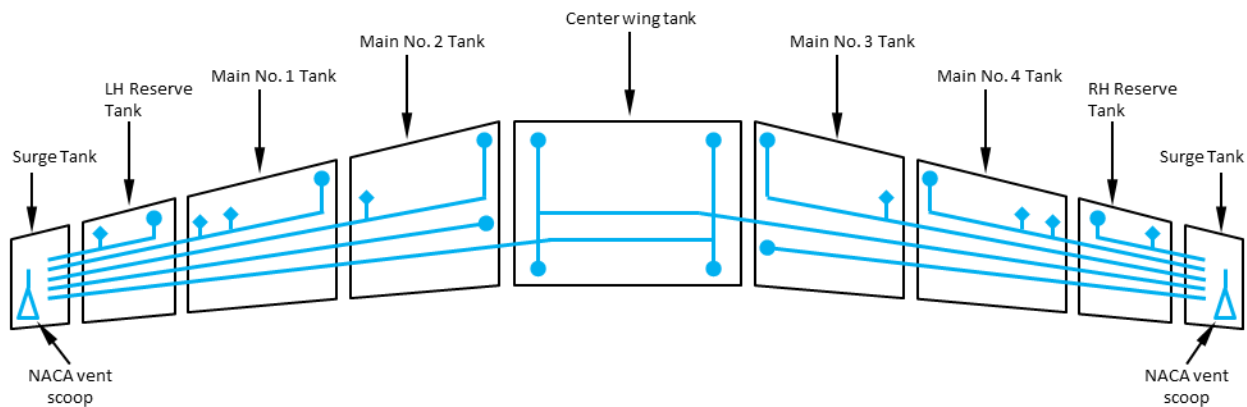
B727



A320



B747-100



Appendix D Empirical Equations for Fuel System Weight Estimation

Roskam fuel system weight estimation equations:

$$\text{Cessna} \quad W_{fs} = \begin{cases} 0.40W_F/K_{fsp} & \text{For aircraft with internal fuel systems} \\ 0.70W_F/K_{fsp} & \text{For aircraft with external fuel systems} \end{cases}$$

$$\text{USAF} \quad W_{fs} = 2.49 \left[\left(\frac{W_F}{K_{fsp}} \right)^{0.6} \left(\frac{1}{1+int} \right)^{0.3} N_t^{0.20} N_e^{0.13} \right]^{1.21}$$

$$\text{Torenbeek Piston Propeller Aircraft (PPA)} \quad W_{fs} = \begin{cases} 2 \left(\frac{W_F}{K_{fsp}} \right)^{0.667} & \text{For single-engine piston propeller aircraft} \\ 4.5 \left(\frac{W_F}{K_{fsp}} \right)^{0.60} & \text{For multi-engine piston propeller aircraft} \end{cases}$$

$$\text{Torenbeek Commercial Transport Aircraft (CTA)} \quad W_{fs} = \begin{cases} 1.6 \left(\frac{W_F}{K_{fsp}} \right)^{0.727} & \text{For non-self-sealing bladder tanks} \\ 80(N_e + N_t - 1) + 15N_t^{0.5} \left(\frac{W_F}{K_{fsp}} \right)^{0.333} & \text{For Integral tanks} \end{cases}$$

NASA FLOPS fuel system weight estimation equations:

$$WFSYS = 1.07 \times FMXTOT^{0.58} \times FNENG^{0.43} \times VMAX^{0.34} \text{ for transport category aircraft}$$

$$WFSYS = 1.07 \times FMXTOT^{0.58} \times FNENG^{0.43} \text{ for general aviation aircraft}$$